

## Accepted Manuscript

Paleozoic reactivation structures in the Appalachian-Ouachita-Marathon foreland: Far-field deformation across Pangea

John P. Craddock, David H. Malone, Ryan Porter, John Compton, John Luczaj, Alex Konstantinou, James E. Day, Stephen T. Johnston



PII: S0012-8252(16)30439-1  
DOI: doi: [10.1016/j.earscirev.2017.04.002](https://doi.org/10.1016/j.earscirev.2017.04.002)  
Reference: EARTH 2401  
To appear in: *Earth-Science Reviews*  
Received date: 21 November 2016  
Revised date: 3 April 2017  
Accepted date: 3 April 2017

Please cite this article as: John P. Craddock, David H. Malone, Ryan Porter, John Compton, John Luczaj, Alex Konstantinou, James E. Day, Stephen T. Johnston , Paleozoic reactivation structures in the Appalachian-Ouachita-Marathon foreland: Far-field deformation across Pangea. The address for the corresponding author was captured as affiliation for all authors. Please check if appropriate. Earth(2017), doi: [10.1016/j.earscirev.2017.04.002](https://doi.org/10.1016/j.earscirev.2017.04.002)

This is a PDF file of an unedited manuscript that has been accepted for publication. As a service to our customers we are providing this early version of the manuscript. The manuscript will undergo copyediting, typesetting, and review of the resulting proof before it is published in its final form. Please note that during the production process errors may be discovered which could affect the content, and all legal disclaimers that apply to the journal pertain.

**Paleozoic Reactivation Structures in the Appalachian-Ouachita-Marathon  
Foreland: Far-Field Deformation across Pangea**

John P. Craddock, Geology Department, Macalester College, St. Paul, MN  
55105 USA (Craddock@Macalester.edu)

David H. Malone, Department of Geography-Geology, Illinois State  
University, Normal, IL USA

Ryan Porter and John Compton, School of Earth Sciences and Environmental  
Sustainability, Northern Arizona University, Flagstaff, AZ USA

John Luczaj, Department of Natural & Applied Sciences, University of Wisconsin  
-Green Bay, 2420 Nicolet Drive, Green Bay, WI 54311

Alex Konstantinou, Cyprus Hydrocarbons Company, Nicosia, Cyprus

James E. Day, Department of Geography-Geology, Illinois State  
University, Normal, IL USA

Stephen T. Johnston, Department of Geology, University of Alberta, Edmonton,  
Alberta, Canada

**Abstract**

The Proterozoic Grenville orogeny (~1300-980 Ma) reactivated the Archean-hosted Kapuskasing suture in Laurentia which then propagated west and south initiating the Keweenaw rift (1141-1085 Ma) which closed by thrust shortening at 1060 Ma. Late Proterozoic-Paleozoic sediments were then deformed in association with the amalgamation of Pangea in the late Paleozoic causing ~30 km of thrust shortening along this 4000 km paired (inverted) fault system, preserved by numerous 2<sup>nd</sup> and 3<sup>rd</sup> order footwall structures in adjacent basement and Paleozoic cover rocks. We present the descriptions of twenty field sites of deformed Paleozoic sediments in the Appalachian-Ouachita-Marathon foreland to further document the subtleties of far-field tectonic stress transmission in the midcontinent of North America. Field observations are also complimented with 63 new foreland calcite twinning strain results and, when compiled with 260 older twinning strain results, document a complex Paleozoic far-field stress-strain field. Appalachian-Ouachita-Marathon orogenic fluid pulses in the foreland were also complex, namely the so-called Mississippi Valley type (MVT) Pb-Zn ore deposits, and mineralization is constrained by thrust faulted highlands with occasional fluid sourcing from underlying Precambrian

basement. The amalgamation of Pangea was a complex process in the late Paleozoic involving oblique convergence along the Gondwana margin and a central Laurussian collisional belt where far-field stresses initiated inversion structures in the centers of the African and N. American cratons, including the Kiri and Keweenaw-Kapuskasung uplifts, respectively.

### Introduction

Laurentia grew by subduction-related accretion around the ~15 terrane core of the Archean Canadian shield (Card, 1990) with orogenic events at 1.85 Ga (Penokean; Schultz and Cannon, 2007; Holm et al. 1998), 1.75 Ga (Yavapai; Bickford et al., 2008; Medaris et al., 2003), 1.63 Ga (Mazatzal; Romano et al. 2000; Medaris et al. 2003; Foster et al., 2006), 1.3-1.0 Ga (Grenville-Keweenaw; Donaldson and Irving, 1972; Gordon and Hempton, 1986; Paces and Miller, 1993; Eriksson et al. 2003, Heaman et al. 2007; Rainbird et al. 2012) and the 3 Paleozoic phases of the Appalachian orogeny (Rodgers, 1967; Hatcher, 1987; Hatcher et al. 1989). These orogenic belts young to the southeast and are oriented ~SW-NE (Hoffman, 1988; Whitmeyer and Karlstrom, 2007) with the exception being the Keweenaw rift system, with its central hotspot and 5 failed rift arms (Sutcliffe, 1991). The Kapuskasing suture has a long history of fault reactivation in Ontario (Percival and McGrath, 1986; Evans and Halls, 2010) and is interpreted by Manson and Halls (1994, 1997) to continue to the southwest as the Keweenaw-Lake Owen-Hastings thrust fault system in Michigan, Wisconsin, Minnesota, Iowa, Kansas and Oklahoma thereby forming a single thick-skinned, reverse fault system from near James Bay, Ontario, Canada to central Oklahoma, USA (Figure 1). The Kapuskasing-Keweenaw reverse fault (KKF) crosscuts all the terranes mentioned above (2.65 Ga Wawa to 1.63 Ga Mazatzal) over a distance of ~4000 km where the youngest exposed rocks offset along this boundary are late Devonian (Hamblin, 1958, 1961; Milstein, 1987). In the subsurface, Mississippian-Permian sediments are offset by reverse motion (Woelk and Hinze, 1991) and both observations require a late Paleozoic reverse fault motion in the

midcontinent of North America. This fault system may be the longest, and longest-lived, intracratonic fault system on earth.

Transmission of compressional tectonic stresses is well-documented in active settings from plate boundary to plate boundary (Zoback et al. 1989) thereby connecting tectonic stresses to absolute plate motions (DeMets et al., 2009). Far-field tectonic stresses are also preserved in older rocks as measurable finite strains in foreland settings that are proximal (Nichelsen, 1966; Engelder and Engelder, 1977) and up to 2000 km inboard of a thrust belt (Craddock and van der Pluijm, 1989; Lacombe et al., 1989; Craddock et al., 1993) where both differential stress and strain magnitudes decrease into the foreland of a given orogeny (van der Pluijm et al. 1997). Our goal in this study was to further document late Paleozoic Appalachian-Ouachita-Marathon (AOM) deformation in the midcontinent of North America. Specifically, we have documented thick-skinned fault offsets and local footwall deformation associated with the KKF, and employ twinned calcite strain and seismic reflection data to attempt to understand related far-field deformation associated with the amalgamation of Pangea (Daly et al. 1991; Trouw and DeWit, 1999).

### **Previous Work**

Cratonic North America is characterized by a broad patchwork of low amplitude, long wavelength basins and domes, such as the Michigan basin, Wisconsin arch and Williston basin, that formed early in the Paleozoic in what became the Appalachian-Ouachita-Marathon (AOM) foreland (Quinlan and Beaumont, 1984; Howell and van der Pluijm, 1990). Most of these basins were depocenters throughout the Paleozoic, and again received sediment in the Jurassic-Cretaceous. Chapple (1978) modeled the mechanics of Appalachian foreland deformation, as preserved by small finite strains or large-scale salt-cored rootless folds (Wiltschko and Chapple, 1977), as thin-skinned and lacking

involvement of basement crust. This model was supported by the many examples of subtle foreland deformation (Nickelson, 1966; Engelder and Engelder, 1977; Craddock and van der Pluijm, 1989) and 2<sup>nd</sup> order features that resulted from the flushing of orogenic fluids into the foreland (Oliver, 1986): Permian remagnetizations (McCabe and Elmore, 1989), magnetic anisotropy fabrics (Jackson et al. 1989, 1991; Sun et al. 1993) and Mississippi Valley type Pb-Zn deposits of Permian age (MVT; Leach and Rowan 1986, Christensen et al. 1995; Leach et al. 2010). Chapple (1978) did not envision the development of an antithetic thick-skinned reverse fault motion 1000 km inboard of an evolving thin-skinned fold-and-thrust belt, which is what we will argue for here.

Klasner and Schulz (1982) presented evidence that the Kapuskasing shear zone in Ontario, which crosscuts the Archean Wawa (Abitibi) and Quetico-Omanica terranes from James Bay to eastern Lake Superior, is a positive Bouguer gravity anomaly that is continuous with the main trace of the Proterozoic Keweenaw rift, also known as the midcontinent gravity high (Chase and Gilmer, 1973). The terranes of this Archean crust were in place by ~ 2.6 Ga, followed by cooling and modest erosion to establish the Superior Province as a craton by ~ 2.5 Ga. Rifting along its southern margin formed the Huronian basin (2.5-2.45 Ga; see Craddock et al. 2013a), and was followed by the emplacement into the craton of the radiating 2.4 Ga Matachewan dyke swarm (Halls and Bates 1990, Halls et al. 1994). Subsequent dike intrusion events in the Wawa terrane at 2.22, 2.17, 2.14 and 2.04 Ga mark plume impingement related to distal rifts (Ernst and Buchan, 2001). All of these mafic dike swarms were affected by a variety of fault motions along the Kapuskasing suture including distortion of the Matachewan swarm in the hanging wall of the Kapuskasing uplift by 90 km of dextral transpression before the 1850 Ma Penokean orogeny (Ernst and Halls, 1984; Evan and Halls, 2010). A profile of Ar-Ar, K-Ar and Rb-Sr radiometric ages across the Wawa terrane reveals a history of differential fault-related uplift that ended by ~1.9 Ga

(Easton, 2000; Manson and Halls, 1997; Percival and McGrath, 1986, Percival and West, 1994), and included the formation of pseudotachylite (1940 Ma Ar-Ar age on microlites; Percival, 1981). Seismic profiles across the Kapuskasing suture confirm the presence of a thick-skinned, north-dipping ( $50^\circ$ ) reverse fault (27 km of offset; Ivanhoe Lake fault) that places a  $\sim 10$  km section of granulitic crust ( $V_p > 6.8$  km/s) over greenschist-grade footwall rocks (Percival et al. 2006). The Archean Abitibi crust is locally thickened thickened by 8 km along the Kapuskasing suture and granulite facies hanging wall rocks are replaced toward the north along the fault strike indicating an oblique offset (Percival and McGrath, 1986). The Kapuskasing uplift event has not been dated directly but field and geophysical evidence in eastern Lake Superior suggest that the older Kapuskasing suture was reactivated in the Neoproterozoic and influenced the westward and southward propagation of faults which became the Keweenaw rift (Manson and Halls, 1994, 1997) in a back-arc setting parallel to the Grenville margin. The Keweenaw rift system was localized around a mantle plume with five failed extensional arms (Figure 2; Sutcliffe, 1991) including the Kapsukasing suture along which the Abitibi dikes (1141 Ma; 6 km of offset; Ernst and Buchan, 1993; Queen et al. 1996) and many rift-aged carbonatite and lamprophyre dikes (1141 Ma) were intruded and later deformed (Sage, 1988; Halls and Shaw, 1988; Hanes et al. 1994; Percival and West, 1994) during the Ottawan stage of the Grenville orogen. Craddock et al. (2017) report a Grenville age for a top-to-the-SE granoblastic mylonite (Ottawan; 1102 Ma Ar-Ar on biotite and 1093 Ma on zircon) along the Keweenaw thrust hangingwall near Mellen, WI (Fig. 2) suggesting that Grenville far-field shortening may have dominated the early stages of the Keweenaw system. Hnat et al. (2006) have argued that the curvature of the Keweenaw thrust is a primary plane influenced by propagation of the Kapuskasing suture from the east.

The Midcontinent rift (also Midcontinent Rift System [MRS] and

Keweenaw Rift) was a short-lived, bimodal igneous province (1115–1085 Ma [30 Ma]; Davis and Sutcliffe 1985; Davis and Paces 1990; Heaman and Machado 1992; Paces and Miller 1993; Davis and Green 1997; Zartman et al. 1997; Vervoort et al. 2007) that formed in the back-arc setting of the SW-NE Grenville orogen (~1300–980 Ma), largely parallel to the southeast margin of Laurentia (Donaldson and Irving, 1972; Gordon and Hempton, 1986; Cannon 1992, 1994; Hauser 1996). Heaman et al. (2007) have proposed a 4-stage magmatic history across the region with rift-related igneous rocks spanning 1141–1085 Ma (56 Ma). Gravity (Craddock et al. 1963, 1969; Chandler and Sharp 1991), magnetic (Chandler et al., 1989; NICE, 2006), and seismic (Cannon et al. 1989; Mariano and Hinze, 1994) profiles give the full three-dimensional extent of the rift structure (fig. 1; King and Zietz 1971; Chase and Gilmer 1973). The extensional phase of the rift, dominated initially by mafic rock extrusion, was also the southwestern arm of a failed mantle plume–triple junction that was centered in present-day Lake Superior (Fig. 2), and the bimodal igneous suite (basalt, rhyolite, granophyre, gabbro, etc.; Winchell 1897; Grout et al. 1959; Miller et al. 2002) was immediately buried in 2–3 km of unfossiliferous red clastic sediments of the Oronto and Bayfield Groups (Thwaites 1912; Stauffer 1927; Morey and Ojakangas 1982; Ojakangas and Morey 1982), including the Jacobsville Sandstone on the east side of the Keweenaw thrust (Kalliokoski, 1982). Craddock et al. (2013) evaluated the detrital zircon populations of the rift clastic sediments and report no significant changes to the unfossiliferous rift stratigraphy, including the duration of the unconformity between the rift section and the overlying middle Cambrian Mt. Simon and Munising Formation sandstones (Webers, 1972). The youngest detrital zircons in the basal Jacobsville Sandstone, from a structurally high location in the middle of the basin at Little Presque Isle, are 933 and 996 Ma; Malone et al. (2016) now report a maximum depositional age for the Jacobsville of 959 Ma based on analysis of 2080 detrital zircons. The rift shortened, by thrusting on pre-existing rift-margin normal faults, shortly after filling with

clastic debris (Bornhorst et al. 1987; Cannon, 1993; Stein et al. 2015; see also Craddock et al. 2017). The bounding reverse (thrust) faults are the Douglas-Isle Royale-Michipicoten (north side, S or SE dip) and the Keweenaw-Lake Owen-Hastings (S and E side, NW dip) faults. The Midcontinent rift crosscuts the Minnesota River Valley (MRV; Southwick and Chandler 1996; Bickford et al. 2006; Schmitz et al. 2006) and the Wawa, Quetico, and Wabigoon terranes of the Archean Superior province (Van Schmus 1976, 1980; Card 1990; Percival et al. 2006).

The Jacobsville Sandstone and older Keweenaw rift igneous rocks are folded and offset by thrust faults within, and south of, the Kapuskasing suture zone east of Lake Superior leading Manson and Halls (1994, 1997) to propose that the Kapuskasing faults continue to the west and connect with the Keweenaw thrust in Michigan (Figure 2). Here, the rift-aged Portage Lake volcanics are thrust over the Jacobsville Sandstone and Ordovician-Devonian limestones are deformed in the footwall requiring a midcontinental orogenic event in the late Paleozoic (Hamblin, 1958, 1961; Craddock et al. 1993).

## Methods

### *Calcite Twin Analysis*

The calcite strain-gage technique (CSGT) of Groshong (1972) allows investigation of intraplate stresses as constrained by intracrystalline twinning of rock-forming calcite grains. Although the result is actually a strain tensor, a similar orientation of the stress tensor appears likely in case of coaxial deformation (Turner, 1953, 1962). The CSGT has been used to constrain strain tensor directions in veins (Kilsdonk and Wiltschko, 1988; Paulsen et al. 2014), limestones (Engelder, 1979; Spang and Groshong, 1981; Wiltschko et al., 1985; Craddock and van der Pluijm, 1988; Mosar, 1989; Ferrill, 1991; Craddock et al., 2000), marble (Craddock et al., 1991; Craddock and Craddock, 2012),

amygdaloidal basalts (Craddock and Pearson, 1994; Craddock et al., 1997, 2004) and lamprophyres (Craddock et al., 2007b).

Under temperatures of ca. 200 °C intracrystalline deformation of calcite results in the formation of e-twins. The formation of calcite e-twins requires a shear stress exceeding ca. 10 MPa (Wenk et al., 1987; Burkhard, 1993; Lacombe and Laurent, 1996; Ferrill, 1998). Calcite offers three glide systems for e-twinning. From U-stage measurements of width, frequency and orientation of twins, and the crystallographic orientation of the host crystals, a strain tensor can be calculated using a least-squares technique (Groshong, 1972). In order to remove “noise” from the dataset, a refinement of the calculated strain tensor can be achieved by stripping 20% twins with highest deviations (Groshong et al., 1984a). This procedure has been used if the number of measured grains were large ( $n > 20$ ). In cases where the data appear to be inhomogeneous, the separation of incompatible twins (“NEV”=negative expected values) from compatible twins (“POS”=positive expected values) of the initial dataset allows separate calculation of two or more least-squares deviatoric strain tensors. Thus, the CSGT can be used to obtain information on superimposed deformations (Groshong, 1972; 1974) and differential stress magnitudes (Rowe and Rutter, 1990).

The validity of this stripping procedure was demonstrated in experimental tests where the reliability depends on the overall complexity of deformation and the number of grains with twins (Groshong, 1974; Teufel, 1980). The stripping procedure was used in cases of high proportions of NEV and a large number of measured grains. An experimental re-evaluation of the CSGT has shown that measurements of about 50 grains on one thin-section or 25 grains on two mutually perpendicular thin-sections yield the best results (Groshong et al., 1984; Evans and Groshong, 1994; Ferrill et al., 2004). The chance to extract the records of more than two deformations from one dataset is limited when dealing

with natural rocks (Burkhard, 1993). Individual analyses of veins, matrix, nodules, etc. allows the acquisition of several strain tensors without applying statistical data stripping. The complexity of rotational strains in fault zones has limited the application of this method to the efforts of Gray et al. (2005). Application of the CSGT requires the following assumptions to be valid: (1) low temperatures (dominance of Type I and Type II twins), (2) random c-axis orientations of calcite, (3) homogenous strain, (4) coaxial deformation, (5) volume constancy, (6) low porosity materials and (7) low strain (<15%). If these conditions are not fully met, the underlying dataset of the calculated strain tensor could be biased, modified or random. Strain tensors were calculated from calcite e-twin datasets using the software package of Evans and Groshong (1994).

#### *Stable Isotope Geochemistry*

Stable isotopes were analyzed at the University of Michigan stable isotope laboratory. Carbonate samples weighing a minimum of 10 micrograms are placed in stainless steel boats. Samples are then placed in individual borosilicate reaction vessels and reacted at  $77^{\circ} \pm 1^{\circ}\text{C}$  with 4 drops of anhydrous phosphoric acid for 8 minutes (a total of 12 minutes for dolomites, 17 minutes for apatite, and 22 minutes for siderites) in a Finnigan MAT Kiel IV preparation device coupled directly to the inlet of a Finnigan MAT 253 triple collector isotope ratio mass spectrometer.  $\text{O}^{17}$  corrected data are corrected for acid fractionation and source mixing by calibration to a best-fit regression line defined by two NBS standards, NBS 18 and NBS 19. Data are reported in ‰ notation relative to VPDB.

Precision and accuracy of data are monitored through daily analysis of a variety of powdered carbonate standards. At least four standards are reacted and analyzed daily. Measured precision is maintained at better than 0.1 ‰ for both carbon and oxygen isotope compositions.

#### *Microprobe Analyses*

Analyses were performed on a JEOL JXA-8200 electron microprobe equipped with 5 wavelength-dispersive spectrometers, and a JEOL (e2v / Gresham) silicon-drift energy-dispersive spectrometer at Washington University. Analyses were acquired using either the Probe for EPMA or JEOL analysis software, and x-ray correction was performed using the CITZAF correction software. Typical operating conditions were 15 KV accelerating potential and 25 nA probe current, but conditions appropriate for analysis of special materials warrant other values. Standards used in the facility ranged from pure elements and oxides to simple or complex silicates and glasses recognized throughout the analytical community. A wide range of standards appropriate to specific analytical problems were used.

#### *U-Pb Geochronology*

We analyzed igneous zircons (n=5) from the Lincoln folds, New Mexico using LA-ICPMS at the Laserchron lab at the University of Arizona. Methods are posted on their webpage.

#### *Seismic Investigations*

We use earthquake data collected by the Earthscope Transportable Array to calculate receiver functions for stations across the region and from these generate Common Conversion Point (CCP) stacks. These new cross sectional images of seismic impedance contrasts across the KKF system provide insight into crustal scale structures. This analysis was limited by the sparsity of seismic stations where the fault crosses through Ontario, Canada.

## **Results**

We present a collage of evidence to support the hypothesis that the Kapuskasing-Keweenaw fault system was active in the late Paleozoic in response to far-field orogenic stresses propagated to the North American midcontinent by

the amalgamation of Pangea. Nine field areas are included here, presented from northeast to southwest, between James Bay, Ontario, eastern Lake Superior, Michigan's upper peninsula, Wisconsin, Minnesota, Iowa, Indiana, central Illinois, the Lincoln folds of central New Mexico, and the Sacramento Mountains of south central New Mexico, USA (Figs. 1 and 2, Appendix 1). We also present a collection of supporting field sites on either side of the fault system that are examples of footwall deformation related to the inverted motion on this fault system (Figures 3-16). Calcite twinning results are in Table 1 and Appendices 1 and 2, stable isotopes (O,C) in Table 2, microtektite geochemistry and conodont results for Limestone Mountain in Tables 3 and 4, respectively, and U-Pb results for an intrusion in the Lincoln folds, NM in Table 5.

#### *Moose River Basin, James Bay*

To the northwest of James Bay, Ordovician-Devonian marine sediments are poorly exposed over a wide area as part of the Moose River basin (Fig. 2). Flat-lying Cretaceous and Quaternary sediments unconformably overlie the Paleozoic section. Dips of 35° are reported in the Paleozoic section (Thurston, 1977), and one anticline (330° trend with 20° limb dips) is reported near Moose Junction, 30 km from the Kapuskasing suture to the southeast (Ontario Geological Survey, 1967). The Devonian section includes potential economic gypsum deposits, perhaps from Mt. Gypsum, also near Moose Junction (Bezys, 1990). Devonian marine sediments both overlie and are cross-cut (with a 15° NW dip) by the Kapuskasing suture (Stott, 2008). Calcite is mechanically twinned in Devonian limestones near Moosonee, Ontario with a layer-parallel shortening strain oriented N10°W (Craddock et al. 1993; see Discussion) requiring a post-Devonian deformation. Devonian carbonate xenoliths are found in the region in younger kimberlite pipes (McCracken et al. 2000).

#### *Kapuskasing Shear Zone & Island Lake Fault*

The Kapuskasing shear zone (KSZ) includes many faults that strike ~E-W at the eastern end of Lake Superior between Batchawana Bay and Mamainse Point north to the Montreal River (~50 km). The Mamainse Point and Montreal River thrusts narrow and become a single fault plane with a northerly strike near James Bay (Fig. 2). Rift-aged carbonatites are also common forming a belt that runs parallel to the KSZ (Sage, 1988) and the Abitibi mafic dike swarm (Ernst and Buchan, 1993; Fig. 2). In eastern Lake Superior most of the faults have steep dips to the north or south and reverse fault offsets that commonly include folded (isoclinal in places) and overturned Jacobsville Sandstone, the youngest rift-aged sediment (Craddock et al. 2007b, 2013; Malone et al. 2016).

To the southeast of Batchawana Bay, Bennett (2006, Site 2.1) reports a reactivated fault that juxtaposes Archean Wawa terrane rocks and a rift-aged rhyolite. The Island Lake fault strikes N-S and preserves sinistral synfaulting calcite slickenfibers with a small offset. The twinned calcite, from 10 thin sections throughout the sample (n=236; horizontal planes A-E in Fig. 3), record a sub-horizontal shortening strain that is parallel to the fault strike and normal to the trace of the Kapuskasing suture (Fig. 3; Table 1). Normal data cleaning resulted in eliminating 37 of the 236 grains (15%) leaving a PEV analysis (n=199) with a robust result. We chose to analyze the strain overprint (n=37) and the sinistral calcite fault gouge also records a steep westerly shortening strain overprint. Stable isotopes (O, C) suggest the synfaulting calcite precipitated from metamorphic fluids (Table 2). The strike-slip faulting and twinning is younger than the rift-aged rhyolite.

#### *Mamainse Point & Batchawana Bay Thrusts*

Manson and Halls (1994, 1997) report mapping and geophysical data that supports the trace of the Keweenaw thrust being continuous to eastern Lake Superior forming part of the Kapuskasing shear zone (KSZ; Percival and Card, 1983; Sage, 1988). In Batchawana Bay, the Jacobsville Sandstone is folded (E-W

anticlines and synclines, shallow plunges) and is locally vertical or overturned where it is in fault contact (E-W, 60°S dips) with Archean and rift-aged rocks (Fig. 4). Synfaulting calcite (n=118) in these reverse faults records NNW-SSE sub-horizontal shortening. Vertical calcite veins that cross-cut the deformed Jacobsville Sandstone at nearby Mamainse Point record the same shortening strain (Table 1). Stable isotope values from the synfaulting calcite and Mamainse veins also suggest a metamorphic fluid source (Table 2). The youngest detrital zircon in the basal Jacobsville Sandstone at Little Presque Isle is 933 Ma (Craddock et al. 2013), so the fault offsets that overturned the Jacobsville and the cross-cutting calcite veins are younger.

#### *Limestone Mountain Klippe*

Approximately 7 km east of the Keweenaw thrust, which places rift-aged Portage Lake Volcanics over sub-vertical Jacobsville Sandstone, is a curious series of outliers in the vicinity of Pelkie, MI, that consist of assemblages of folded Ordovician-Devonian limestone (Figs. 5 and 6; Milstein, 1987). Cannon and Nicholson (2001) have mapped twelve outliers of Paleozoic carbonate resting on Jacobsville Sandstone in Houghton County, Michigan. Three outliers are small outcroppings (no strike and dip data reported), seven outcrops have dips that range from 5°-70° and the two largest are Limestone Mountain and Sherman Hill (quarry, little outcrop remains). The stratigraphy of the klippen does not correlate with the Michigan basin stratigraphy 300 km to the southeast and Ordovician carbonates are in fault contact with the underlying Jacobsville Sandstone, which has a maximum depositional age of 959 Ma (Malone et al., 2016; Fig. 6f).

Limestone Mountain is an upright syncline (N-S trend, no plunge) with Ordovician-Devonian limestones that cover an area of ~10 km<sup>2</sup> that are in fault contact with Jacobsville Sandstone. The Cambrian Munising Fm. sands, found in

the conformable section in the Michigan Basin, are missing between the Jacobsville Sandstone and Ordovician limestones. The Jacobsville Sandstone underlies the region but dips gently west ( $20^\circ$ ) toward the Keweenaw thrust on the west side of Limestone Mountain, and east of Limestone Mountain the Jacobsville is folded ( $\sim$ N-S trends, steep northerly plunges) into chevron shapes which are best seen from the air (Fig. 5d). There are a number of classic exposures of the Keweenaw thrust near Larium, MI where rift basalts are thrust over contorted Jacobsville Sandstone (Fig. 5b; Daniels and Elmore, 1988). Fault offsets are estimated at  $\sim$ 6000 feet, and the overturned folds in the footwall are spectacular. The Paleozoic section at Limestone Mountain, best exposed in a quarry on the southeast side, is also a syncline that is offset internally by a west-dipping thrust fault based on the detailed conodont biostratigraphy. The basal section in the quarry contains 30 meters of upright middle-late Ordovician conodonts (faunal zones 10 and 11; *Plectodina furcata*, *Belodina compressa* and *Periodon grandis*) that are overlain by older Ordovician carbonates (faunal zones 7 and 8; *Plectonida aculeate*; Fig. 6b and c). Gastropods from Limestone Mountain are *Maclurites sp.*, and likely *Hormotoma sp. cf. H. trentonensis*. The latter has been illustrated from the Chandler Falls Formation from the upper peninsula of Michigan classifying this unit as part of the Middle Ordovician (Darwillian Stage) with closest equivalents in this area being the upper part of the Galena Group with a similar large species known from northeast Iowa. Small, partial fragments of probable Pennsylvanian conodonts were identified, a regional phenomena common in Paleozoic carbonates with active karst processes (Day, 1990; Day et al. 1996, 2008). Farther north, on the west side of Limestone Mountain, an upright 15 meter section of Silurian Lime Island Dolomite and 20 meters of Devonian Erian Fm. carbonates are present in the hinge of the syncline. Dissolution of the carbonate material for conodonts also revealed the presence, in faunal zone 10, of a population of glassy microtektites  $\sim$ 50 microns in diameter (Fig. 6c). Microprobe analysis of these glassy spheres revealed a deficiency of Al

(1.3%) and enrichment of Na (15.3%) relative to Si (73%; Table 3; see Shaller et al. 2016). Translucent spheres in dissolved carbonate residues can be microtektites or aeolian zircons (Malone et al. 2017).

Nearby Sherman Hill is composed of Ordovician limestones and is folded into a gentle, upright syncline (25° limb dips) with the underlying Jacobsville sands (60° dips) thrust upward along the fault contact without the Cambrian Munising sands (Fig. 6e). The Sherman Hill section of middle Ordovician carbonates contains *Periodon grandis*, *Belondina compressa*, *Plectodina furcata* and *Penderodus* sp. conodonts, and is thus assigned to conodont faunal zone 9. All the conodonts recovered are yellow and show no signs of thermal alteration.

The carbonates at Limestone Mountain and Sherman Hill both preserve layer-parallel calcite twin shortening strains with the shortening axes oriented parallel to the regional Appalachian transport direction (SE-NW; Fig. 5d). This deformation is related to far-field stresses that twinned the calcite, reactivated the nearby Keweenaw thrust (Hamblin, 1958, 1961), thereby folding the footwall Jacobsville Sandstone and Paleozoic carbonates as the region was overthrust from the northwest by the Keweenaw thrust hangingwall (Fig. 6a). A NW-SE palinspastic reconstruction has a few end-member choices constrained by the 12 km distance between the Keweenaw thrust and carbonate outliers. If the carbonate outliers were originally in the Keweenaw hangingwall a displacement of 12 km is required, plus the displacement on the thrust. If the outliers were in the footwall, 12 km of thrust offset is required plus the distance of thrusting over the footwall to deform the outliers. If carbonate outliers were in the Keweenaw hangingwall (no eroded away), options 1 and 2 could be additive and we need to include deformation in the footwall Jacobsville and perhaps, the allochthonous Silver Mountain inlier for a total offset approaching 30 km. These curious carbonate outliers, 300 km northwest from the nearest Paleozoic strata in the

Michigan basin, are klippe rather than related to an astrobleme impact (Milstein, 1987), kimberlite collapse (Cannon and Mudrey, 1981) or a kimberlite eruption (Craddock et al. 2009; Malone et al. 2014). There are no breccia pipes or shatter cones, and the microtektites (faunal zone 10) are debris from an Ordovician impact that hit ~200 million years before post-Devonian thrust deformation of the region.

#### *Keweenaw Thrust*

The Keweenaw thrust is observed as a <100 m scarp from Copper Harbor, MI southwestward to near Mellen, WI where the topography becomes subtle and swampy. Along the thrust, the Portage Lake Volcanics, often copper-bearing, are in fault contact with Jacobsville Sandstone which overlies Archean Wawa terrane crystalline rocks and Proterozoic Animikie Basin sediments (Morey et al. 1982). There are synthetic thrust faults that offset crystalline rocks, like the Marenisco fault (Cannon and Nicholson, 2001), along which undated pseudotachylite was generated (Bjornerud, 2010; see also Craddock et al. 2017). Just north of Hurley, WI the Keweenaw thrust places rift volcanics over Proterozoic Tyler Fm. (Craddock et al., 2013b), and both units have the same orientation (75°, 70°N) and younging direction (north). Argillites in the footwall Tyler Fm. have a well-developed cleavage (75°, 58°N) that is difficult to explain as a Penokean orogeny axial-planar cleavage (Atwater, 1938; Schmidt and Hubbard, 1972; LaBerge et al. 1991; Klasner et al., 1991) but likely formed by reactivation of the Keweenaw thrust. This same rift-parallel, sub-vertical undated cleavage is found directly to the west in the Douglas thrust footwall near Duluth (Foster and Hudleston, 1986).

#### *Midcontinent Footwall Mesostructures*

Fault scarps (50-100 m) along the Keweenaw and Douglas thrusts in northern Wisconsin and Michigan, and offsets of Cambrian-Devonian sediments, suggest late Paleozoic fault offsets. Additional field observations suggest that

deformation in the footwall of the Kapuskasing-Keweenaw fault system is fairly common on both sides of the inverted rift up to 200 km from the fault boundary. We present four areas on the northwest side of the structure in the footwall of the Douglas-Isle Royale thrust (NE strike, SE dip) in Minnesota and Wisconsin (Figure 2) and six sites in the footwall of the Keweenaw-Lake Owen-Hastings thrust (NE strike, NW dip) in Wisconsin and Minnesota (Figures 7-9). The NICE (2007) tectonic terrane map provides a base for understanding these local structures; rift-aged rocks are exposed along the St. Croix river at Taylors Falls, MN and are everywhere buried by Paleozoic and younger sediments to the south (Fig. 7). Aeromagnetic maps aid in interpreting plunging folds in, and along, the rift margin (Figs. 8a, 9d).

#### *Douglas Thrust Footwall*

Thirty miles west of Grand Marais, MN, near the west end of Gunflint Lake, is a fault contact (E-W, 40°S dip) that thrusts Proterozoic Gunflint Fm. and rift-aged Logan Intrusions (gabbro) over Archean Saganaga tonalite (Jirsa, 2011). The fault is post-rift with a displacement of ~10 km and is in an odd orientation. Just west of Grand Marais, MN is a spectacular exposure of a rift-aged interflow sediment (Jirsa, 1984) overlain by a basalt flow. The basalt flow is in depositional contact with a younger rhyolite flow and this contact has been reactivated as a thrust fault (N80°W, 38°S) with stepped striations in the fault plane and fault drag joints indicating top-to-the-north fault motion (Fig. 7a). The Cutface Creek interflow sediment contains largely rift-aged detrital zircons (Craddock et al. 2013). Farther south, the Silver Creek Cliff tunnel was created along Highway 61 in 1994 and exposed a section of gabbro thrust over a series of disharmonic flow folds in rhyolite. The fault zone (110°, 37°S) is a 1 meter thick calcite-supported fault gouge with top-to-the-northeast kinematics. The matrix calcite is twinned and preserves a layer-parallel shortening strain parallel to the fault's dip direction (Figs. 8c, d; Table 1; high <sup>204</sup>Pb levels prevented acquisition of a U-Pb

calcite crystallization age). Bardon Peak is southwest of Duluth, MN and is part of the Duluth Gabbro (1076 Ma) complex. The gabbro preserves an undated penetrative, regularly spaced cleavage that is rift-parallel over an area of 30 km<sup>2</sup> (SW-NE strike, vertical dip; Foster and Hudleston, 1986). Bardon Peak also provides a vista of the southeast-dipping Douglas thrust scarp to the southeast which places rift-aged basalts over the Hinckley, Fon du Lac, or Bayfield Group sandstones (Craddock et al. 2013b). This contact is best observed at Amnicon and Pattison state parks. (Fig. 8).

#### *Keweenaw Thrust Footwall*

On the east side of the Keweenaw thrust, in the vicinity of Hudson, WI, and including Willow River State Park (Dott and Attig, 2004), one can observe the subtle differences in lower Paleozoic stratigraphic fault offset and dip. Paleozoic sediments within the Keweenaw rift form the Twin Cities (Forest Lake) basin (SW-NE trend, no plunge) across this structure one traverses the Afton anticline (SW-NE trend, no plunge; Thiel and Schwartz, 1941; St. Croix horst of Craddock, 1972 and Morey, 2001), then the Keweenaw (Hastings) thrust, which caused the footwall River Falls syncline (SW-NE trend, no plunge) with southeast dips of 35° in the Ordovician section. The hanging wall rift-aged Chegwatana volcanics (Wirth et al., 1997) also dip west (7-15°) and flow-parallel quartz-calcite fillings preserve top-to-the-east thrust offsets (Fig. 9a; Leslie et al., 1994). Winchell and Upham (1884) first mapped the Cottage Grove fault along the railroad cuts on the northeast side of the Mississippi river where the Cambrian Jordan Sandstone and Ordovician Prairie du Chien Limestone are in fault contact. The reverse fault strikes NE-SW, has a fault breccia zone and an offset of ~10 meters (Fig. 9b; Matsch, 1962). The Red Wing fault at Barn Bluff, Red Wing, MN juxtaposes older Cambrian Franconia Sandstone against Jordan Sandstone in a nearly-vertical reverse fault. The fault strikes ~NE-SW and, to accommodate the stratigraphic offset, must dip west and become listric at depth.

The thrust offset is on the order of tens of meters and, again, is parallel to the Keweenaw thrust nearby (Fig. 9c). Just northwest of the berg of Pepin, WI is a quarry in the Ordovician Prairie du Chien Fm. with SW-NE trending folds that are locally harmonic and in the footwall of a thrust fault that strikes N30°E and dips west (Fig. 9d; Cordua, 1985; French et al., 2004). Houston, MN, in the southeasternmost corner of the state, contains a small, overgrown roadcut of Cambrian Franconia Fm. sandstones and shaly limestones offset by an east-dipping thrust fault. The fault strikes N35°E and dips to the southeast with a 3 meter offset, strike-parallel folds, and top-to-the-northwest striations (Fig. 9e). Denzer, WI is on the southside of the Proterozoic Baraboo syncline deformed by the Mazatzal orogeny (1.63 Ga; Medaris et al., 2003; see also Craddock and McKiernan, 2007). There is a beautifully exposed angular unconformity of middle Cambrian sandstones around the synclinal topographic high and, near Denzer, on the southern margin, there are some folded structures (N25°E, no plunge) in the Cambro-Ordovician section which are parallel to the Keweenaw thrust boundary (Fig. 9f). Additional folds of similar geometry and orientation are found along Highway 12 to the south and in the parking lot behind the Post Office in Middleton, WI.

#### *Twinning Strains, Iowa*

Mississippian limestones were collected along a SE-NW traverse across northern Iowa. Seven samples were collected, and 3 were suitable for twinning study. The layer-parallel shortening strain is oriented ~170° and the strain magnitudes are all <1% (Fig. 10, Table 1). Five active quarries in Pennsylvanian cyclothem were visited in southwest Iowa resulting in 2 strain analyses that are similar to the Mississippian results. Both sample suites cross the Keweenaw rift structure in the subsurface and there is no strain overprint (low NEVs); reverse fault offsets of 500-750 ft. are reported along the Keweenaw fault based on offsets

in the Mississippian-Pennsylvanian section in active quarries (R. Anderson and G. Schildberg, personal comm., 2015).

#### *LaSalle Anticline, Illinois Basin*

The foreland of east-central North America is a patchwork of low amplitude, long wavelength basins and domes that seem to have been present since the mid-Cambrian (see Quinlan and Beaumont, 1984). Superimposed on these regional structures are a host of local, 2<sup>nd</sup> order features including the N-S trending LaSalle anticline in the central Illinois basin where Cambrian-Pennsylvanian sediments are folded (Nelson et al. 1996; McBride and Nelson, 1999; Figure 11). The LaSalle anticline has limb dips of 5° on the east and 30° on the west (Nelson et al. 1996; Shields et al., 2005). Four calcite strain results, two for the Pennsylvanian McLeansboro Group and two from the Ordovician Platteville Formation, preserve a layer-parallel shortening strain. The Platteville preserves a shortening strain normal to the fold axis whereas the McLeansboro records a shortening strain parallel to the fold axis (340°; Fig. 11). Differential stress and strain magnitudes are modest and there is no strain overprint (Table 1).

#### *Twinning Strains, Indiana*

Mississippian limestones (n=8) were collected from limestones from an outcrop belt (e.g. Dodd et al., 1993) between Leavenworth and Crawfordsville, IN (~200 km). Four twinning strains record a layer-parallel shortening strain oriented ~160°, normal to the inferred thrust transport direction of the Appalachian belt to the south. One sample has a 20° shortening axis plunge to the south, somewhat anomalous within the greater data set where shortening axis plunges are 2-5° (Fig. 10, Table 1).

#### *Lincoln Folds, New Mexico*

Harmonic folds are exposed in the Permian Yeso Fm. with ~flat-lying Permian carbonates above and below over an area of 9000 km<sup>2</sup>. Folds are oriented ~SW-NE with shallow plunges and are periodically cored by gypsum along a detachment surface that dips 1° to the southeast (Craddock, 1960, 1964; Fig. 12). Fold wavelength and amplitude decrease to the northwest, away from the Marathon belt, and fold vergence is generally to the northwest similar to the evaporate-cored footwall folds described in the Appalachian foreland by Wiltschko and Chapple (1977). The Lincoln folds are proximal to the Marathon belt (south; 300 km) and the Ancestral Rockies orogeny (west; 150 km). Quartz monzonite sills and dikes cross-cut the folds and are dated at 47.7 Ma (Fig. 12; Table 5) thereby bracketing fold formation between the Permian and Eocene. We also report xenocrystic zircons of Proterozoic age. Much of the Yeso Formation is a micritic limestone but we did measure calcite twinning strains in 3 limestones and 6 calcite veins (Fig. 13); sub-horizontal shortening is common and seven of nine shortening axes are ~parallel to the Lincoln fold axes and the other 2 strain results record shortening normal to fold axes. Strain magnitudes are modest, differential stress magnitudes are common for a foreland setting and there is no strain overprint (low NEVs; Table 1).

#### *Sacramento Mountains, N. Mexico*

A complete, flat-lying Ordovician-Permian stratigraphic section is exposed in the Sacramento Mountains in southcentral New Mexico, accessed at Oliver Lee State Park (Pray 1961; Scholle, 2003; Fig. 14). Most of the section is marine carbonate and is an ideal setting to study changes in the stress-strain history, as recorded by mechanically twinned calcite, through a continuous horizontal section representing ~400 Ma. This 2700 m section was also in proximity to the southwest margin of North America in the Paleozoic, including deformation associated with the Pennsylvanian Ancestral Rockies orogen (Kluth, 1986) and the Permian Marathon fold belt (Hickman et al., 2009).

The Ordovician-Mississippian section is flat-lying and a layer-parallel shortening strain is preserved and oriented N-S in limestones and a calcite vein. The overlying Pennsylvanian carbonates are deformed (Bedding: N20°W, 45°W) and record a layer-parallel shortening strain oriented SW-NE as part of the Ancestral Rockies deformation (Kluth and Coney, 1981; Marshak et al., 2000). The uppermost Pennsylvanian and Permian limestones are flat-lying and, again, preserve a layer-parallel shortening strain with a N-S orientation (Fig. 15, Table 1). There is no twinning strain overprint.

### *Seismic Interpretations*

We focus our seismic observations on two receiver function cross sections across the midcontinent rift. These cross-sections highlight large-scale crustal structure across the midcontinent rift and correlate well with previous active-source seismic data in the region (Fig. 16). The northeastern cross-section (A-A') extends across the western edge of Lake Superior. Crustal thicknesses in this cross section are ~40 km with only minor variation across the rift. The amplitude of the crustal Ps conversion shows significant variation across the rift, likely indicative of a change in velocity contrast at the Moho. The weak Ps conversion beneath the rift is indicative of a minor change in velocity at the Moho, while the higher amplitude conversions adjacent to the rift are likely indicative of a stronger velocity contrast. The weak conversion across the rift is likely indicative of fast lower crustal or slow upper mantle velocities. This interpretation is supported by the presence of a positive conversion at 30 km depth, which likely represents the top of this high velocity lower crust. The southern cross-section (B-B') extends across the midcontinent rift in southern Iowa. Within this cross-section crustal thickness increases slightly beneath the rift. Similar to the previous cross sections, the Moho conversion has a weak amplitude beneath the rift, and there is a positive conversion present in the mid-crust. This mid-crustal conversion likely represents the top of this high velocity lower crustal layer or

the boundary between rift volcanic and sediments deposits and crystalline basement. Within this cross-section there is also a negative conversion present in the upper-crust which may reflect sedimentation into the rift. These results are similar to the active source results of Cannon et al. (1989), which show a thick sedimentary layer beneath the rift underlain by volcanics, and crystalline basement. However, the active source results do not provide evidence for a high-velocity lower crust beneath the rift. Shen et al. (2013) use a joint receiver function/ambient noise tomography surface wave inversion to examine the structure of the Earth, these results also highlight thickened crust along the rift adjacent to these cross sections and the presence of a weak velocity contrast at the base of the crust in the region.

### Discussion

The North American midcontinent presents a unique opportunity to observe thick-skinned foreland deformation associated with thin-skinned accretion of the Appalachian-Ouachita-Marathon orogen. First order deformation is in the form of small amplitude, long wavelength basins and arches (Howell and van der Pluijm, 1990) superimposed on Precambrian crystalline basement (Whitmeyer and Karlstrom, 2007) with localized small-offset normal faults (Pinet et al. 2013; Pinet, 2016). Second order deformation includes outcrop-scale faults, folds, cleavages, magnetic fabrics, MVT deposits and microstructures (e.g., twinned calcite). Craddock and van der Pluijm (1989) and Craddock et al. (1993) reported a layer-parallel shortening strain fabric, as recorded by mechanical twins in Paleozoic limestone calcite, up to 2000 km inboard of the AOM thrust front. The AOM strain fabric is unique when compared to the older Keweenaw (calcite amygdules, veins cements; see also, Craddock et al. 1997) and Grenville (marble; see also Craddock et al. 2017) twinning strains, and there is no strain overprint in the calcite of the older terranes. The AOM foreland data also included three layer-parallel shortening

strains results that are inconsistent (~E-W shortening in samples 9, 10 and 47 in Craddock et al. 1993) with the regional AOM thrust transport-parallel fabric. This study was initiated by those three anomalous strain results, gaps in the foreland strain dataset (Iowa, Indiana, Illinois, New Mexico), field observations of late Paleozoic deformation near the KKF (Figures 3-12) and the realization that the Pennsylvanian Ancestral Rockies orogen on the western margin of North America could have influenced deformation in the midcontinent (McBride and Nelson, 1999; Marshak et al. 2000) including the inversion of the Kapuskasing-Keweenaw fault.

The Archean Superior province formed by accretion from the southeast between ~2.7 to 2.6 Ga with north-dipping subduction (Card, 1990). Following ~200 Ma of quiescence and erosion, the Huron Supergroup (2.4-2.2 Ga) and Animikie Group (2.2-1.8 Ga; Craddock et al. 2013a) were deposited and both basins were deformed by the Penokean orogen (1.85 Ga; Schulz and Cannon, 2007). Penokean accretion was along the continent's southeast margin, followed by accretion of the Yavapai, Mazatzal and Central Plains crust (Hoffman, 1988; Whitmeyer and Karlstrom, 2007). The Kapuskasing suture crosscuts the Superior province terranes at an acute angle and has a long, complex displacement history (Wilson, 1968, Watson, 1980; Goodings and Brookfield, 1992; Burke and Dewey, 1973; Thurston et al., 1977) and is an anomaly within stable Archean cratons (Percival, 2004, 2006). The Superior province contains two other anomalous suture zones, the Trans-Superior suture (50 km offset; Manson and Halls, 1994) and the Quetico fault in northern Minnesota. The Quetico fault has ~50 km of dextral motion that crosscuts the Wabigoon, Quetico and Wawa terranes but does not offset the 2.1 Ga Marathon LIP (Kenora-Kabetogama) dikes so it was a short-lived Archean fault (Chandler, 1991). The Kapuskasing suture was presumed to terminate along the southern Wawa (Abitibi) boundary with the Minnesota River valley (MRV) terrane somewhere in eastern Lake Superior with

its last motion being related to Penokean accretion (1.9 Ga pseudotachylite; Percival and Card, 1983). As the Grenville (1300-980 Ma) orogen evolved, the Kapuskasing suture, which is ~parallel to the Grenville front (Carr et al., 1991) and 300 km inboard, became one of the 5 arms radiating from the Keweenaw hotspot (Sutcliffe, 1991; 1100-1060 Ma) and rift-aged mafic dikes and carbonatites are common within the KKF (Sage, 1988; Ernst and Buchan, 1993). The tectonic connection of the Grenville terrane collisions and evolution of the short-lived igneous phase of the rift in a back-arc setting is a controversial topic (Cannon, 1994; Stein et al. 2011; Craddock and Craddock, 2012; Merino et al., 2013; Stein et al. 2014; Malone et al., 2016). Manson and Halls (1994, 1997) make a compelling argument that the Kapuskasing suture propagated to the west and south, and the Kapuskasing-Keweenaw fault became a single inverted fault boundary 4000 km in length that is parallel to the Grenville and younger Appalachian orogens (Figure 1) and may be related to lateral viscosity gradients in the low-velocity layer at the base of the lithosphere (Doglioni and Panza, 2015). The Jacobsville Sandstone (Figure 2) is a synorogenic deposit deformed in the hanging and footwalls of the Kapuskasing-Keweenaw thrust, a fault displacement that includes deformation of the Paleozoic section.

The Keweenaw and Douglas thrusts have the best-preserved fault scarps which may correlate with the greatest fault offsets along the KKF system (see below). The youngest rocks offset along the KKF are the Ordovician-Devonian Limestone Mtn. and Sherman Hill Paleozoic outliers near Pelkie, MI and these sediments are in fault contact (65° dip) with the underlying Jacobsville Sandstone. We interpret these two synclines to be the result of motion of the nearby KKF in the late Paleozoic and that the folds are footwall structures and are allochthonous. The KKF structure includes periclinal anticlines and synclines along its length bounded on the northwest by a southeast-dipping thrust and on the southeast by a northwest-dipping thrust, structures best seen with magnetic data (Figs. 7-9).

Other, structurally related footwall deformation (Figures 3-15) show a variety of contractional features <200 km from the KKF system; the KKF foreland is then the area between the NE-striking KKF and the NE-striking Appalachian thrust (e.g., Pine Mountain) front. Three small-offset thrust faults are also reported within the Keweenaw North Shore volcanic suite in Minnesota and these north-vergent thrusts are interpreted to be the response of Ouachita convergence in the Douglas thrust footwall (Figures 7, 8).

The Transcontinental Arch (TCA) is another structural feature that is present in the North American midcontinent, specifically from Thunder Bay, Ontario to Tucson, AZ (Carlson, 1999), throughout the Paleozoic. The arch influenced sedimentation, both the environments of deposition and sediment thickness, and could be interpreted as a footwall anticline northwest of, and parallel to, the KKF structure. The Transcontinental Arch could be a positive crustal flexure formed late in the Grenville-rift (Ottawan) orogen, later reactivated by shortening associated with the AOM thrusting, or both. Seismic velocity studies at 6 km depth (sedimentary cover removed) support the presence of a remnant of the Transcontinental Arch including the alternating highs and sags along strike (Fig. 17). The TCA-KKF highland in the late Paleozoic influenced Pennsylvanian sedimentation (deposition east of the high) and Permian (sedimentation west of the high; Figure 18). Detrital zircons in the Pennsylvanian of the Forest City and Illinois basins suggest a zircon supply from the east in the Appalachian and Grenville Mountains with some, but little sediment traversing the sags in the TCA to deliver sediment in the west.

All the AOM twinning data is compiled in Figure 19 (see Appendices 1 and 2) and the result presented by Craddock and van der Pluijm (1989) and Craddock et al. (1993) is complimented with a few second order observations. The layer-parallel shortening fabric ( $-\epsilon_1$ ) is consistently parallel to the inferred

thrust transport direction regardless of location along the curved AOM thrust belt (Hnat and van der Pluijm, 2001; Ong and van der Pluijm, 2007). For this fabric, despite a wide variety in limestone ages and grain sizes, there was a remarkably consistent differential stress ( $-30$  MPa) that caused twinning (Table 1) and remarkably few NEVs. We plotted the shortening strain axes for the AOM foreland by the age of the host limestone (Figure 17 a-c) and found a consistent result indicating a uniform stress-strain field existed throughout the Paleozoic of North America. The age of twinning was not necessarily shortly after limestone deposition. We also found layer-parallel shortening strains that are parallel ( $\sim$ E-W) with the anomalous shortening strains reported in Craddock et al. (1993; samples 9, 10, 47) and that these strain orientations are parallel to the thrust transport direction of the Pennsylvanian Ancestral Rockies in New Mexico (Figure 17d). The Sacramento Mountain section preserves three shortening directions: N-S (Ordovician-Mississippian), E-W (Pennsylvanian; Ancestral Rockies orogen) and N-S (Permian; Marathon orogen). The LaSalle anticline in Illinois is particularly anomalous with a fold-axis normal ( $\sim$ E-W) shortening strain in Ordovician limestones and a fold-axis parallel LPS strain in the overlying Pennsylvanian limestones.

Plots of the layer-parallel shortening strain magnitude ( $-\epsilon_1$ ) vs. orogenic distance show high strains in the Appalachian thrust belt that decrease into the foreland (Fig. 20b; van der Pluijm et al. 1997) except in the vicinity of the KKF (Figure 20a). Limestones and calcite veins in the southeast footwall of the KKF record high strain values; for the Batchawana, Mamainse and Island fault suites these metamorphic calcite veins are proximal, or within, the KKF and the shortening strains are parallel to the inferred KKF thrust transport direction and unique when compared to the twinning strains of the Grenville and rift sequences (Craddock et al. 1993, 1997 and Craddock and Craddock, 2012). It is also possible to argue that the high twinning strain values along the KKF are cumulative (co-axial), meaning twinning has occurred more than once with the

stress field in the same orientation (i.e., KKF-Alleghenian *after* Taconic deformation). With this result, shown schematically in Fig. 21, we can define the large region to the southeast of the KKF and northwest of the Appalachian front as a foreland basin between a thick-skinned and thin-skinned thrust belt of the same age. This is a basinal region that contains all the effects of the migration of Permian orogenic fluids (Oliver, 1986; Leach et al. 2010) but did the fluid migrate to the northwest from the Appalachian's or southeast from the KKF, or both (see below)?

The Permian Yeso Formation limestones presented an opportunity to measure calcite strains over a wide area north of the Marathon fold belt. Our reconnaissance of the Lincoln folds resulted in 9 strain results from 32 samples as much of the Yeso is a micrite and not amenable to our strain analysis (Table 1). The Lincoln folds are older than 47.4 Ma (U-Pb age on zircon) as the monzonite cross-cuts the folds. The layer-parallel shortening axes are not normal to the Lincoln fold axes so the twinning strains are older and the folding is post-twinning. The E-W shortening axes in the Lincoln folds could be the result of shortening between the KKF western footwall and the Ancestral Rockies footwall to the west (see samples 11-13, 16 from the Sacramento Mountains) but this requires late Permian deformation. Is the twinning strain fabric related to Marathon shortening (N-S), or Laramide shortening (E-W)??? The opening of the Rio Grande rift and related igneous intrusions have been proposed as a mechanism to induce widespread gravity sliding that shortened the Lincoln folds (Kehle, 1970), thereby creating a landslide that moved to the southeast larger than the volcanically-triggered slides reported in Wyoming by Malone et al. (2014) and Craddock et al. (2015).

*Mississippi Valley-Type Mineralization, K-silicates, and the Timing of Hydrothermal Alteration in the Midcontinent*

The distribution of late Paleozoic MVT deposits and disseminated MVT mineralization is known to occur between the Appalachian-Ouachita front (south and east) and the KKF (north and west; Figure 21). Paleozoic rocks in this region were influenced by multiple fluid flow events that have precipitated various metal sulfide minerals, dolomite (both saddle and planar), fluorite, quartz, sulfates, and other minerals, which are together known as the Mississippi Valley-Type (MVT) mineral assemblage. These minerals are interpreted to have formed by hydrothermal brines that moved from adjacent sedimentary basins via regional sandstone aquifers onto adjacent arches and platforms. Although early work proposed a direct tectonic-related driving mechanism for the movement of the brines (Oliver, 1986), most researchers have settled on topography driven fluid flow as the most reasonable mechanism to move the brines away from the Appalachian-Ouachita front (e.g., Bethke, 1986; Sverjensky, 1986; Garven et al., 1993; Leach et al., 2010). Other fluid flow mechanisms have been proposed for various MVT ore deposits worldwide, including overpressurized gas reservoirs, density reflux, compaction, etc. (Leach et al., 2010). It is recognized that no one mechanism can be applied to explain all MVT deposits and that the flow of ore-bearing fluids was multi-directional.

Evidence for timing of mineralization reveals a complex pattern across the midcontinent, and includes K-Ar or Ar-Ar dates on feldspar and illite, Rb-Sr dates on sphalerite, U-Th-Pb dates on calcite, fission-track ages, paleomagnetic interpretations, and others (Figure 21). Precipitation temperatures of Paleozoic-hosted MVT mineralization and associated minerals are variable due to differences in paleodepth, distance from sedimentary basins and orogenic fronts, and position of the mineral in the paragenetic sequence. In general, however, there is a well-recognized decrease in ore-stage MVT mineral precipitation temperature with distance from the Appalachian-Ouachita orogenic front (e.g.,

Leach and Rowan, 1986) that satisfies data for many deposits, with the exception of the Upper Mississippi Valley (UMV) district in southwestern Wisconsin and some areas nearer to the KKF. This is broadly consistent with decreasing vitrinite reflectance values (e.g., Rowan et al., 2002; East et al., 2012) and conodont alteration indices (e.g., Harris, 1979) that decrease away from the Appalachian-Ouachita front, requiring brief episodic fluid pulses to account for elevated fluid-inclusion temperatures but low organic maturation indices.

Broadly, at least two distinct sets of ages have been reported for U.S. Midcontinent mineral assemblages, but there is evidence of multiple mineralization events in some areas. Diagenetic K-silicate minerals occur throughout the Midcontinent and the central and southern Appalachian region (e.g., Woodard, 1972; Marshall et al., 1986; Hearn et al., 1987; Hay et al., 1988; Duffin, 1989; Duffin et al., 1989; Aleinikoff et al., 1993; Elliott and Aronson, 1993; Girard and Barnes, 1995). Several authors have suggested that at least some of the potassic diagenesis is related to MVT ore deposition (Hearn et al., 1987; Wheeler, 1989; Aleinikoff et al., 1993). Luczaj (2000) recognized that two distinct age signatures for diagenetic K-silicate minerals occur in the region bounded by the KKF and the Appalachian-Ouachita front. A northern province, ranging from southeastern Minnesota through Wisconsin, northern Illinois, and Michigan yields mid-Paleozoic age dates, mainly Devonian to Middle Carboniferous, for potassic diagenetic minerals (Hay et al., 1988; Matthews, 1988; Girard and Barnes, 1995; Liu et al. 2003). A second province, ranging from Oklahoma through Missouri and southern Illinois into the central and southern Appalachians, yields mainly Late Carboniferous and Permian age dates (e.g., Bass and Ferrara, 1969; Rothbard, 1983; Hearn et al., 1987; Wheeler, 1989; Aleinikoff et al., 1993; Elliott and Aronson, 1993). Here, radiometric ages on the MVT ores generally cluster around 270 Ma (e.g., Nakai et al. 1990; Brannon et al. 1992), directly relating the ore fluids to the Alleghenian-Ouachita orogeny. Although mid-Paleozoic ages for

authigenic K-silicates dominate in the UMV region and areas to the north, lesser amounts of Permian K-silicates are also observed (Hay et al., 1988). Additional ages constrained by U-Pb, paleomagnetic and fission-track methods for regions closer to the Appalachian-Ouachita front also yield late Paleozoic to early Mesozoic ages (e.g., Desborough et al., 1985; Bachtadse et al., 1987; Leach et al., 2001).

Several challenges remain with regard to fully understand MVT mineralization events, especially in areas farther from the Appalachian-Ouachita front. These challenges include the following: fluid-inclusion temperatures that exceed those predicted by topography-driven flow models, the brief duration of MVT events on the order of  $10^5$  years (e.g., Rowan et al., 2002) in a topography-driven regime, evidence for fluids penetrating the Precambrian basement, and the lack of a sensible topography-driven mechanism for the Michigan basin's radial fluid flow evidence.

In general, most radiometric age dates on K-silicate minerals from Midcontinent MVT ore deposits seem to match radiometric age dates from ore-stage minerals (e.g., Wheeler, 1989; Brannon et al., 1996; Leach et al., 2001). However, the UMV ore district contains the most obvious discrepancy in the Midcontinent with regard to the age of most of the K-silicate mineralization, which is Devonian-Mississippian in age, and the reported Permian age for the MVT mineralization. If accurate, fluid-inclusion temperatures reported for sphalerite in the UMV up to 120-150°C (McLimans, 1977) are difficult to explain with thin sedimentary cover and steady topography-driven fluid flow systems discharging from the Illinois basin, although Rowan et al. (2002) showed that a brief interval of mineralization could occur with a heat pulse in the southern Illinois region superimposed on a long lived fluid flow system and deep burial. However, fluid-inclusion homogenization temperatures for 360 Ma authigenic K-feldspar reported by Liu (1997) along the Precambrian-Cambrian contact in

northwestern Wisconsin (106°C) are difficult to explain with any existing numerical models for topography-driven flow developed for the region (e.g., Rowan et al., 2002). Broad areas of Wisconsin's Paleozoic section were exposed to hydrothermal fluids of at least 100-115°C in the absence of deep burial (McLimans, 1977; Kutz and Spry, 1989; Liu, 1997; Luczaj, 2006).

Several lines of evidence have emerged recently that suggest Precambrian basement rocks played a substantial role in the origin, fluid flow pathways, and geochemistry of hydrothermal fluids that have passed through the Paleozoic section. These are relevant because fluids from deeper within the crust may have originated in part in the KKF or have been influenced by thermal events centered in the midcontinent rift during the Phanerozoic Era. Luczaj (2006) called for a radially distributed flow pattern out of the Michigan basin during the Paleozoic instead of a flow pattern simply away from the Appalachian-Ouachita front. Subsequent work by Ma et al. (2009) using crustal noble gas signatures in deep brines demonstrates that there was indeed a reactivation of the midcontinent rift system beneath the Michigan basin that was likely responsible for the upward transport of heat and mantle derived gases into the basin via deep-seated faults and fracture zones. A thermal reactivation of the Midcontinent rift system, along with compressional stresses from the KKF might have allowed gas generated within the rift and deeper portions of the Michigan basin to force fluids out of Precambrian rocks, perhaps even radially outward from the Michigan basin, similar to conceptual models used by Cathles (1993), Eisenlohr et al. (1994), and Cathles (1997).

With regard to Paleozoic mineralizing fluids, the KKF might have acted as either a hydrologic-structural buttress, as there are no MVT deposits northwest of the KKF or, as a source of hydrothermal fluids in the late Paleozoic. As a result, mineralizing fluids likely travelled through the Precambrian basement

and along early Paleozoic aquifers, and were eventually forced upward through younger strata during one or more episodes in the Paleozoic in areas distal from the Appalachian-Ouachita front. Petroleum fluid inclusions have been observed in Ordovician-hosted quartz cements from Hudson, Wisconsin near Paleozoic faults related to the midcontinent rift (Luczaj, unpublished data), which is closer to the KKF than any Paleozoic sedimentary basin. Newell (1997) observed excess maturation and elevated fluid-inclusion homogenization temperatures in Ordovician saddle dolomite near the Humboldt fault and the Midcontinent Rift in central and southern Kansas that greatly exceed the predicted temperatures from burial models. This led Newell to infer a thermal event and localized heating by vertical and lateral movement of formation waters.

Luczaj et al. (2007) demonstrated that proximal vertical circulation must occur between the Precambrian basement and Paleozoic units during mineralization based on Pb-isotopes on Paleozoic hosted galena. Regional gradients in the  $^{206}\text{Pb}/^{204}\text{Pb}$  isotopic signature of the galena stretch from northeastern Wisconsin to Iowa, Illinois, and Minnesota. These values are similar to the late-stage Pb-isotopic signature of Pb and Au mineralization in a Paleoproterozoic deposit in central Wisconsin (Haroldson et al., 2016), suggesting that fluids exchanged in both directions between Precambrian and Paleozoic rocks. Doe et al. (1983) and Afifi et al. (1984) inferred at least one lead-leaching event in the northern Illinois and northern Wisconsin between 400 Ma and 250 Ma. Even Proterozoic rocks in the iron ranges of the upper peninsula of Michigan contain adularia (K-feldspar) with ages in the Devonian to Mississippian range (420 to 327 Ma) (Robinson and LaBerge, 2013). Together with the 106°C fluid-inclusion data from 360 Ma authigenic K-feldspar from northwestern Wisconsin (Liu, 1997), these data suggest one or more Paleozoic thermal events affected some regions much closer to the KKF than the Appalachian-Ouachita front (Figure 21).

### *Seismic Sections*

Based on our results we are able to determine a marked difference between cross sections A-A' and B-B' in terms of crustal thickness variations and mid-crustal reflectors beneath the KKF which are consistent with oblique offset along the fault strike (Percival et al. 2006) and variable thrust displacement along the KKF; Cannon et al. (1993) argued that the KKF system has been shortened by 21-34 km of thrust motion since the Proterozoic extension phase when the rift was 32-54 km wider, a tectonic scenario and result very different than that proposed by Stein et al. (2015). Both the Keweenaw and Douglas thrusts have thrust fault scarps and the Keweenaw (SE side, NW dip) was most recently active as it offsets the Douglas thrust, has a greater offset and more prevalent footwall deformational structures (Fig. 9). Due to the station spacing of the EarthScope USArray stations and the low frequency content of receiver function data relative to active source seismic data, we are unable to directly image the fault or determine its exact geometry, however the location of the negative conversion within the upper crust does give insight into the bounds of the rift and therefore the fault locations. Based on seismic results we are also unable to distinguish how much thrust shortening occurred on the KKF system in the Proterozoic (~1060 Ma; Bornhorst et al., 1986) versus thrust motions in the late Paleozoic. The palinspastic fault calculations near Limestone Mountain of ~12-30 km is one constraint. However our seismic results, when compared to additional seismic observations from the region (Shen et al., 2013), show variations in crustal thickness along the rift likely indicative of variable crustal thickening along the KKF.

### *Pangea*

The Appalachian (Alleghenian) Ouachita-Marathon (including the twinning strains in Pennsylvanian limestones in the Sacramento Mountains)

orogen records the closure of the Rheic ocean and subsequent collision of Gondwana and Laurussia, and hence the formation of Pangea. Our study suggests that far-field stresses resulting from this collisional event were responsible for the reactivation and inversion of the KKF in the late Paleozoic which begs the question: “Are there other intracratonic structures attributable to far-field stress transmission related to the Pangea-forming continental collisions?” Additional collisional orogens that record Pangea-formation include the Permian Variscan of western Europe and the Permian Gondwanides of southern and western Gondwana.

A compilation of Late Paleozoic twinning strains associated with the final amalgamation of Pangea in the Permian includes the North American data set (Fig. 19; Appendices 1 and 2), and strain results from the now separated components of the Gondwanides including the Ellsworth Mountains of Antarctica, the Ventana Mountains of Argentina, the Cape fold belt of Southern Africa (Craddock et al. 2007), the Tasmanides (Craddock et al., 1997) and the Himalaya's (Paulsen et al., 2003). Layer-parallel shortening strains in these Gondwanide orogens have been rotated clockwise from their initial thrust transport-parallel direction in response to oblique convergence along the orogen, an interpretation based in part on the twinning strains preserved in autochthonous Permian limestones in the southern Karoo basin, just north of the Cape Fold Belt (Craddock et al. 2007). We have taken the liberty of projecting this orogenic stress-strain field across Gondwana to Laurussia (or vice versa; Fig. 22) recognizing there is no strain data for S. America and only the Gondwanide (southern) margin of Africa. This is a simplistic approach based on the strain data at hand, and we are aware of the many complications and controversies of different orogens (i.e., Taconic, Acadian, Alleghenian vs. Variscan, Hercynian, Caledonian) and local collisional events that can vary along strike in a convergent margin.

Projection of this late Paleozoic stress-strain field across Gondwana to Laurussia (Fig. 22) is consistent with the far-field stress required for reactivation of the KKF in Laurussia, and suggests that the Kiri uplift of central Africa may comprise a similar inversion structure. Daly et al. (1991), using seismic reflection and drilling data, demonstrated that Archean crystalline rocks that core the Kiri uplift are bound by steep reverse faults (~40 km total crustal shortening) that cut Permian strata and are unconformably overlain by undeformed Cretaceous strata (Fig. 22). Trouw and DeWitt (1999) interpreted the Kiri uplift as an inversion structure located 2000 km inboard of, but attributable to far-field stresses originating in, the Gondwanide orogen. The Kiri uplift, in the present-day Congo basin, was a highland and experienced an orogenic thermal pulse in the late Paleozoic (Linol et al. 2015; Kasanzu et al. 2016). Alternatively, if we argue that the highest differential stress gradient was generated along the Gondwana-Laurussia collisional boundary then the KKF and Kiri inversion structures are ~2000 and 3000 km, respectively, inboard of the collisional boundary. The KKF and Kiri uplifts may, therefore, represent coeval intracratonic pop-up structures that attest to the significance of the far-field stresses that developed throughout Pangea during supercontinent amalgamation. There are undoubtedly other such late Paleozoic offsets of crystalline structures within Pangea.

### Conclusions

The Grenville-Keweenaw system reactivated the Kapuskasing shear zone which propagated and formed the Keweenaw rift system (1141-1085 Ma), after which the Kapuskasing-Keweenaw-Douglas thrust system became an inverted structure in the center of North America in the late Paleozoic. This paired thick-skinned structure accommodated 30 km of crustal shortening along its 4000 km

length and initiated a wide variety of 2<sup>nd</sup> (folds) and 3<sup>rd</sup> (twinned calcite) order deformations in its footwall. Analysis of calcite twin strain patterns in the North American midcontinent are complex and suggest tectonic stress transmission originated from different directions at different times as a result of changes in orogenic convergence, not exclusively from the AOM margin; this observation is complimented by the complexity of fluid flow associated with the wide range of ages and origins for Paleozoic-hosted MVT deposits between the KKF and AOM thrust margins. The late Paleozoic amalgamation of Pangea, including the central Alleghenian (North America) and Variscan (Europe-Africa) orogens accentuated the far-field deformation in central North America (KKF) and central Africa (Kiri uplift; 40 km of fault offset), and included far-field Gondwanide stresses from oblique convergence along Gondwana's southern margin.

### **Acknowledgements**

The ideas presented here were initiated for Craddock and Malone on a 3 week University of Wisconsin Lake Superior region field trip run by Cam Craddock in 1990. Conversations with Mike Easton, Derek Armstrong, Ron Sage, Henry Halls, Maarten deWit and John Percival, over the decades, helped with resolution of the importance of the Kapuskasing boundary and its connection to the Keweenaw system. Jerry Webers and Michelle McGovern separated and analyzed the Limestone Mountain conodonts and microtektites. Zircon analyses were greatly aided by the folks at the University of Arizona Laserchron lab. Field assistance of Clara Thomann, Hayley Malone, Monica Mustain, Annie Craddock and Joey Affinati is greatly appreciated. Reviews by Rick Groshong and Carol Stein greatly improved the clarity of the manuscript.

### **Figures**

Figure 1: Regional basemap showing the Kapuskasing-Keweenaw fault system, based in part on the Bouguer gravity anomaly map of N. America (inset A) relative to the Grenville tectonic front and the Appalachian front. Inset B is pseudotachylite (1940 Ma; see text) hosted in granulite along the Kapuskasing fault. Study sites across the region are indicated.

Figure 2: Geologic overview of the Lake Superior region showing the 5 failed arms of the Keweenaw rift system (red) and the post-rift connection of the older Kapuskasing suture with the Keweenaw-Douglas thrusts as a thick-skinned

inversion structure (Manson and Halls, 1994, 1997). Shaded regions include the rift-aged Duluth complex, Archean granulites in the hanging wall of the Kapuskasing fault and the Proterozoic Jacobsville Sandstone. Solid circles are rift-aged carbonatites, red lines are the Pigeon River and Abitibi mafic dikes (1141 Ma), the Island Lake sinistral fault is represented by the white star, and the red star is the location of the top-to-the-SE granoblastic mylonite near Mellen, WI (Craddock et al. 2017).

Figure 3: Synfaulting calcite on the Island Lake fault (sinistral) field sample (A), sliced for multiple horizontal thin sections (A-E) which show sinistral kinematics (B & C). Calcite twin results in D (PEV) and E (NEV).

Figure 4: Deformation in Mamainse Point and Batchawana Bay (Figs 1 and 2). A: Overtaken crossbeds in the Jacobsville Sandstone. B: South-dipping reverse fault with syn-faulting calcite offsetting rift-aged rhyolites, C: Lower hemisphere projection of shortening axes for calcite twin analyses from 4 syn-faulting calcite samples. Great circle is the fault. D: Calcite strain results for veins crosscutting Mamainse Point rift rhyolites (Table 1).

Figure 5: DEM basemap showing the location of the Keweenaw thrust, the Paleozoic outliers in the footwall and the location of the cross section in Fig. 6 (A). Footwall deformation includes the vertical Jacobsville Sandstone at Larium, MI (B), the faulted Jacobsville under the Sherman Hill Ordovician outlier (C), and the north-plunging chevron folds in the Jacobsville on a false-color image(D). Calcite strain data are plotted stereographically (see Table 1).

Figure 6: Cross section interpretation for the Keweenaw thrust and Paleozoic limestone klippe (A) with the corresponding stratigraphic column (B). Conodonts confirm the age relations of the section and we also recovered microtektites (Table 3; C). Clastic dikes also cross-cut the Jacobsville Sandstone (D) which can dip  $60^\circ$  as at Sherman Hill quarry (E). The Jacobsville Sandstone has a maximum depositional age of 959 Ma based on 2080 detrital zircons (Malone et al., 2016).

Figure 7: NICE (2007) basemap showing the Keweenaw rift crosscutting Archean and Proterozoic terranes and locations of late Paleozoic footwall structures (A). Thrust fault with a rhyolite breccia over a flat-lying basalt, Cutface Creek along Highway 61 west of Grand Marais, MN (B). Detrital zircon results ( $n=99$ ) for the adjacent interflow sediment are described Craddock et al. 2013 (sample KP-16).

Figure 8: Aeromagnetic basemap showing the internal deformation of the Keweenaw rift (A) and Bardonia Peak site (B) with rift-parallel cleavage in the Duluth Gabbro. Composite photo C is from north of the Silver Cliff Creek tunnel

on Highway 61 where thrust faulting has offset flow folds in rift-aged rhyolites. View southeast from Bardon Peak (D) shows the Douglas fault scarp. Calcite twinning strain for fault gouge in (C) is plotted on the stereonet inset in D.

Figure 9: Aeromagnetic basemap of the Twin Cities (Forest City) basin in Minnesota and Wisconsin with offset Chengwatana basalts near Dresser, WI (A), offset Ordovician sediments along the Hastings fault (B), the Red Wing fault (C; Barn Bluff), overthrust and folded Ordovician carbonates near Lake Pepin, WI (D), drag folds along a thrust in the Cambrian Franconia Fm., Houston, MN (E) and folded Ordovician carbonates near Denzer, WI (F). See Figure 7 for additional details.

Figure 10: Calcite twinning results from the Mississippian and Pennsylvanian of Iowa (top) and the Mississippian of Indiana. Lower hemisphere projections, bedding is horizontal. See Table 1.

Figure 11: Bedrock geologic map of the LaSalle County, area, Illinois (from Kolata, 2005). Bedrock exposures are limited to quarries and stream cuts along the Illinois River and its tributaries. Red stars = sampling localities. The trace of the axis of the LaSalle Anticline is indicated. Blue = Pennsylvanian strata; Pink = Ordovician strata (see inset field photo). Lower hemisphere plots are for the four calcite twinning strain samples (Table 1).

Figure 12: Traces of the Lincoln fold anticlines of east-central New Mexico exposed near the Cretaceous El Capitan intrusion and north of the Marathon fold and thrust belt (A). One example of a Lincoln fold (B) is cored by evaporites (photo from J. Amato). The folds are crosscut by a monzonite with zircons that yield a crystallization age of 47.7 Ma (C) from rounded zircons (D; backscatter image).

Figure 13: Geologic basemap (see outline on Fig. 12) from Jones (1994) with red stars the locations of calcite twinning samples and the yellow star the location of the dated monzonite. All samples from the Permian Yeso Fm. (see stratigraphic column, upper right; orange box highlights Yeso Fm.). Lower hemisphere stereoplots include principal strain axes, contoured Turner compression axes and either bedding or vein great circles (see Table 1).

Figure 14: Geologic map of the western Sacramento Mountains, NM (modified from Scholle, 2003) with inset map of N. Mexico. Sampling localities are indicated by red stars (samples 3, 6-9 from Oliver Lee Park, others from the north). Yellow = Quaternary; Purple = Ordovician-Mississippian; Blue = Pennsylvanian and Permian; Tim = Tertiary intrusive rocks. See Figure 15 and Table 1.

Figure 15: Stratigraphic column for the Sacramento Mountains, New Mexico (A; orange highlight denotes units sampled) with a photomicrograph of twinned calcite in a brachiopod (inset, B). Lower hemisphere plots are for twinned calcite strain results (Table 1).

Figure 16: Earthscope receiver function cross sections across the KKF (see inset above and Fig. 20 for section lines A-A' and B-B').

Figure 17: Mississippian-Permian features in the Midcontinent along the KKF including the structurally high Mississippian Nemeha Arch (NA), deposition of Pennsylvanian sediments east of the KKF which include detrital zircons (sample sites indicated) only from eastern sources (Kissock et al. 2016), and the lack of Permian sedimentation west of the KKF.

Figure 18: Shear wave velocities at 6 km calculated using ambient noise tomography and wave gradiometry (Porter et al., 2016; percent perturbation is calculated from the average for the region) with the supracrustal sediments removed to accentuate the relationship of the KKF and the Transcontinental Arch (Carlson, 1999).

Figure 19: Layer-parallel shortening strain ( $\epsilon_1$  axes; Table 2) recorded by twinned calcite presented by age of host limestone and correlative Appalachian-Ouachita-Marathon orogenic stages (A-C). Figure D includes shortening axes hosted by late Pennsylvanian limestones in the proximal Ancestral Rockies foreland and other AOM misfits that are better interpreted with this data grouping (eastern 3 samples from Craddock and van der Pluijm, 1989 and Craddock et al. 1993).

Figure 20: Layer-parallel shortening strain calcite twinning data for the Appalachian-Ouachita thrust belt and foreland (Appendices 1 and 2) with all the data (A) and then with the data proximal to the KKF removed (B). Closed circles are twinning strains for limestones, open circles are for veins (Table1).

Figure 21: Map showing age dates for diagenetic minerals in the Midcontinent region of the United States. Major Mississippi Valley-type ore districts include: (1) Tri-State, (2) Northern Arkansas, (3) Viburnum Trend, (4) Old Lead Belt, (5) Southeast Missouri Barite, (6) Central Missouri Barite, (7) Upper Mississippi Valley, (8) Illinois-Kentucky Fluorispar, (9) Central Tennessee and Kentucky, (10) Central Kentucky, (11) Eastern Tennessee. Shapes indicate types of age dating techniques used: triangles indicate various age dates on ore-stage minerals such as sphalerite and calcite; circles indicate ages dates on on K-silicate minerals (feldspare and illite-smectite); and squares indicate paleomagnetic

age dates. Age ranges for colors are shown in the inset legend. Data are from Duffin et al. (1989), Elliot and Aronson (1993), Girard and Barnes (1995), Hay et al. (1988), Leach et al. (2001, and references therein), Liu et al (2003), Marshal et al. (1986), Matthews (1988), Nakai et al. (1990), Robinson and LaBerge (2013) and Wheeler (1989).

Figure 22: Pangea at ~240 Ma with closure of the Atlantic Ocean and corresponding orogenic belts (Alleghenian and Hercynian-Atlas) in the north, and the oblique Gondwanide orogen on the southern margin of Gondwana. Thick black lines are layer-parallel shortening axes, thin lines are the projection of that strain field across continents. Cross sections A-B, across the KKF, are from Figure 16 and the Kiri uplift profile is included here (Daley et al. 1991; C-C').

### Tables

- 1: Calcite Strain data
- 2: Stable Isotope (C, O) data
- 3: Tektite Microprobe data
- 4: Limestone Mountain klippe conodont data
- 5: U-Pb zircon ages, Lincoln folds monzonite

### References

- Aleinikoff, J. N., Walter, M., Kunk, M. J., and Hearn, P. P., 1993, Do ages of authigenic K-feldspar date the formation of Mississippi Valley-type Pb-Zn deposits, central and southern United States?: Pb isotopic evidence. *Geology*, v. 21, p. 73-76.
- Atwater, Gordon I. "Correlation of the Tyler and the Copps formations of the Gogebic iron district." *Geological Society of America Bulletin* 49.2 (1938): 151-194.
- Barth, A.P., and Wooden, J.L., 2010, Coupled elemental and isotopic analyses of polygenetic zircons from granitic rocks by ion microprobe, with implications for melt evolution and the sources of granitic magmas: *Chemical Geology*, v. 277, p. 149-159.
- Bennett, G. 2006. The Huronian Supergroup between Sault Ste. Marie and Elliot Lake. Institute on Lake Superior Geology, 52nd Annual Meeting (Sault Ste. Marie, Ontario), field trip guidebook, pt. 4, 65 p.
- Bethke, C.M., 1986, Hydrologic constraints on the genesis of the Upper Mississippi Valley mineral district from Illinois basin brines. *Econ. Geol.*, v. 81, 233-249.
- Bezys, R.K., 1990, Geology of Gypsum Deposits in the James Bay Lowland: Ontario Geological Survey Open File Report 5278, 109 p.
- Bjørnerud, M. G. "Evidence for Grenville-Age Seismicity and Thick-Skinned Deformation in Northern Wisconsin, USA." *The Journal of Geology* 118.1 (2010): 45-58.

- Black, L.P., Kamo, S.L., Allen, C.M., Davis, D.W., Aleinikoff, J.N., Valley, J.W., Mundil, R.M., Campbell, I.H., Korsch, R.J., Williams, I.S., and Foudoulis, C., 2004, Improved  $^{206}\text{Pb}/^{238}\text{U}$  microprobe geochronology by the monitoring of a trace-element-related matrix effect: SHRIMP, ID-TIMS, ELA-ICP-MS, and oxygen isotope documentation for a series of zircon standards: *Chemical Geology*, v. 205, p. 115-140.
- Bickford, M. E.; Wooden, J. L.; and Bauer, R. L. 2006. SHRIMP study of zircons from Early Archean rocks in the Minnesota River Valley: implications for the tectonic history of the Superior Province. *Geol. Soc. Am. Bull.* 118:94-108.
- Bickford M.E., Mueller, P.A., Kamenov, G.D., Hill, B.M., 2008. Crustal evolution of southern Laurentia during the Paleoproterozoic: insights from zircon Hf isotopic studies of ca. 1.75 Ga rocks in central Colorado. *Geology* 36, 555-558.
- Bornhorst, P. J.; Paces, J. B.; Grant, N. K.; Obradovich, J.D.; and Huber, N. K. 1987. Age of native copper mineralization, Keweenaw Peninsula, Michigan. *Econ. Geol.* 83:619-625.
- Brannon, J. C., Podosek, F. A., and McLimans, R. K., 1992, Alleghenian age of the Upper Mississippi Valley zinc-lead deposit determined by Rb-Sr dating of sphalerite. *Nature*, v. 356, p. 509-511.
- Burke, K., & Dewey, J. F. (1973). Plume-generated triple junctions: key indicators in applying plate tectonics to old rocks. *The Journal of Geology*, 406-433.
- Burkhard, M., 1993. Calcite twins, their geometry, appearance and significance as stress-strain markers and indicators of tectonic regime: a review. *Journal of Structural Geology* 15, 351-368.
- Cannon, William F., and M. G. Mudrey. *The potential for diamond-bearing kimberlite in Northern Michigan and Wisconsin*. No. 842. US Geological Survey, 1981.
- Cannon, W. F., and Nicholson, S. W. 2001. Geologic map of the Keweenaw Peninsula and adjacent area, Michigan. U.S. Geol. Surv. Map I-2696, scale 1 : 100,000.
- Cannon, W., 1994, Closing of the Midcontinent Rift – A far-field effect of Grenvillian compression: *Geology*, v. 22, p. 155-158, doi: 10.1130/ 0091-7613(1994)0222.3.CO
- Cannon, W.F., Green, A.G, Hutchinson, D.R., Lee, M., Milkereit, B., Behrendt, J.C., Halls, H.C., Green, J.C., Dickas, A.B., Morey, G.B., Sutcliffe, R., and Spencer, C., 1989, The North American Midcontinent Rift beneath Lake Superior from GLIMPCE seismic reflection profiling: *Tectonics*, v. 8, p. 305-332.
- Card, K. D. 1990. A review of the Superior Province of the Canadian Shield, a product of Archean accretion. *Precambrian Res.* 48:99-156.

- Carlson, M.P., 1999, Transcontinental Arch- a pattern formed by rejuvenation of local features across central North America: *Tectonophysics* 305, p. 225-233.
- Chandler, V. W., McSwiggen, P. L., Morey, G. B., Hinze, W. J., and Anderson, R. R., 1989, Interpretation of seismic reflection, gravity, and magnetic data across the Middle Proterozoic Midcontinent rift system, northwestern Wisconsin, eastern Minnesota, and central Iowa: *American Association of Petroleum Geologists, Bulletin*, v. 73, p. 261-275
- Chandler, V. M., and Schaap, B. D. 1991. Bouguer gravity anomaly map of Minnesota. *Minn. Geol. Surv. Map S-16*, scale 1 : 500,000.
- Chapple, W.M., 1978, Mechanics of thin-skinned fold and thrust belts: *Geological Society of America Bulletin*, v. 89, p. 1189-1198.
- Chase, C.G. and Gilmer, T.H., 1973, Precambrian plate tectonics: The midcontinent gravity high: *Earth and Planetary Science Letters*. v. 21. P. 70-78.
- Chinn, A.A. and R.H. Konig, 1973, Stress inferred from calcite twin lamellae in relation to regional structure in northwest Arkansas: *GSA Bulletin* 84, p. 3731-3736.
- Christensen, J.N., Halliday, A.N., Leigh, K.E., Randell, R.N., and Kesler, S.E., 1995, Direct dating of sulfides by Rb-Sr., A critical test using the Polaris Mississippi-type Zn-Pb deposit: *Geochimica et Cosmochimica Acta*, v. 59, p. 5190-5197. Geological Survey State Map S-17, scale 1:500,000.
- Cordua, W. S. (1985). Rock Elm structure, Pierce county, Wisconsin: A possible cryptoexplosion structure. *Geology*, 13(5), 372-374.
- Craddock, C. (1960). The origin of the Lincoln fold system, southeastern New Mexico. *Structure of the earth's crust and deformation of rocks: Internat. Geol. Cong., 21st, Norden, Rept., pt, 18, 34-44.*
- Craddock, C., 1964, The Lincoln Fold system: *New Mexico Geological Society, 15<sup>th</sup> Field Conference*, p. 122-133.
- Craddock, C., 1972, Keweenaw geology of east-central and southeastern Minnesota: *Geology of Minnesota: a centennial volume*, p. 416-424.
- Craddock, C., E.C. Theil and B. Gross, 1963, A gravity investigation of the Precambrian of southeastern Minnesota and western Wisconsin: *J. Geophys. Res.* 68, p. 6015-6032.
- Craddock, C., Mooney, H.M. and V. Kolehmainen, 1969, Simple Bouguer gravity map of Minnesota and northwestern Wisconsin: *Minnesota Geological Survey Map M-10.*
- Craddock, J.P., van der Pluijm, B.A., 1989. Late Paleozoic deformation of the cratonic carbonate cover of eastern North America. *Geology* 17, 416-419.
- Craddock, J.P. and Pearson, A., 1994. Non-coaxial horizontal shortening strains preserved in amygdale calcite, DSDP Hole 433C, Suiko Seamount. *Journal of Structural Geology* 16, 719-724.

- Craddock, J.P. and van der Pluijm, B., 1988, Kinematic analysis of an en echelon-continuous vein complex: *Journal of Structural Geology*, v. 10, p. 445-452.
- Craddock, S.D. and J.P. Craddock, 2012, Strain Variations in Carbonates across the Proterozoic Grenville Orogen: 58<sup>th</sup> ILSG (Thunder Bay), p. 21.
- Craddock, J.P., Moshoin, A., Pearson, A.M., 1991. Kinematic analysis from twinned calcite strains in the marble mylonites of the central Grenville province, Canada. Geological Society of America, Abstracts with Programs 15, 236.
- Craddock, J.P., Jackson, M., van der Pluijm, B.A., Versical, R., 1993, Regional shortening fabrics in eastern North America: far-field stress transmission from the Appalachian–Ouachita orogenic belt: *Tectonics* 12, 257–264.
- Craddock, J.P., Pearson, A., McGovern, M., Kropf, E.P., Moshoin, A., and Donnelly, K., 1997, Post-extension shortening strains preserved in calcites of the Keweenaw rift: Middle Proterozoic to Cambrian Rifting, Central North America, R.W. Ojakangas, A.B. Dickas and J.C. Green (Eds.) Geological Society of America Special Paper 213 , p. 115-126.
- Craddock, J.P., McGillion, M.S., Webers, G.F., & Yoshida, M., 1998, Strain analysis across the Ventana-Ellsworth fold-and-thrust belt: *South African Journal of Earth Sciences*, 27, n. 1A., p. 49-50.
- Craddock, J.P. , Farris, D. and Roberson, A., 2004, Calcite-twinning constraints on stress-strain fields along the Mid-Atlantic Ridge, Iceland: *Geology* 32, n. 1, p. 49-52 (and two electronic repository files).
- Craddock, J. P., & McKiernan, A. W. (2007). Tectonic implications of finite strain variations in Baraboo-interval quartzites (ca. 1700Ma), Mazatzal orogen, Wisconsin and Minnesota, USA. *Precambrian Research*, 156(3), 175-194.
- Craddock, J.P., Anziano, J., Wirth, K.R., Vervoort, J.D., Singer, B. and Zhang, X., 2007b, Structure, geochemistry and geochronology of a lamprophyre dike swarm, Archean Wawa terrane, Michigan, USA: *Precambrian Research*, 157, p. 50-70.
- Craddock, J.P., Malone, D.H., #Cook, A.L., \*Rieser, M.E., and Doyle, J.R., 2009, Dynamics of emplacement of the Heart Mountain allochthon at White Mountain: constraints from calcite twinning strains, anisotropy of magnetic susceptibility and thermodynamic calculations: *Geological Society of America Bulletin*, v. 121, n. 5, p. 919-938, doi:10.1130/B26340.
- Craddock, J. P., Rainbird, R. H., Davis, W. J., Davidson, C., Vervoort, J. D., Konstantinou, A., ... & Lundquist, B. (2013a). Detrital Zircon Geochronology and Provenance of the Paleoproterozoic Huron (~ 2.4–2.2 Ga) and Animikie (~ 2.2–1.8 Ga) Basins, Southern Superior Province. *The Journal of Geology*, 121(6), 623-644.
- Craddock, J. P.; Konstantinou, A.; Vervoort, J. D.; Wirth, K. R.; Davidson, C.; Finley-Blasi, L.; Juda, N. A.; and E. Walker. 2013b. Detrital zircon provenance of the Proterozoic midcontinent rift, USA. *J. Geol.* 121:57–73.

- Craddock, J.P., Malone, D.H., MacNamee, A.F., Mathisen, M., Leonard, A.M., and Kravits, K., 2015, Structural Evolution of the Eocene South Fork Landslide, Northwest Wyoming: *Journal of Geology*, v. 123, n. 5, p. 311-335.
- Craddock, J.P., Craddock, S.D., Konstantinou, A., Kylander-Clark, A., and Malone, D.H., 2017, Calcite Twinning Strain Variations across the Proterozoic Grenville Orogen and Keweenaw-Kapuskasung Inverted Foreland, USA and Canada. Manuscript accepted at **Geoscience Frontiers** pending revisions on December 26, 2016.
- Davis, D.W. and Sutcliffe R.H., 1985, U-Pb ages from the Nipigon plate and northern Lake Superior. *Geological Society of America Bulletin*, v. 96, p. 1572-1579.
- Davis, D.W. and Paces, J.B. 1990, The resolution of geologic events on the Keweenaw Peninsula and implications for the development of the Midcontinent Rift System, *Earth and Planetary Science Letters*, v. 97, p.379-398.
- Davis, D.W., and Green, J.C., 1997. Geochronology of the North American Midcontinent rift in western Lake Superior and implications for its geodynamic evolution. *Canadian Journal of Earth Sciences*, v. 34, pp. 476-488.
- Day, J., 1990, The Upper Devonian (Frasnian) conodont sequence in the Lime Creek Formation of north-central Iowa and comparison with Lime Creek Ammonoid, brachiopod, foraminifer, and gastropod sequences: *Journal of Paleontology*, v. 64, p. 614-628.
- Day, J., 1996, Faunal signatures of Middle-Upper Devonian depositional sequences and sea level fluctuations in the Iowa Basin: U.S. Midcontinent, in Witzke, B.J., Ludvigson, G.A., and Day, J., eds., *Paleozoic sequence stratigraphy, views from the North American craton*: Geological Society of America, Special Paper 306, p. 277-300.
- Day, J., Witzke, B.J., and B. Bunker, 2008, Overview of Middle and Upper Devonian Cedar Valley Group and Lime Creek Formation Carbonate Platform Facies, Faunas, and Event Stratigraphy of Northern Iowa. *Iowa Geological Survey Guidebook 28*, p. 15-39.
- Daly, M.C., Lawrence, S.R., Kimun'a, D. and M. Binga, 1991, Late Paleozoic deformation in central Africa: a result of distant collision? *Nature* 350, p. 605-7.
- DeMets, C., Gordon, R.G., and Argus, D.F., 2009, Geologically Current Plate Motions. *Geophys. J. Int.* 181, 1-80 doi: 10.1111/j.1365-246X.2009.04491.x GJ
- Daniels Jr, P. A., and R. D. Elmore. "Upper Keweenawan rift-fill sequence, Mid-Continent rift system." *Upper Keweenawan rift-fill sequence, mid-continent rift, Michigan: Michigan Basin Geological Society Annual Field Excursion* (1988): 1-23.
- Donaldson, J.A. and Irving., E., 1972, Grenville Front and Rifting of the Canadian

- Shield, *Nature Phys. Sci.*, v. 237, p.139-140.
- Dodd, J. R., Zuppann, C. W., Harris, C. D., Leonard, K. W., & Brown, T. W. (1993). Petrologic method for distinguishing eolian and marine grainstones, Ste. Genevieve Limestone (Mississippian) of Indiana. *Mississippian Oolites and Modern Analogs: American Association of Petroleum Geologists, Studies in Geology*, 35, 49-59.
- Dogliani and Panza, 2015, Polarized Plate Tectonics, *Advances in Geophysics, Volume 56*, 1-167, <http://dx.doi.org/10.1016/bs.agph.2014.12.001>)
- Dott, R.H. & J.W. Attig, 2004, *Roadside geology of Wisconsin*: Mountain Press, 354 p.
- Duffin, M. E., 1989, Nature and origin of authigenic K-feldspar in Precambrian basement rocks of the North American midcontinent. *Geology*, v. 17, 765-768.
- Duffin, M. E., Lee, M., Klein, G, deV., and Hay, R. L., 1989, Potassic diagenesis of Cambrian sandstones and Precambrian granitic basement in UPH-3 deep hole, Upper Mississippi Valley, U.S.A. *Journal of Sedimentary Research*, v. 59, 848-861.
- East, J.A., Swezey, C.S., Repetski, J.E., and Hayba, D.O., 2012, Thermal Maturity Map of Devonian Shale in the Illinois, Michigan, and Appalachian Basins of North America. US Geological Survey Scientific Investigations Map, no. 3214.
- Easton, R. M. (2000), Metamorphism of the Canadian shield, Ontario, Canada. I. The Superior Province, *Can. Mineral.*, **38**, 287-317, doi:10.2113/gscanmin.38.2.287.
- Elliott, W. C., and Aronson, J. L., 1993, The timing and extent of illite formation in Ordovician K-bentonites at the Cincinnati Arch, the Nashville Dome, and north-eastern Illinois basin. *Basin Research*, v. 5, p. 125-135.
- Ernst, R.E. and Halls, H.C. (1984). Paleomagnetism of the Hearst dike swarm and implications for the tectonic history of the Kapuskasing Structural Zone, northern Ontario. *Canadian Journal of Earth Sciences* 21: 1,499-1,506.
- Ernst, R.E., and Buchan, K.L., 2001, Large mafic magmatic events through time and links to mantle-plume heads, in Ernst, R.E., and Buchan, K.L., eds., *Mantle plumes: Their identification through time*: Geological Society of America Special Paper 352, p. 483-566.
- Engelder, T. and Engelder, R., 1977, Fossil distortion and decollement tectonics of the Appalachian plateau: *Geology* 5, p. 457-460.
- Engelder, T., 1979. The nature of deformation within the outer limits of the central Appalachian foreland fold-and-thrust belt in New York state. *Tectonophysics* 55, 289-310.
- Eriksson, K.A., Campbell, I.H., Palin, J.M., Allen, C.M., 2003. Predominance of Grenvillian magmatism recorded in detrital zircons from modern Appalachian rivers. *J. Geol.* 111, 707-717.
- Evans, M. and Groshong R. H. 1994. "A Computer Program for the Calcite Strain-

- Gage Technique." *Journal of Structural Geology* 16 (2): 277-281.
- Ferrill, D.A., 1991. Calcite twin widths and intensities as metamorphic indicators in natural low-temperature deformation of limestone. *Journal of Structural Geology* 13, 675-677.
- Ferrill, D.A., 1998. Critical re-evaluation of differential stress estimates from calcite twins in coarse-grained limestone. *Tectonophysics* 285, 77-86.
- Ferrill, David A., Alan P. Morris, Mark A. Evans, Martin Burkhard, Richard H. Groshong, and Charles M. Onasch. 2004. "Calcite Twin Morphology: A Low-Temperature Deformation Geothermometer." *Journal of Structural Geology* 26(8): 1521-1529.
- Foster, D.A., Mueller, P.A., Mogk, D.W., Wooden, J.L., Vogl, J.J., 2006. Proterozoic evolution of the western margin of the Wyoming craton: implications for the tectonic and magmatic evolution of the northern Rocky Mountains. *Can. J. Earth Sci.* 43, 1601-1619.
- Foster, M.E. and Hudleston, P.J., 1986, "Fracture cleavage" in the Duluth complex, northeastern Minnesota: *Geol. Soc. America Bull.* 97, p. 85-96.
- French, B. M., Cordua, W. S., & Plescia, J. B. (2004). The Rock Elm meteorite impact structure, Wisconsin: Geology and shock-metamorphic effects in quartz. *Geological Society of America Bulletin*, 116(1-2), 200-218.
- Gordon, M.B. and Hempton, M.R., 1986. Collision-induced rifting: The Grenville Orogeny and the Keweenaw rift of North America, *Tectonophysics*, 17: 1-25.
- Garven, G.; Ge, S.; Person, M.A.; Sverjensky, D.A., 1993, Genesis of stratabound ore deposits in the midcontinent basins of North America. 1. The role of regional groundwater flow. *Am. J. Sci.*, v. 293, 497-568.
- Gasteiger, C.M., 1980, Strain analysis of a low amplitude fold in north-central Oklahoma using calcite twin lamellae: M.S. Thesis, University of Oklahoma, Norman, Oklahoma, 90 p.
- Gehrels, G.E., Valencia, V., and Ruiz, J., 2008, Enhanced precision, accuracy, efficiency, and spatial resolution of U-Pb ages by laser ablation-multicollector-inductively coupled plasma-mass spectrometry: *Geochemistry Geophysics Geosystems*, v. 9, Q03017, doi: 10.1029/2007GC001805.
- Girard, J. P., and Barnes, D. A., 1995, Illitization and paleothermal regimes in the Middle Ordovician St Peter Sandstone, central Michigan basin: K-Ar, oxygen isotope, and fluid inclusion data. *AAPG Bulletin*, v. 79, p. 49-69.
- Goodings, C. R., & Brookfield, M. E. (1992). Proterozoic transcurrent movements along the Kapuskasing lineament (Superior Province, Canada) and their relationship to surrounding structures. *Earth-Science Reviews*, 32(3), 147-185.
- Gordon, M. B., and Hempton, M. R., 1986, Collision-induced rifting: The Grenville orogeny and the Keweenaw rift of North America: *Tectonophysics*, v. 127, p. 1-25.

- Gray, Mary Beth, John A. Stamatakos, David A. Ferrill, and Mark A. Evans. 2005. "Fault-Zone Deformation in Welded Tuffs at Yucca Mountain, Nevada, USA." *Journal of Structural Geology* 27 (10): 1873-1891.
- Grout, F. F.; Sharp, R. P.; and Schwartz, G. M. 1959. The geology of Cook County, Minnesota. *Minn. Geol. Surv. Bull.* 39.
- Groshong, R.H., Jr. 1972, Strain calculated from twinning in calcite: *Bull. geol. Soc. Am.* 83, 2025-2038.
- Groshong, R.H., Jr. 1974, Experimental test of least-squares strain calculations using twinned calcite: *Bull. Geol. Soc. Am.* 85, 1855-1864.
- Groshong, R.H., Jr. Strain, fractures, and pressure solution in natural single-layer. *Bull. Geol. Soc. Am.* 1975, 86, 1363-1376.
- Groshong, R.H. Jr, Teufel, L.W., Gasteiger, C.M., 1984. Precision and accuracy of the calcite strain-gage technique. *Bulletin of the Geologic Society of America* 95, 357-363.
- Hamblin, W. K. (1958). The Cambrian sandstones of northern Michigan: Michigan Geologic Survey Publication 51.
- Hamblin, W. K., and Horner, W. J. 1961. Sources of Keweenaw conglomerate of northern Michigan. *J. Geol.* 69:204-211.
- Halls, H.C. and E.G. Shaw, 1988, Paleomagnetism and orientation of Precambrian dykes, eastern Lake Superior region, and their use in estimates of crustal tilting: *Canadian Journal of Earth Sciences* 25, p. 732-743.
- Halls, H. C., and M. P. Bates (1990), The evolution of 2.45 Ga Matachewan dyke swarm, Canada, in *Mafic Dykes and Emplacement Mechanisms*, edited by A. J. Parker, P. C. Rickwood, and D. H. Tucker, pp. 237 - 250, A. A. Balkema, Brookfield, Vt.
- Halls, H. C., H. C. Palmer, M. P. Bates, and W. C. Phinney (1994), Constraints on the nature of the Kapuskasing structural zone from the study of Proterozoic dyke swarms, *Can. J. Earth Sci.*, 31, 1182 - 1196.
- Hanes, J.A., D.A. Archibald, M. Queen and E. Farrar, 1994, Constraints for  $^{40}\text{Ar}$ - $^{39}\text{Ar}$  geochronology on the tectonothermal history of the Kapuskasing uplift in the Canadian Superior province: *Canadian Journal of Earth Sciences* 31, p. 1146-1171.
- Haroldson, E., Beard, B., Satkoski, A., Johnson, C., Brown, P., 2016, Phanerozoic Au in a Paleoproterozoic Cu Vein deposit of Central Wisconsin; Evidence from Pb Isotopes Using LA-ICP-MS, *Geological Society of America Abstracts with Programs*. Vol. 48, No. 7, p.0.
- Harris, A. G., 1979, Conodont color alteration, and organo-mineral metamorphic index, and its application to Appalachian basin geology. in, P. Scholle and P. Schluger, eds., *Aspects of diagenesis: SEPM Special Publication*, v. 26, p. 3-16.
- Hatcher, R.D., 1987, Tectonics of the southern and central Appalachians: *Annual Review of Earth and Planetary Sciences*, v. 15, p. 337-362.
- Hatcher, R.D., Thomas, W.A., and Viele, G.W., editors, 1989, *The Appalachian-*

- Ouachita orogeny in the United States: Boulder, Colorado, Geological Society of America, Geology of North America, v. F-2, 767 p.
- Hauser, E., 1996, Midcontinent Rifting in a Grenville embrace, in Van Schmus, W.R., Bickford, M.E., and Turek, A., eds., Proterozoic geology of the east-central Midcontinent basement: Geological Society of America Special Paper 308, p. 67-75.
- Hay, R. L., Lee, M., Kolata, D. R., Matthews, J. C., and Morton, J. P., 1988, Episodic potassic diagenesis of Ordovician tuffs in the Mississippi Valley area. *Geology*, v. 16, 743-747.
- Heaman, L.M., and Machado, N., 1992. Timing and origin of midcontinent rift alkaline magmatism, North America: evidence from the Coldwell Complex. *Contributions to Mineralogy and Petrology*, v. 110, pp. 289-303.
- Heaman, L.M., R.M. Easton, T.R. Hart, P. Hollings, C.A. MacDonald and M. Smyk, 2007, Further refinement of the timing of Mesoproterozoic magmatism, Lake Nipigon region, Ontario: *Canadian Journal of Earth Sciences* 44, p. 1055-1086.
- Hearn, P. P., Sutter, J. F., and Belkin, H. E., 1987, Evidence for Late-Paleozoic brine migration in Cambrian carbonate rocks of the central and southern Appalachians: Implications for Mississippi Valley-type sulfide mineralization. *Geochimica et Cosmochimica Acta*, v. 51, p. 1323-1334.
- Hickman, R. G., Varga, R. J., & Altany, R. M. (2009). Structural style of the Marathon thrust belt, west Texas. *Journal of Structural Geology*, 31(9), 900-909.
- Hnat, J.S., van der Pluijm and R. Van Der Voo, 2006, Primary curvature in the Mid-Continent Rift: Paleomagnetism of the Portage Lake Volcanics (northern Michigan, USA): *Tectonophysics* 425, p. 71-82.
- Hnat, J.S.; van der Pluijm, B.A., 2011, Foreland signature of indenter tectonics: Insights from calcite twin analysis in the Tennessee salient of the southern Appalachians, USA. *Lithosphere*, 3, 317-327.
- Hoffman, P.F., 1988, United Plates of America, the birth of a craton: early Proterozoic growth and assembly and growth of Laurentia: *Annual Review of Earth and Planetary Sciences*, v. 1, p. 543-603.
- Holm, D.K., Schneider, D., and Couth, C.D., 1998. Age and deformation of Early Proterozoic Quartzites in the southern Lake Superior region: implications for the extent of foreland deformation during the final assembly of Laurentia. *Geology*, v. 26, p. 907-910.
- Howell, P. D., and van der Pluijm, B. A., 1990, Early history of the Michigan basin: Subsidence and Appalachian tectonics: *Geology*, v. 18, p. 1195-1198.
- Jackson, M., Craddock, J.P., Ballard, M., Van Der Voo, R., and McCabe, C., 1989, Anhyseretic remanent magnetic anisotropy and calcite strains in Devonian carbonates from the Appalachian Plateau, NY: *Tectonophysics*, v. 161, p. 43-53.
- Jackson, M. 1991. Anisotropy of magnetic remanence: a brief review of

- mineralogical sources, physical origins, and geological applications, and comparison with susceptibility anisotropy. *Pure Appl. Geophys.* 136, 1–28. doi: 10.1007/BF00878885.
- Jirsa, M.A., 1984, Interflow sedimentary rocks in the Keweenaw North Shore Volcanic Group, northeastern Minnesota. *Minn. Geol. Surv. Rep. Invest.* 30, 20 p.
- Jirsa, M.A., 2011, Bedrock geology of the western Gunflint Trail area, northeastern, Minnesota: Minnesota Geological Survey Map M-191, 1:24,000.
- Kalliokoski, J. 1982. Jacobsville sandstone. In Wold, R.J., and Hinze, W. J., eds. *Geology and tectonics of the Lake Superior basin.* *Geol. Soc. Am. Mem.* 156:147–155.
- Kasanzu, C.H., Linol, B., de Wit, M.J., Brown, R., Persano, C. and F.M. Stuart, 2016, From source to sink in central Gondwana: Exhumation of the Precambrian basement rocks of Tanzania and sediment accumulation in the adjacent Congo basin: *Tectonics* 35, doi:10.1002/2016TC004147.
- King, E. R, and Zietz, I., 1971, Aeromagnetic study of the Midcontinent gravity high of central United States: *Geological Society of America, Bulletin*, v. 82, p. 2,187-2,208.
- Kissock, J.K., Finzel, E.S., Malone, D.H., Craddock, J.P., in review, Lower-Middle Pennsylvanian strata in the North American midcontinent record the interplay between erosional unroofing of the Appalachians and eustatic sea level rise: *Basin Research*.
- Klasner, J.S. and Schulz., K.J., 1982, Concentrically zoned pattern in the Bouger gravity anomaly map of North America: *Geology*, v. 10, p. 537-541.
- Klasner, J. S., Ojakangas, R. W., Schulz, K. J., & LaBerge, G. L. (1991). Nature and Style of deformation in the foreland of early Proterozoic Penokean Orogen, Northern Michigan: *USGS Bull* 1904-K, p. K1-K22.
- Kluth, C. F., & Coney, P. J. (1981). Plate tectonics of the ancestral Rocky Mountains. *Geology*, 9(1), 10-15.
- Kluth, C.F., 1986, Plate Tectonics of the Ancestral Rockies: *AAPG Memoir* 41, p. 353-369.
- Kehle, R.O., 1970, Analysis of gravity sliding and orogenic translation: *GSA Bulletin* 81, p. 1641-1664.
- Kilsdonk, W., Wiltschko, D.V., 1988. Deformation mechanisms in the southeastern ramp region of the Pine Mountain block, Tennessee. *Geological Society of America Bulletin* 100, 644–653.
- Kolata, D.R., 2005, *Geologic Map of Illinois: Illinois State Geological Survey, Map 14.*
- Koppers, Anthony AP. "ArArCALC – software for 40 Ar/39 Ar age calculations." *Computers & Geosciences* 28.5 (2002): 605-619.
- Kutz, K. B., and Spry, P. G., 1989, The genetic relationship between Upper Mississippi Valley district lead-zinc mineralization and minor base metal

- mineralization in Iowa, Wisconsin, and Illinois. *Economic Geology*, v. 84, p. 2139-2154.
- LaBerge, G. L., Klasner, J. S., & Myers, P. E. (1991). *New observations on the age and structure of Proterozoic quartzites in Wisconsin* (No. 1904-B).
- Lacombe, O., Laurent, P., 1996. Determination of deviatoric stress tensors based on inversion of calcite twin data from experimentally deformed monophase samples: preliminary results. *Tectonophysics* 255, 189–202.
- Leach, D.L. and Rowan, E.N., 1986, Genetic link between Ouachita fold-belt tectonism and the Mississippi Valley-type lead-zinc deposits of the Ozarks: *Geology*, v. 14, p. 931-935.
- Leach, D.L., Bradley, D., Lewchuk, M.T., Symons, D.R.A., de Marsily, G., Brannon, J., 2001, Mississippi Valley-type lead-zinc deposits through geological time: implications from recent age-dating research. *Mineralium Deposita*, v. 36, p. 711-740.
- Leach, D.L.; Taylor, R.D.; Fey, D.L.; Diehl, S.F.; Saltus, R.W., 2010, A Deposit Model for Mississippi Valley-Type Lead-Zinc Ores. Chapter A of *Mineral Deposit Models for Resource Assessment*; United States Geological Survey, Scientific Investigations Report. United States Geological Survey: Reston, VA, USA.
- Leslie, M., Wetzel, T., Wirth, K.R., and Craddock, J.P., 1994, Petrography and structure of the Keweenaw-Chengwatana volcanics near Dresser, WI: 40th Annual Proceedings of the Lake Superior Institute, p. 35-6.
- Linol, B., M. J. de Wit, F. Guillocheau, R. Cecile, and O. Dauteuil (2015), Multiphase Phanerozoic subsidence and uplift history recorded in the Congo basin: A complex successor basin, in *Geology and Resource Potential of the Congo basin*, Regional Geol. Rev., pp. 213–227, Springer.
- Ludwig, R.K. 2003. User's Manual for Isoplot 3.00. A geochronological Toolkit for Microsoft Excel®. *Berkeley Geochronology Center*. Special Publication No. 4.
- Liu, J., Hay, R.L., Deino, A., and Kyser, T.K., 2003, Age and origin of authigenic K-feldspar in uppermost Precambrian rocks in the North American Midcontinent. *GSA Bulletin*, v. 115, no. 4, p. 422-433.
- Luczaj, J. A., 2000, Epigenetic dolomitization and sulfide mineralization in Paleozoic rocks of eastern Wisconsin: Implications for fluid flow out of the Michigan Basin: Ph.D. dissertation, Johns Hopkins University, Baltimore, Maryland, 443 p.
- Luczaj, J. A., Millen, T., and Martin, J., 2007, A lead-isotopic study of Galena from Eastern Wisconsin: Evidence for lead sources in Precambrian basement rocks. Geological Society of America, North-Central/South Central Meeting in Lawrence Kansas on April 11-13, 2007. *GSA Abstracts with Programs*, v. 39, no. 3, p. 67.
- Malone, D.H., Craddock, J.P., M.H. Anders and A. Wulff, 2014, Constraints on the emplacement age of the massive Heart Mountain slide, northwest

- Wyoming: *Journal of Geology*, v. 122, p. 675-681.
- Malone, D.H., Carol A. Stein, John P. Craddock, Jonas Kley, Seth Stein, John E. Malone, 2016, Maximum depositional age of the Neoproterozoic Jacobsville Sandstone, Michigan: Implications for the evolution of the Midcontinent Rift: *Geosphere* 12, doi:10.1130/GES01302.1.
- Malone, D.H. Craddock, J.P., Konstantinou, A. and McLaughlin, P.I., 2017, Zircon dust brings Ordovician paleoclimate into focus: U-Pb geochronology of the Bighorn Formation, Wyoming, USA: *Journal of Geology* (in press).
- Manson, M.L. and Halls, H.C., 1994, Post-Keweenaw compressional faults in the eastern Laek Superior region and their tectonic significance: *Canadian Journal of Earth Sciences* 31, p. 640-651.
- Manson, M.L., and Halls, H.C., 1997, Proterozoic reactivation of the southern Superior Province and its role in the evolution of the Midcontinent rift: *Canadian Journal of Earth Sciences*, 1997, 34(4): 562-575, 10.1139/e17-045
- Marshak, S., Karlstrom, K., & Timmons, J. M. (2000). Inversion of Proterozoic extensional faults: An explanation for the pattern of Laramide and Ancestral Rockies intracratonic deformation, United States. *Geology*, 28(8), 735-738.
- Marshall, B. D., Woodard, H. H., and DePaolo, D. J., 1986, K-Ca-Ar systematics of authigenic sanidine from Waukau, Wisconsin, and the diffusivity of argon. *Geology*, v. 14, 936-938.
- Mariano, J. and W.J. Hinze, 1994, Structural interpretation of the Midcontinent rift in eastern Lake Superior from seismic reflection and potential field studies: *Canadian Journal of Earth Sciences* 30, p. 619-628.
- Matsch, C.L., 1962, Pleistocene geology of the St. Paul Park and Prescott quadrangles: Minneapolis, University of Minnesota, M.S. thesis, 49 p.
- McBride, J. H., & Nelson, W. J. (1999). Style and origin of mid-Carboniferous deformation in the Illinois Basin, USA – Ancestral Rockies deformation?. *Tectonophysics*, 305(1), 249-273.
- McCabe, C., and R. D. Elmore (1989), The occurrence and origin of Late Paleozoic remagnetization in the sedimentary rocks of North America, *Rev. Geophys.*, 27(4), 471-494, doi:10.1029/RG027i004p00471.
- McCracken, A.D., Armstrong, D.K. and T.E. Bolten, 2000, Conodonts and corals in kimberlite xenoliths confirm a Devonian seaway in central Ontario and Quebec: *Canadian Journal of Earth Sciences* 37, p. 1651-1663.
- McLimans, R. K., 1977, Geological, fluid inclusion, and stable isotope studies of the Upper Mississippi Valley zinc-lead district, southwest Wisconsin. Ph.D. Dissertation, Pennsylvania State University, 175 p.
- Medaris, G., Singer, B.S., Dott, R.H., Naymark, A., Johnson, C.M., and Schott, R.C., 2003, Late Paleoproterozoic climate, tectonics, and metamorphism in the southern Lake Superior Region and proto-North America: Evidence from Baraboo interval quartzites: *Journal of Geology*, v.111, p 243-257.
- Merino, M., G. R. Keller, S. Stein, and C. Stein (2013), Variations in Mid-

- Continent Rift magma volumes consistent with microplate evolution, *Geophys. Res. Lett.*, 40, 1513–1516, doi:10.1002/grl.50295.
- Morey, G.B., Sims, P.K., Cannon, W.F., Mudrey, M.G. Jr. and D.L. Southwick, 1982, Geologic map of the Lake Superior region, Minnesota, Wisconsin and northern Michigan: Minnesota Geological Survey Map S-13, 1:1,000,000.
- Mosar, J., 1989, Internal deformation in the Prealpes Medianes, Switzerland: *Ecologiae Geologicae Helvetiae*, v. 82, p. 765–793.
- Milstein, R.L., 1987, Anomalous Paleozoic outliers near Limestone Mountain, MI: *Geol. Soc. America DNAG Centennial fieldguide*, p. 263–268.
- Miller, J. D., Jr., and Severson, M. J. 2002. Geology of the Duluth Complex. In Miller, J. D., Jr.; Green, J. C.; Severson, M. J.; Chandler, V. W.; Hauck, S. A.; Peterson, D. M.; and Wahl, T. E., eds. *Geology and mineral potential of the Duluth Complex and related rocks of northeastern Minnesota*. Minn. Geol. Surv. Rep. Investig. 58:106–143.
- Morey, G. B., and Ojakangas, R. W. 1982. Keweenawan sedimentary rocks of eastern Minnesota and northwestern Wisconsin. *Geol. Soc. Am. Mem.* 156:135–146
- Morey, G.B., 2001, Compositions of rift-related volcanic rocks of the Keweenawan supergroup atop the St. Croix hosrt, southeastern MN: Minnesota Geological Survey Info. Circular 47. 1982, Report of Invest. 56.
- Nakai, S., Halliday, A. N., Kesler, S. E., and Jones, H. D., 1990, Rb-Sr dating of sphalerites from Tennessee and the genesis of Mississippi Valley type ore deposits. *Nature*, v. 346, p. 354–357.
- Nelson, R.S., Malone, D.H., Jacobson, R.J., and Frankie, W.T., 1996, Guide to the Geology of Buffalo Rock and Matthiessen State Parks Area, La Salle County, Illinois: *Illinois Geological Survey Field Trip Guidebook 1996C & 1997B*, 56 p.
- NICE (Northern Interior Continental Evolution). 2006, Geologic terrane map of Precambrian basement rocks in Minnesota, Wisconsin and Iowa. <http://www.mngs.umn.edu/nicegeo/niceimgs.htm>.
- Nickelsen. R.P., 1966, Fossil distortion and penetrative rock deformation in the Appalachian plateau, Pennsylvania: *J. Geology* 74, p. 924–31.
- Newell, K. D., 1997, Comparison of Maturation Data and Fluid-inclusion Homogenization Temperatures to Simple Thermal Models--Implications for Thermal History and Fluid Flow in the Midcontinent: Current Research in Earth Sciences, Kansas Geological Survey, Bulletin 240, part 2. <http://www.kgs.ku.edu/Current/1997/newell/newell1.html>
- Ojakangas, R. W., and Morey, G. B. 1982a. Keweenawan pre-volcanic quartz sandstones and related rocks of the Lake Superior region. In World, R. J., and Hinze, E. J., eds. *Geology and tectonics of the Lake Superior basin*. *Geol. Soc. Am. Mem.* 156:85–96.

- Ojakangas, R. W., 1982, Keweenawan sedimentary rocks of the Lake Superior region: a summary. *Geol. Soc. Am. Mem.* 156:157-164.
- Oliver, J. 1986. Fluids expelled tectonically from orogenic belts: their role in hydrocarbon migration and other geologic phenomena: *Geology* 14: 99-102.
- Ong, P.F., van der Pluijm, B.A. and R. Van Der Voo, 2007, Early rotation and late folding in the Pennsylvania salient (U.S. Appalachians): evidence from calcite-twinning analysis of Paleozoic carbonates: *GSA Bulletin* 119, p. 796-804.
- Ontario Geologic Survey, 1967, Kapuskasing sheet (Map 398), Cochrane and Algoma district.
- Paces, J.B., and Miller, J.D., 1993, U-Pb ages of the Duluth Complex and related mafic intrusions, northeastern Minnesota: geochronologic insights into physical, paleomagnetic and tectonomagmatic processes associated with the 1.1 Ga mid-continent rift system: *Journal of Geophysical Research*, v. 98, no. B8, p. 13997-14013.
- Paulsen, T.S., Demosthenous, C.M., Myrow, P.M., Hughes, N.C., and Parcha, S.K., 2007, Paleostrain stratigraphic analysis of calcite twins across the Cambrian-Ordovician unconformity in the Tethyan Himalaya, Spiti and Zaskar valley regions, India: *Journal of Asian Earth Sciences*, v. 31, p. 44-54.
- Paulsen, T.S., Wilson, T.J., Demosthenous, C., Millan, C., Jarrad, R. and A. Laufer, 2014, Kinematics of the Neogene Terror rift: constraints from calcite twinning strains in the ANDRILL McMurdo Ice Shelf (AND-1B) core, Victoria Land Basin, Antarctica: *Geosphere* 10, p. 828-841.
- Percival, J.A., 1981, Geological evolution of part of the central Superior Province based on relationships among the Abitibi and Wawa subprovinces and the Kapuskasing structural zone: Ph. D. thesis, Queen's University, Kingston, Ontario, Canada.
- Percival, J.A., 1994. The Kapuskasing transect of Lithoprobe: Introduction. *Canadian Journal of Earth Sciences*, 31: 1013-1015.
- Percival, J.A., Green, A.G., Milkereit, B., Cook, F.A., Geis, W. and West, G.F., 1989. Seismic reflection profiles across deep continental crust exposed in the Kapuskasing uplift structure. *Nature*, 342: 416-420.
- Percival, J. A., and K. D. Card. "Archean crust as revealed in the Kapuskasing uplift, Superior Province, Canada." *Geology* 11.6 (1983): 323-326.
- Percival, J.A. and McGrath, P.H., 1986, Deep Crustal Structure and Tectonic History of the Northern Kapuskasing Uplift of Ontario: An Integrated Petrological-Geophysical Study: *Tectonics*, 5(4)553-572.
- Percival, J. A., and G. F. West (1994), The Kapuskasing uplift: A geological and geophysical synthesis, *Can. J. Earth Sci.*, **31**, 1256-1286, doi:10.1139/e94-110.

- Percival, J. A.; Sanborn-Barrie, M.; Skulski, T.; Stott, G.M.; Helmstaedt, H.; and White, D. J. 2006. Tectonic evolution of the western Superior Province from NAT-MAP and lithoprobe studies. *Can. J. Earth Sci.* 43:1085–1117.
- Pinet, N., 2016, Far-field effects of Appalachian orogenesis: a view from the craton: *Geology* 44, p. 83-6.
- Pinet, N., Lavoie, D., Dietrich, J., Hu, K., and Keating, P., 2013, Architecture and subsidence history of the Hudson Bay intracratonic basin: *Earth-Science Reviews*, v. 125, p. 1–23, doi:10.1016/j.earscirev.2013.05.010.
- Pray, L. C. (1961). *Geology of the Sacramento Mountains Escarpment: Otero County, New Mexico*. State Bureau of Mines and Mineral Resources, New Mexico Institute of Mining & Technology.
- Queen, M., Heaman, L.M., Hanes, J.A., Archibald, D.A. and E. Farrar, et al. 1996,  $^{40}\text{Ar}/^{39}\text{Ar}$  phlogopite and U-Pb perovskite dating of lamprophyre dykes from the eastern Lake Superior region: evidence for a 1.4 Ga magmatic precursor to the Midcontinent rift volcanism: *Canadian Journal of Earth Sciences* 33, p. 958-965.
- Quinlin, G.M. and Beaumont, 1984, Appalachian Thrusting, lithospheric flexure, and the Paleozoic stratigraphy of the eastern interior of North America: *Canadian Journal of Earth Sciences*, v. 21, p. 973-996.
- Rainbird, R.H., Cawood, P., Gehrels, G., 2012. The great Grenvillian sedimentation episode: record of supercontinent Rodinia's assembly. In: Busby, C., Azor, A. (Eds.), *Tectonics of Sedimentary Basins: Recent Advances*. Wiley, Ch, p. 29.
- Renne, Paul R., et al. "Intercalibration of standards, absolute ages and uncertainties in  $^{40}\text{Ar}/^{39}\text{Ar}$  dating." *Chemical Geology* 145.1 (1998): 117-152.
- Reynolds, R.L., Goldhaber, M.B., and Snee, L.W., 1997, Paleomagnetic and  $^{40}\text{Ar}/^{39}\text{Ar}$  Results from the Grant Intrusive Breccia and Comparison to the Permian Downeys Bluff Sill – Evidence for Permian Igneous Activity at Hicks Dome, Southern Illinois Basin. U.S. Geological Survey, Bulletin, 2097-G, 16 pages.
- Robinson, G.W. and LaBerge, G.L., 2013, Minerals of the Lake Superior Iron Ranges. A.E. Seaman Mineral Museum, Michigan Technological University, Houghton, Michigan, USA, 58 pages.
- Rodgers, J., 1967, Chronology of tectonic movements in the Appalachian region of eastern North America: *American Journal of Science*, v. 265, p. 408-427.
- Romano, D., Holm, D.K., Foland, K.A., 2000. Determining the extent and nature of Mazatzal-related overprinting of the Peokean orogenic belt in the southern Lake Superior region, north-central USA. *Precambrian Res.* 104, 25–46.
- Rowan, E.L., Goldhaber, M.B., and Hatch, J.R., 2002, Regional fluid flow as a factor in the thermal history of the Illinois basin: Constraints from fluid inclusions and the maturity of Pennsylvanian coals. *AAPG Bulletin*, v. 86, p.

257-277.

- Rowe, K.J., Rutter, E.H., 1990. Paleostress estimation using calcite twinning: experimental calibration and application to nature. *Journal of Structural Geology* 12, 1-17.
- Sage, R. P. (1988). *Geology of Carbonatite-alkalic Rock Complexes in Ontario: Goldray Carbonatite Complex, District of Cochrane*. Ontario Ministry of Northern Development and Mines.
- Schulz, K.J., and Cannon, W.F., 2007, The Penokean Orogeny in the Lake Superior region: *Precambrian Research*, v. 157, n. 1-4, p. 4-25.
- Schmidt, R. G., and H. A. Hubbard. "Penokean orogeny in the central and western Gogebic region, Michigan and Wisconsin." *Field Trip A, 18th Annual Institute on Lake Superior Geology, Houghton, Mich* (1972).
- Schmitz, M. D.; Bowring, S. A.; Southwick, D. L.; Boerboom, T. J.; and Wirth, K. R. 2006. High-precision U-Pb geochronology in the Minnesota River Valley sub-province and its bearing on the Neoproterozoic to Paleoproterozoic evolution of the southern Superior Province. *Geol. Soc. Am. Bull.* 115:943-953.
- Scholle, P.A., 2003, *Geologic Map of New Mexico, Scale 1:500,000*: New Mexico Bureau of Geology and Mineral Resources.
- Shields, W.E., Malone, D.H., and Harp, B.R.,\* 2005, *Geologic Map of the LaSalle, IL 7.5 Minute Quadrangle*: Published on-line at the Illinois State Geological Survey, <http://www.isgs.illinois.edu/maps/isgs-quads>
- Smith, M. Elliot, et al. "High-resolution calibration of Eocene strata:  $^{40}\text{Ar}/^{39}\text{Ar}$  geochronology of biotite in the Green River Formation." *Geology* 34.5 (2006): 393-396.
- Spang, J.H. and Groshong, R.H., Jr., 1981, Deformation mechanisms and strain history of a minor fold from the Appalachian Valley and Ridge Province: *Tectonophysics*
- Stauffer, C. R. 1927. Age of the red clastic series of Minnesota. *Geol. Soc. Am. Bull.* 38:469-478.
- Southwick, D. L., and Chandler, V. M. 1996. Block and shear-zone architecture of the Minnesota River Valley sub-province: implications for late Archean accretionary tectonics. *Can. J. Earth Sci.* 26:2145-2158.
- Stacey, J.S. and Kramers, J.D., 1975, Approximation of terrestrial lead isotope evolution by a two-stage model: *Earth and Planetary Science Letters*, v. 26, p. 207-221.
- Stein, S., et al. (2011), Learning from failure: The SPREE Mid-Continent Rift Experiment, *GSA Today*, 21(9), 5-7, doi:10.1130/G120A.1.
- Stein, C.A., S. Stein, M. Merino, G.R. Keller, L.M. Flesch and D.M. Jurdy (2014), Was the Midcontinent Rift part of a successful seafloor-spreading episode?, *Geophys. Res. Letters*, 41, 1465-1470, DOI: 10.1002/2013GL059176.

- Stein, C.A., Kley, J., Stein, S., Craddock, J.P., and Malone, D.H., Age of the Jacobsville Sandstone and Implications for the Evolution of the Midcontinent Rift: Geological Society of America Abstracts with Programs, Vol. 47, No. 6.
- Stott, G.M. 2008. Precambrian geology of the Hudson Bay and James Bay lowlands region interpreted from aeromagnetic data – south sheet; Ontario Geological Survey, Preliminary Map P.3599, scale 1:500 000.
- Sutcliffe, R. H. "Proterozoic geology of the Lake Superior area." *Geology of Ontario, Ontario Geological Survey, Special 4. Part 1* (1991): 627-658.
- Sun, W.W., Jackson, M. and Craddock, J.P., 1993, Relationship between remagnetization, magnetic fabric and deformation in Paleozoic carbonates: *Tectonophysics*, v. 221, p. 361-366.
- Sverjensky, D.A., 1986, Genesis of Mississippi Valley-type lead-zinc deposits. *Annu. Rev. Earth Planet. Sci.*, v. 14, 177-199.
- Teufel, L.W., 1980. Strain analysis of experimental superposed deformation using calcite twin lamellae. *Tectonophysics* 65, 291-309.
- Thurston, P. C., Siragusa, G. M., & Sage, R. P. (1977). *Geology of the Chapleau area, Districts of Algoma, Sudbury, and Cochrane* (Vol. 157). Ontario Division of Mines.
- Thwaites, F.T., 1912, Sandstones of the Wisconsin coast of Lake Superior: Wisconsin Geol. and Nat. History Survey Bull. 25, 117 pp.
- Turner, F.J., 1953. Nature and dynamic interpretation of deformation lamellae in calcite of three marbles. *American Journal of Science* 251, 276-298.
- Turner FJ, 1962, Compression and tension axes deduced from (0112) Twinning in calcite: *J Geophys Res* 67:1660.
- Trouw, R.A.J and M.J. DeWitt, 1999, Relation between the Gondwanide Orogen and contemporaneous intracratonic deformation: *Journal of African Earth Sciences* 28, p. 201-213.
- van der Pluijm, B.A., Craddock, John P., Graham, B.R. & Harris, J.H., 1997, Paleostress in cratonic North America: implications for deformation of continental interiors: *Science*, v. 277, p. 792-6.
- Van Schmus, R. 1976. Early and Middle Proterozoic history of the Great Lakes area, North America. *Philos. Trans. R. Soc. A* 280:605-628.
- Van Schmus, R.. 1980. Chronology of igneous rocks associated with the Penokean orogeny in WI. In Morey, G. B., and Hanson, G. N., eds. Selected studies of Archean gneisses and lower Proterozoic rocks, southern Canadian Shield. *Geol. Soc. Am. Spec. Pap.* 182:159-168
- Vervoort, J.D., Wirth, K., Kennedy B., Sandland, T., and Harpp, K.S., 2007. The magmatic evolution of the Midcontinent rift: New geochronologic and geochemical evidence from felsic magmatism. *Precambrian Research*, v. 157, pp. 235-268.
- Watson, J. (1980). The origin and history of the Kapuskasing structural zone, Ontario, Canada. *Canadian Journal of Earth Sciences*, 17(7), 866-875.

- Wheeler, J. R., 1989, K-Ar dating of authigenic K-feldspar in the Butterfly Dolomite (Lower Ordovician), Arbuckle uplift: Evidence of Late Pennsylvanian-Early Permian tectonically-induced diagenesis and implications for timing of Mississippi Valley-type mineralization. M.S. Thesis, University of Tulsa, 135 pages.
- Whitmeyer, S.J., Karlstrom, K.E., 2007. Tectonic model for the Proterozoic growth of North America. *Geosphere* 3, 220–259.
- Webers, G. F. 1972. Paleocology of the Cambrian and Ordovician strata of Minnesota. In Sims, P. K., and Morey, G. B., eds. *Geology of Minnesota: a centennial volume*. St. Paul, MN, Minn. Geol. Surv., p. 474–482.
- Wenk, H-R, T. Takeshita, E. Bechler, BG Erskine, and S. Matthies. 1987. "Pure Shear and Simple Shear Calcite Textures. Comparison of Experimental, Theoretical and Natural Data." *Journal of Structural Geology* 9 (5): 731-745.
- Wiltchko, D.V., Medwedeff, D.A., Millson, H.E., 1985. Distribution and mechanisms of Schstrain within rocks on the northwest ramp of Pine Mountain block, southern Appalachian foreland: a field test of theory. *Geological Society of America Bulletin* 96, 426–435.
- Wiltchko, D.V., and Chapple, W.M., 1977, Flow of weak rocks in Appalachian Plateau folds, *AAPG Bulletin*, v. 61, p.653-670.
- Wilson, J.T. 1968. Comparison of the Hudson Bay arc with some other features. In *Science, history and Hudson Bay*. Edited by C.S. Beals and D.A. Shenstone. Department of Energy, Mines and Resources, Ottawa, Ont., pp. 1015–1033.
- Winchell, N. H., & Upham, W. (1884). *The Geology of Minnesota, Vol. 1 of the Final Report*.
- Winchell, N. H., 1897, Some new features in the geology of north-eastern Minnesota: *Am. Geologist*, v. 20, p. 41-51.
- Wirth, K. R., Naiman, Z. J., & Vervoort, J. D. (1997). The Chengwatana Volcanics, Wisconsin and Minnesota: petrogenesis of the southernmost volcanic rocks exposed in the Midcontinent rift. *Canadian Journal of Earth Sciences*, 34(4), 536-548.
- Woelk, T. S., and Hinze, W. J., 1991, Model of the Midcontinent Rift System in northeastern Kansas: *Geology*, v.19, p. 277-280.
- Woodard, H. H., 1972, Syngenetic sanidine beds from Middle Ordovician Saint Peter Sandstone, Wisconsin. *Journal of Geology*, v. 80, 323-332.
- Zartman, R.E., Nicholson, S.W., Cannon, W.F., Morey, G.B., 1997. U-Th-Pb zircon ages of some Keweenawan Supergroup rocks from the south shore of Lake Superior. *Canadian Journal of Earth Sciences*, v. 34, pp. 549-561.
- Zoback, M.L., and 27 others, 1989, Global patterns of tectonic stress: *Nature*, v. 341, p. 291–298.

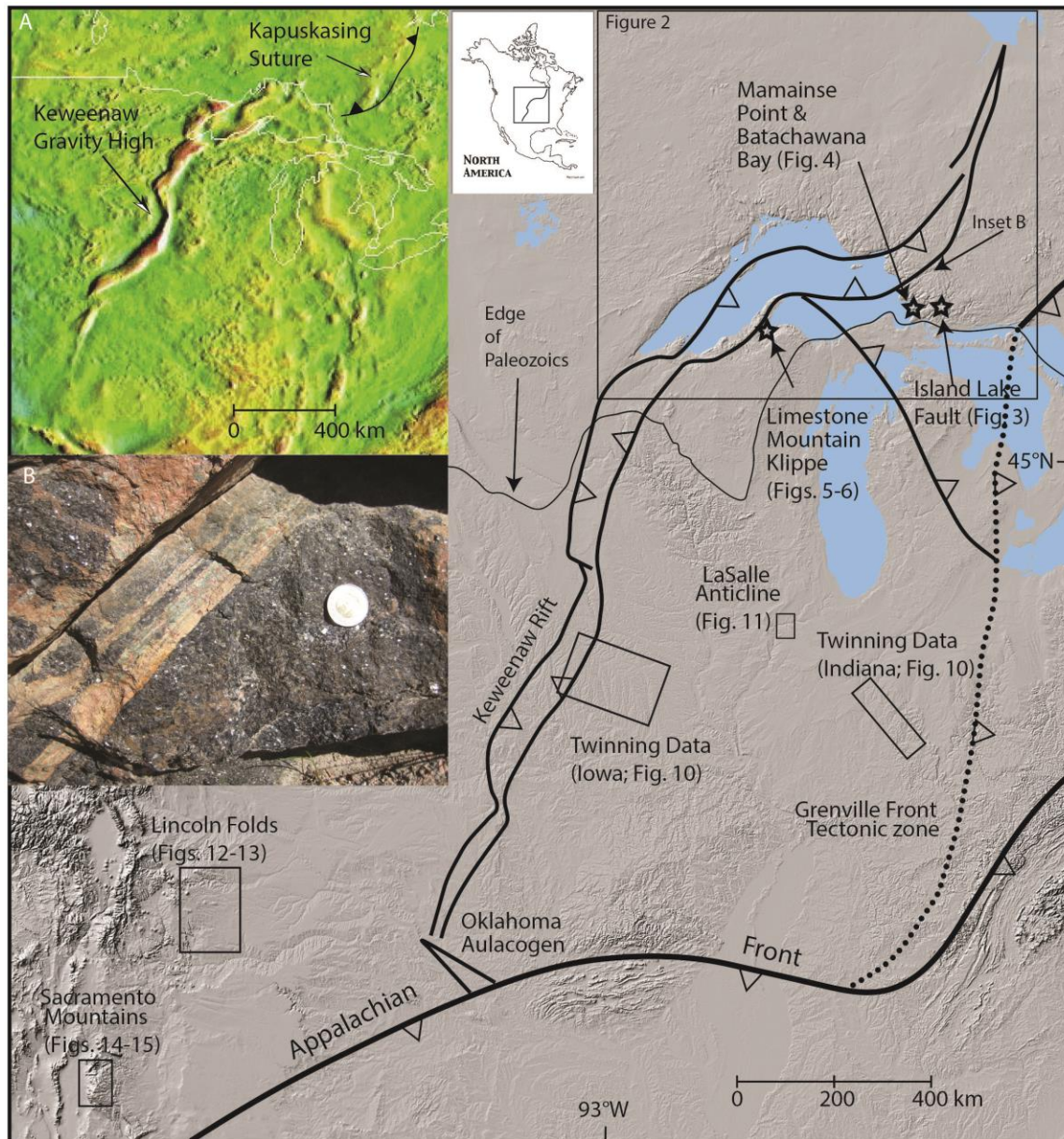


Figure 1: Regional basemap showing the Kapuskasing-Keweenaw fault system, based in part on the Bouguer gravity anomaly map of N. America (inset A) relative to the Grenville tectonic front and the Appalachian front. Inset B is pseudotachylite (1940 Ma; see text) hosted in granulate along the Kapuskasing fault. Study sites across the region are indicated.

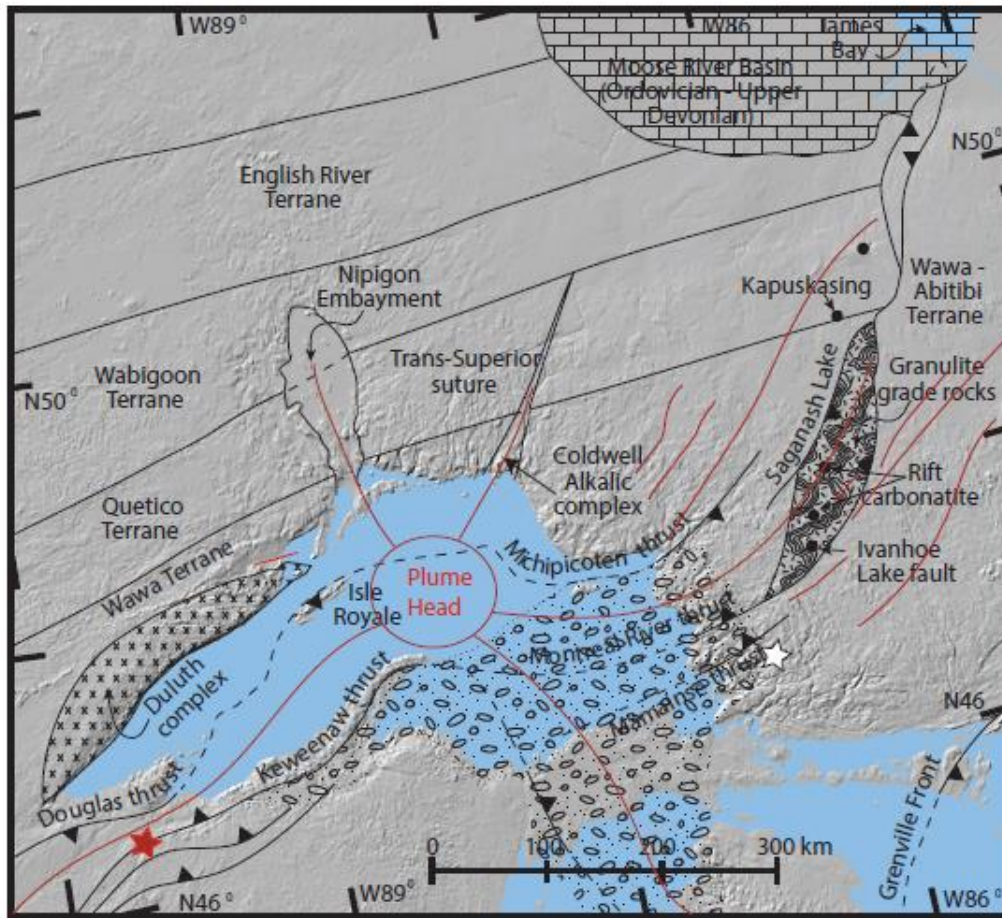


Figure 2: Geologic overview of the Lake Superior region showing the 5 failed arms of the Keweenaw rift system (red) and the post-rift connection of the older Kapuskasing suture with the Keweenaw-Douglas thrusts as a thick-skinned inversion structure (Manson and Halls, 1994, 1997). Shaded regions include the rift-aged Duluth complex, Archean granulites in the hanging wall of the Kapuskasing fault and the Proterozoic Jacobsville Sandstone. Solid circles are rift-aged carbonatites, red lines are the Pigeon River and Abitibi mafic dikes (1141 Ma), the Island Lake sinistral fault is represented by the white star, and the red star is the location of the top-to-the-SE granoblastic mylonite near Mellen, WI (Craddock et al. 2017).

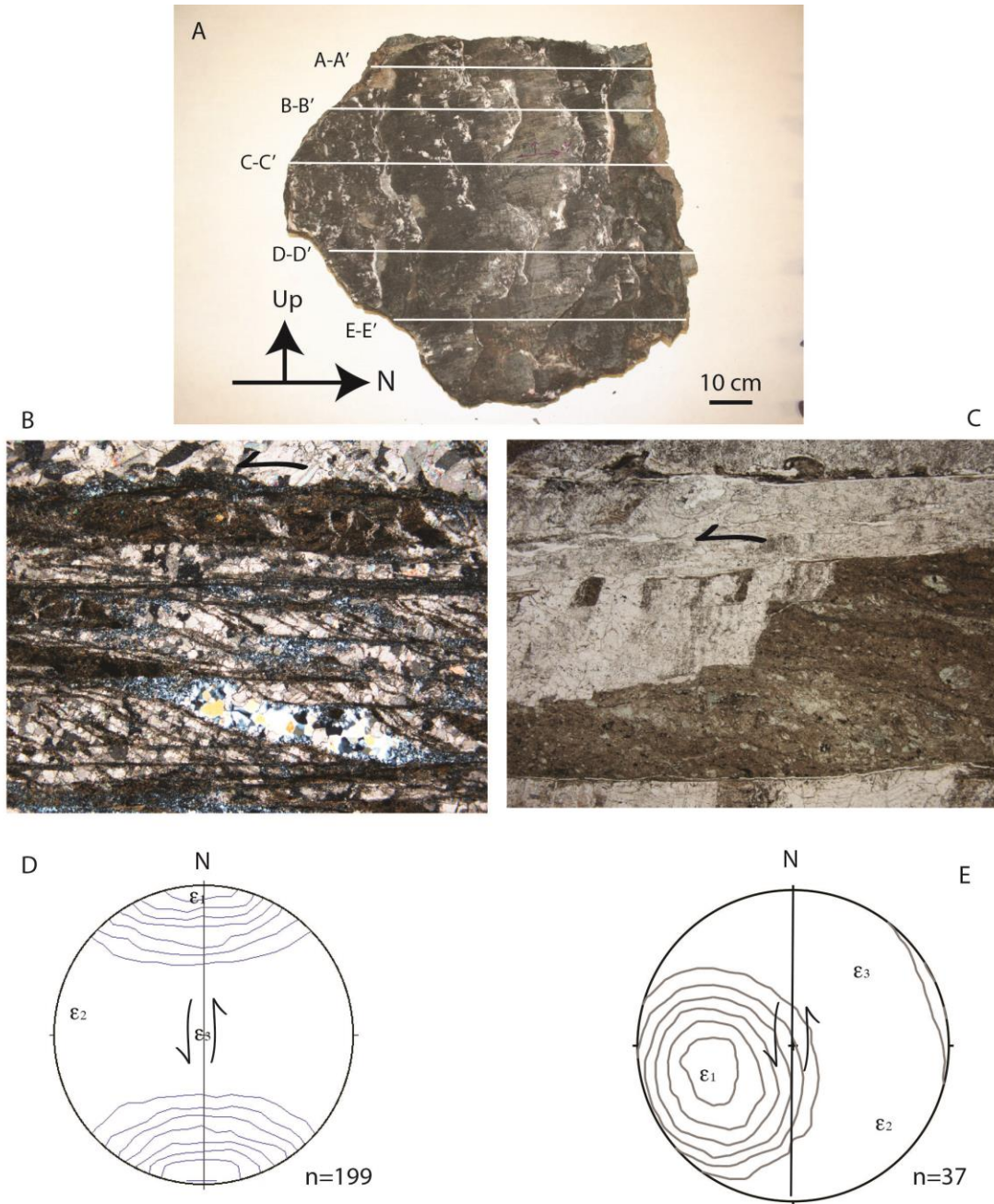


Figure 3: Synfaulting calcite on the Island Lake fault (sinistral) field sample (A), sliced for multiple horizontal thin sections (A-E) which show sinistral kinematics (B & C). Calcite twin results in D (PEV) and E (NEV).

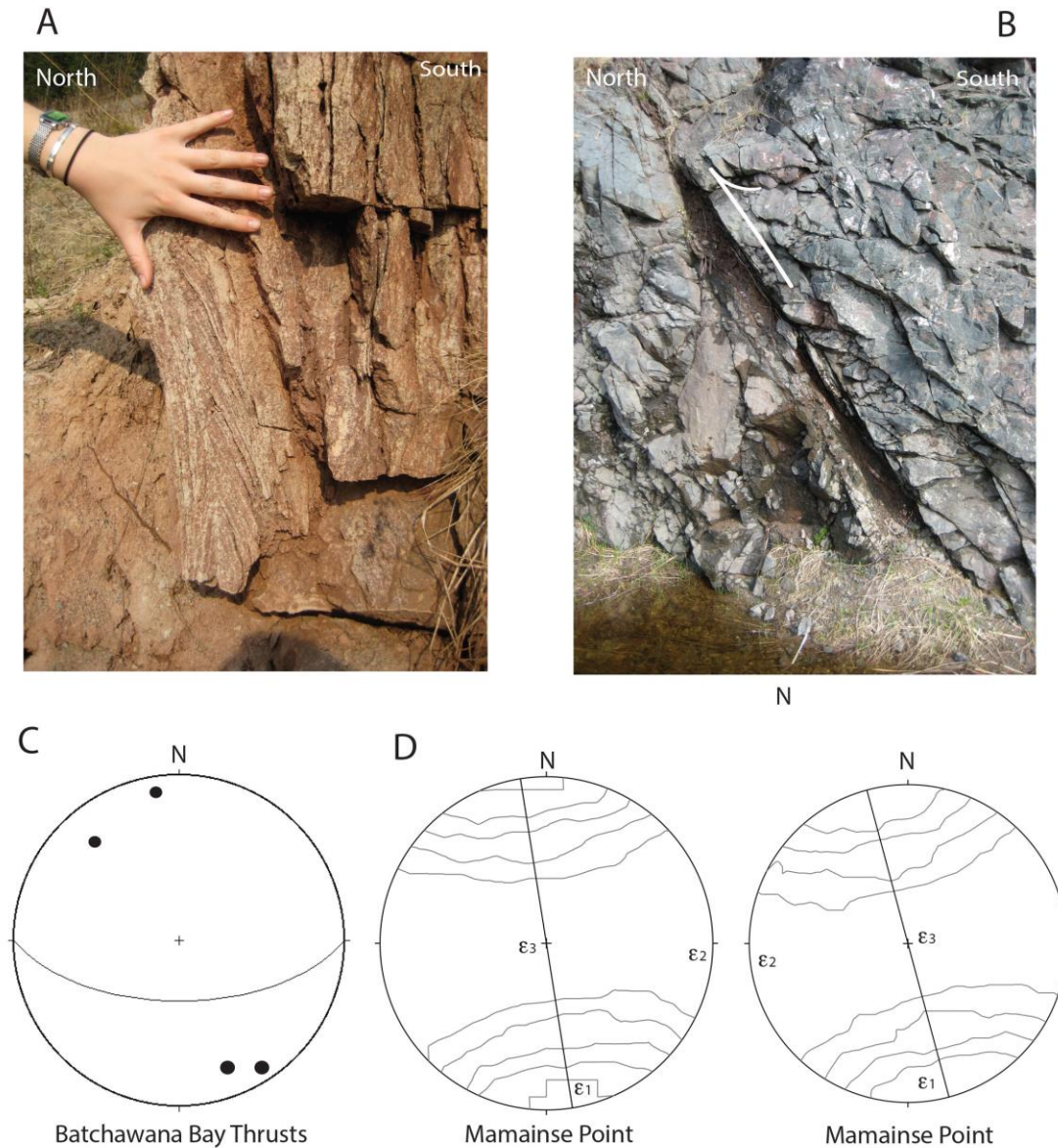


Figure 4: Deformation in Mamainse Point and Batchawana Bay (Figs 1 and 2). A: Overturned crossbeds in the Jacobsville Sandstone. B: South-dipping reverse fault with syn-faulting calcite offsetting rift-aged rhyolites, C: Lower hemisphere projection of shortening axes for calcite twin analyses from 4 syn-faulting calcite samples. Great circle is the fault. D: Calcite strain results for veins crosscutting Mamainse Point rift rhyolites (Table 1).

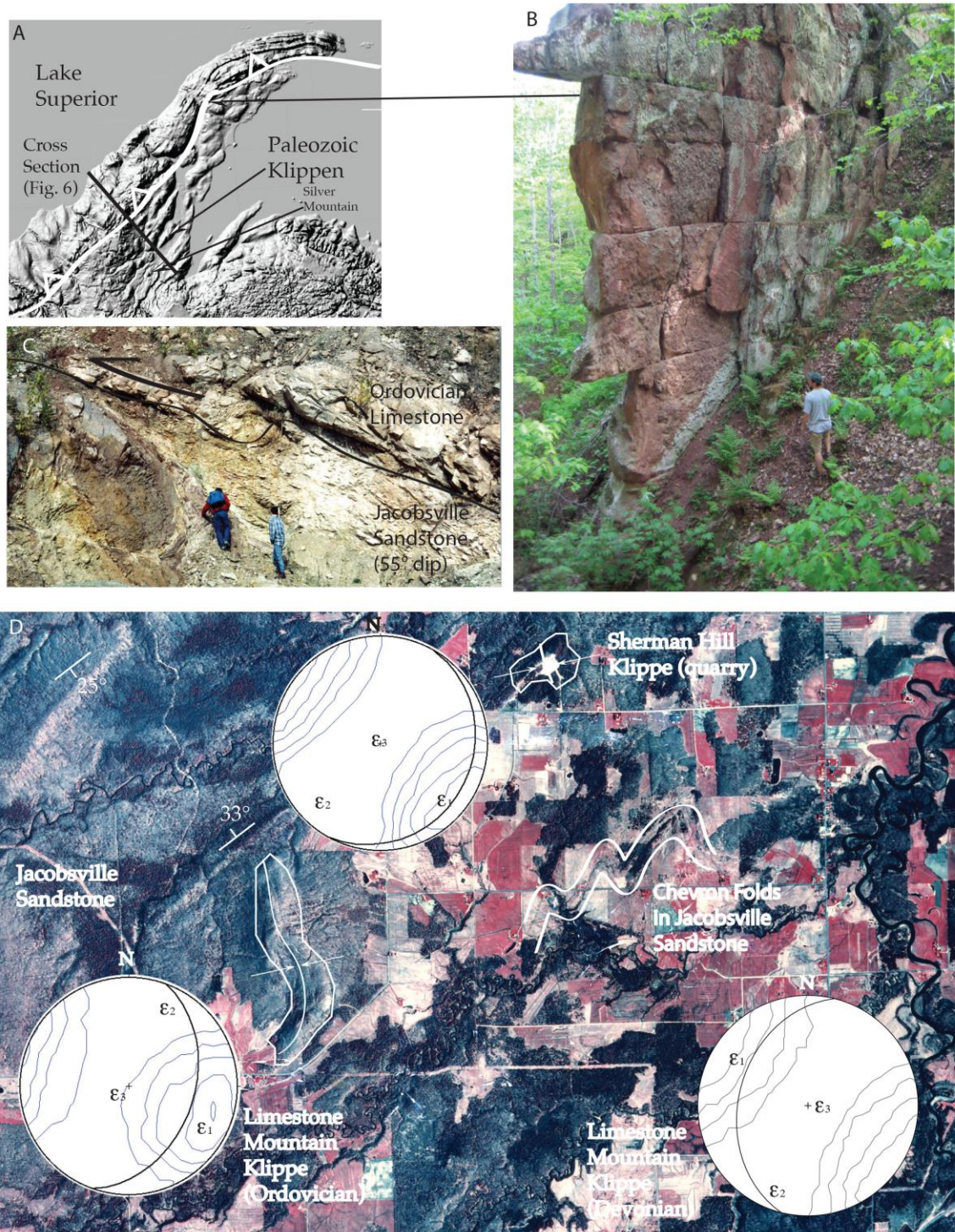


Figure 5: DEM basemap showing the location of the Keweenaw thrust, the Paleozoic outliers in the footwall and the location of the cross section in Fig. 6 (A). Footwall deformation includes the vertical Jacobsville Sandstone at Larium, MI (B), the faulted Jacobsville under the Sherman Hill Ordovician outlier (C), and the north-plunging chevron folds in the Jacobsville on a false-color image (D). Calcite strain data are plotted stereographically (see Table 1).

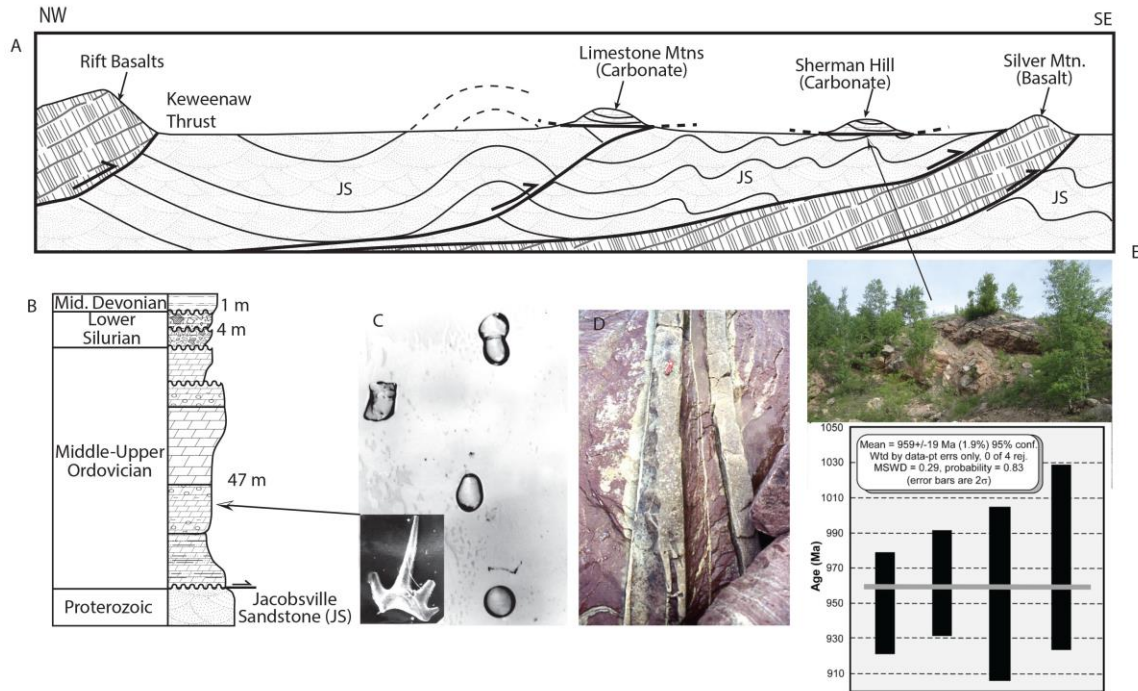


Figure 6: Cross section interpretation for the Keweenaw thrust and Paleozoic limestone klippe (A) with the corresponding stratigraphic column (B). Conodonts confirm the age relations of the section and we also recovered microtektites (Table 3; C). Clastic dikes also cross-cut the Jacobsville Sandstone (D) which can dip 60° as at Sherman Hill quarry (E). The Jacobsville Sandstone has a maximum depositional age of 959 Ma based on 2080 detrial zircons (Malone et al., 2016).

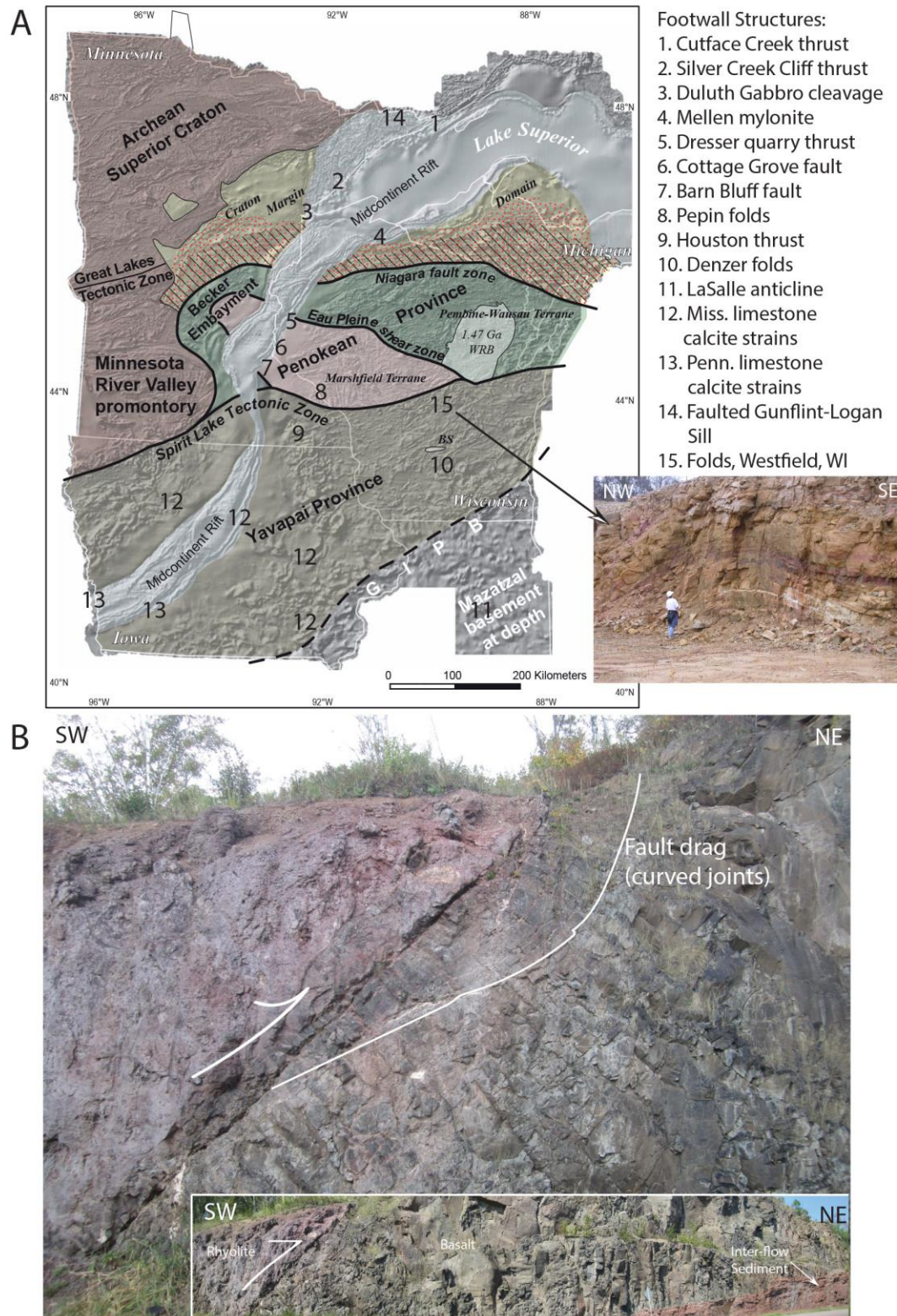


Figure 7: NICE (2007) basemap showing the Keweenaw rift crosscutting Archean and Proterozoic terranes and locations of late Paleozoic footwall structures (A). Thrust fault with a rhyolite breccia over a flat-lying basalt, Cutface Creek along Highway 61 west of Grand Marais, MN (B). Detrital zircon results ( $n=99$ ) for the adjacent interflow sediment are described Craddock et al. 2013 (sample KP-16).

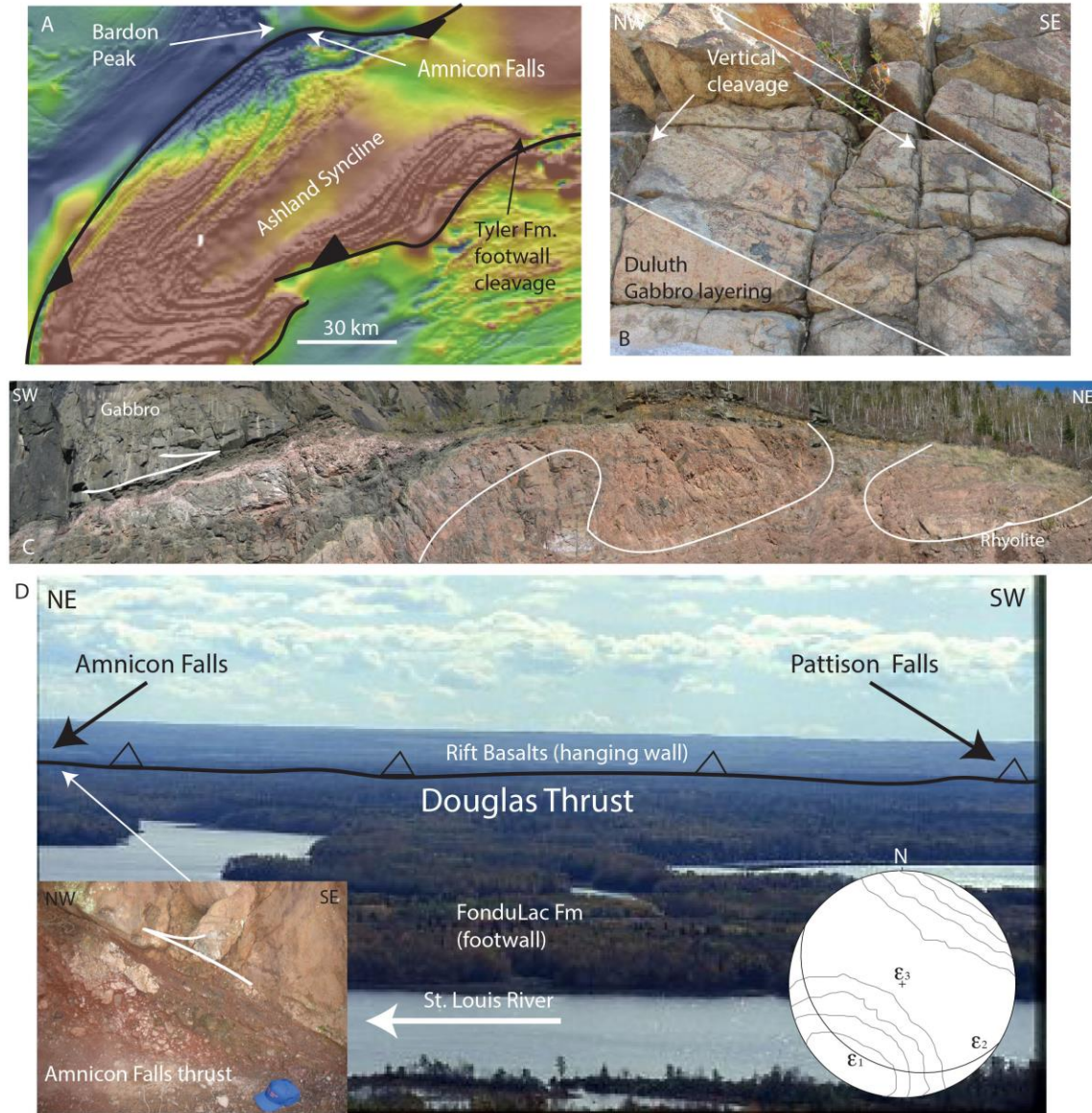


Figure 8: Aeromagnetic basemap showing the internal deformation of the Keweenaw rift (A) and Bardon Peak site (B) with rift-parallel cleavage in the Duluth Gabbro. Composite photo C is from north of the Silver Cliff Creek tunnel on Highway 61 where thrust faulting has offset flow folds in rift-aged rhyolites. View southeast from Bardon Peak (D) shows the Douglas fault scarp. Calcite twinning strain for fault gouge in (C) is plotted on the stereonet inset in D.

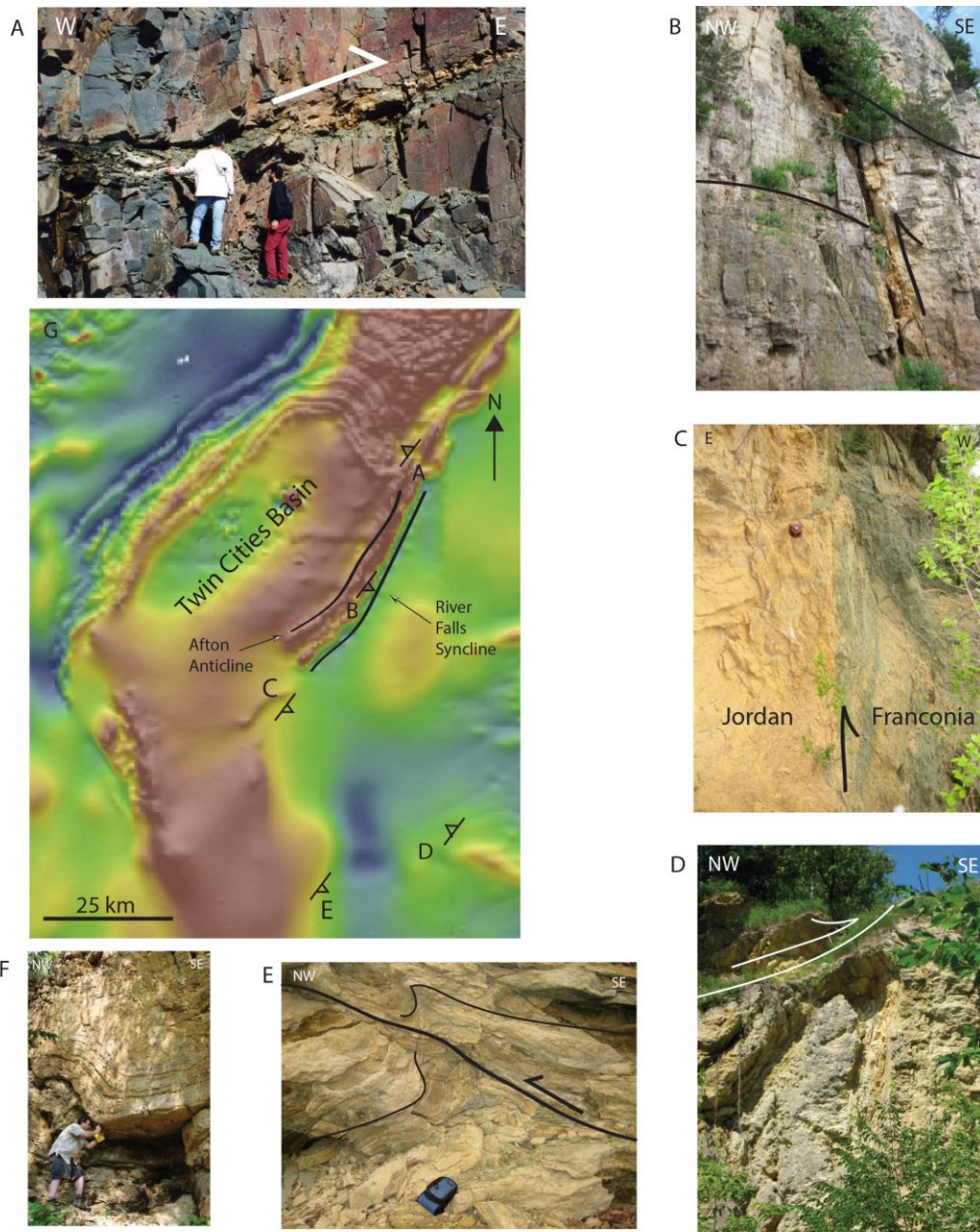


Figure 9: Aeromagnetic basemap of the Twin Cities (Forest City) basin in Minnesota and Wisconsin with offset Chengwatana basalts near Dresser, WI (A), offset Ordovician sediments along the Hastings fault (B), the Red Wing fault (C; Barn Bluff), overthrust and folded Ordovician carbonates near Lake Pepin, WI (D), drag folds along a thrust in the Cambrian Franconia Fm., Houston, MN (E) and folded Ordovician carbonates near Denzer, WI (F). See Figure 7 for additional details.

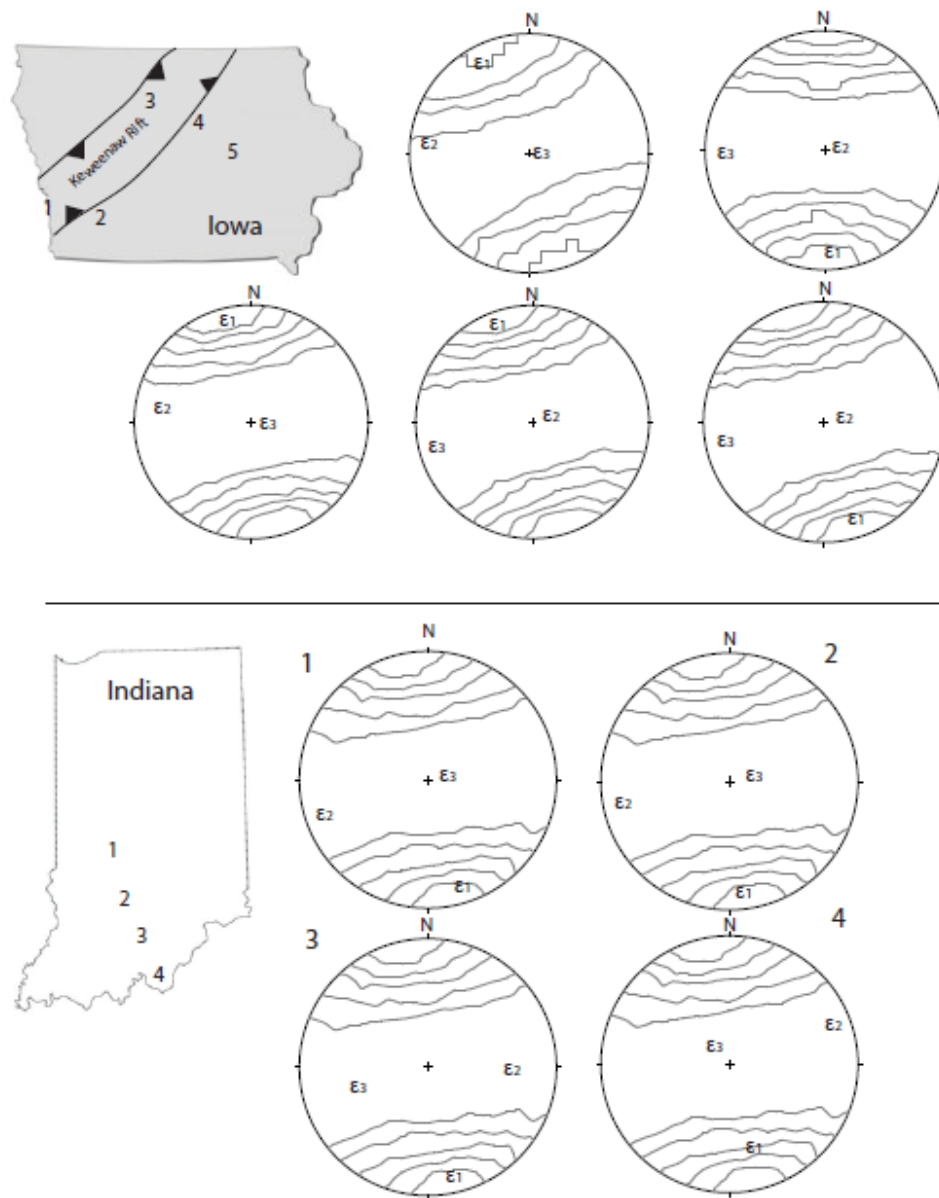


Figure 10: Calcite twinning results from the Mississippian and Pennsylvanian of Iowa (top) and the Mississippian of Indiana. Lower hemisphere projections, bedding is horizontal. See Table 1.

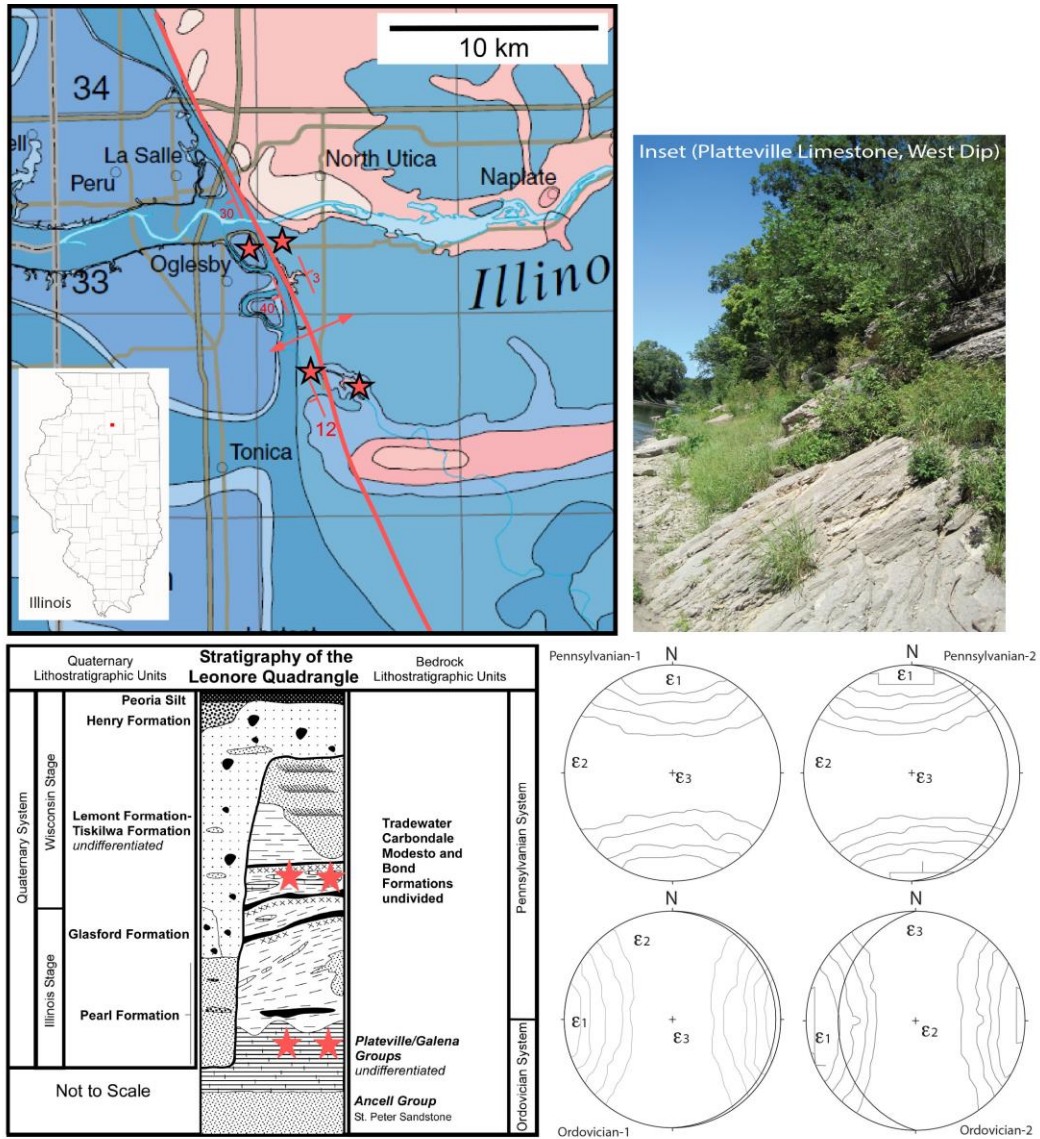


Figure 11: Bedrock geologic map of the LaSalle County, area, Illinois (from Kolata, 2005). Bedrock exposures are limited to quarries and stream cuts along the Illinois River and its tributaries. Red stars = sampling localities. The trace of the axis of the LaSalle Anticline is indicated. Blue = Pennsylvanian strata; Pink = Ordovician strata (see inset field photo). Lower hemisphere plots are for the four calcite twinning strain samples (Table 1).

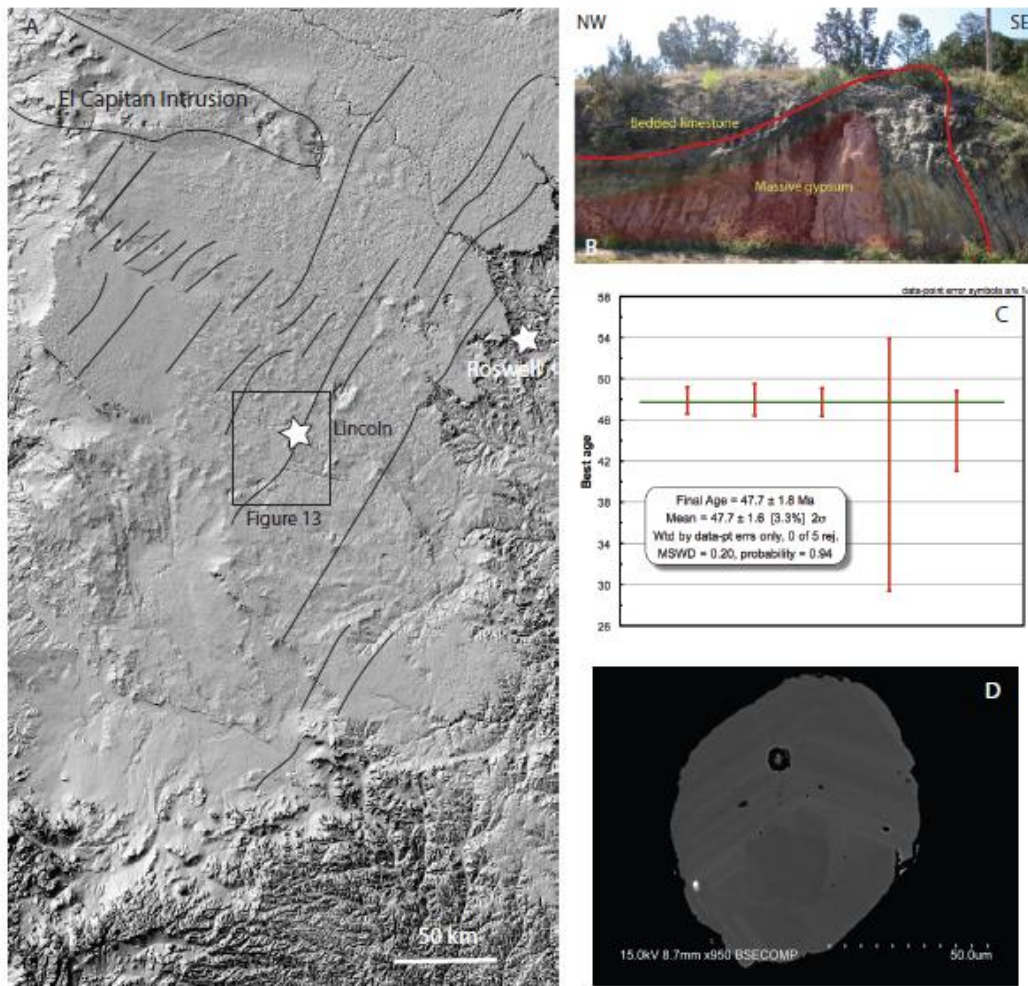


Figure 12: Traces of the Lincoln fold anticlines of east-central New Mexico exposed near the Cretaceous El Capitan intrusion and north of the Marathon fold and thrust belt (A). One example of a Lincoln fold (B) is cored by evaporites (photo from J. Amato). The folds are crosscut by a monzonite with zircons that yield a crystallization age of 47.7 Ma (C) from rounded zircons (D; backscatter image).

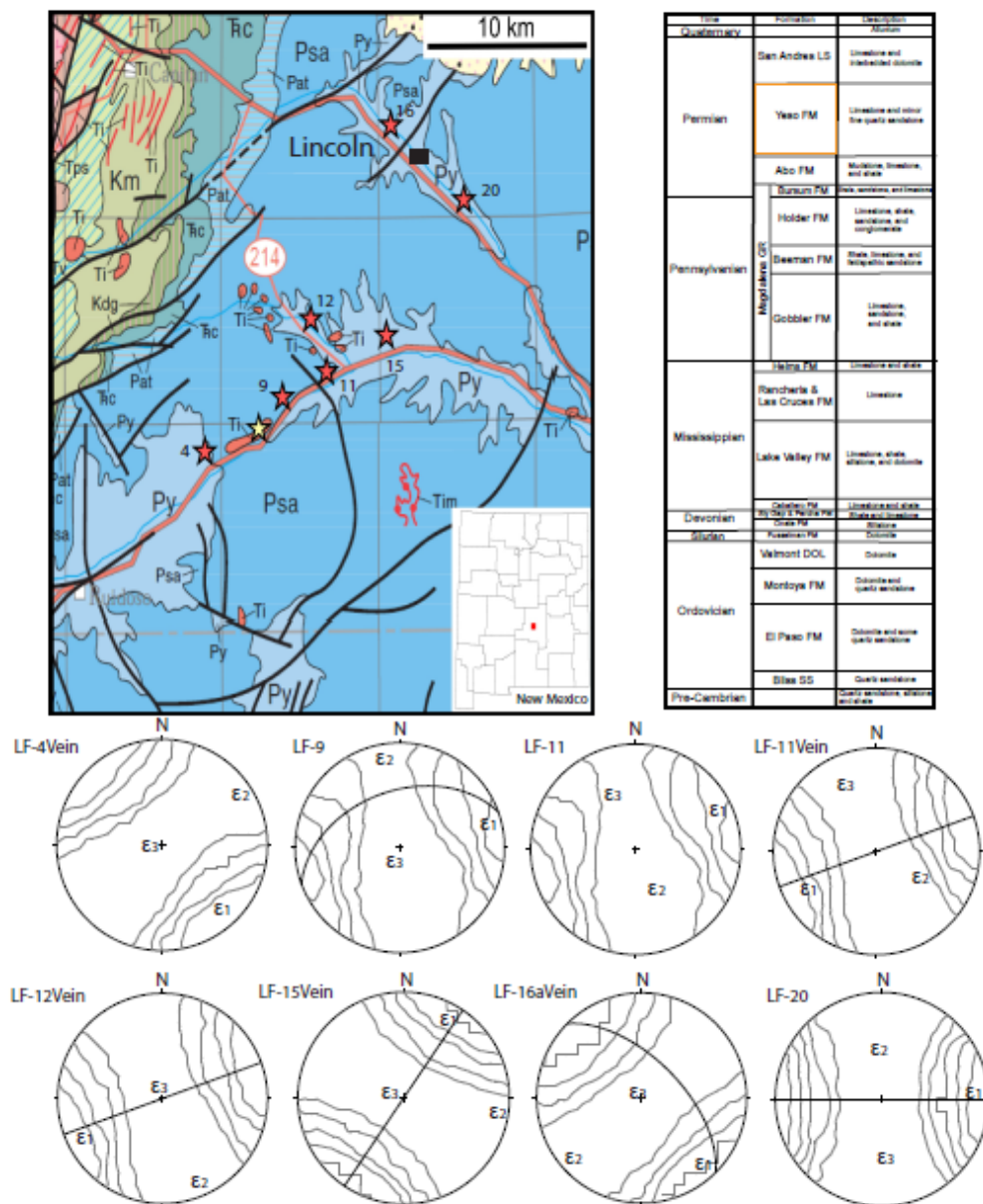


Figure 13: Geologic basemap (see outline on Fig. 12) from Jones (1994) with red stars the locations of calcite twinning samples and the yellow star the location of the dated monzonite. All samples from the Permian Yeso Fm. (see stratigraphic column, upper right; orange box highlights Yeso Fm.). Lower hemisphere stereoplots include principal strain axes, contoured Turner compression axes and either bedding or vein great circles (see Table 1).

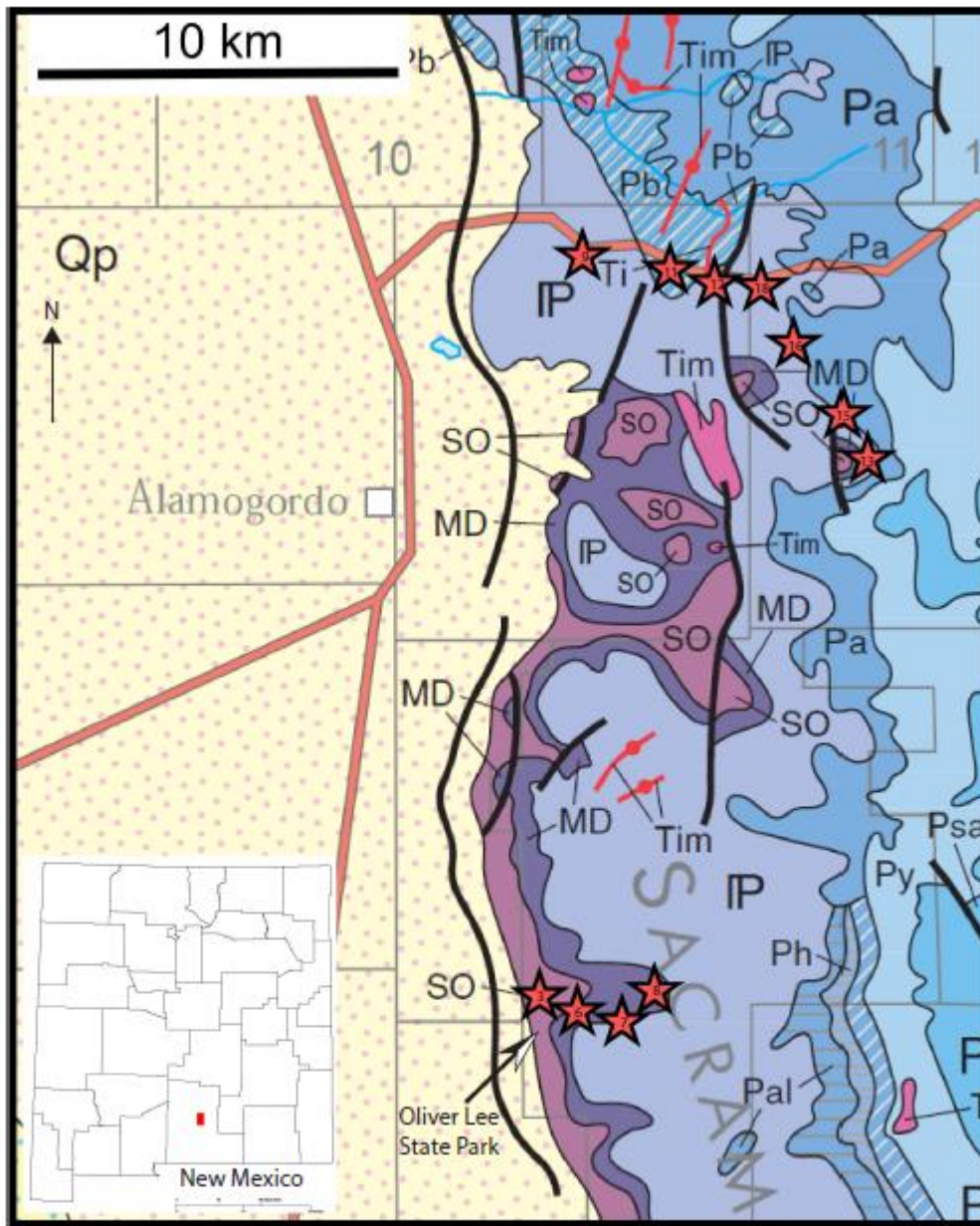
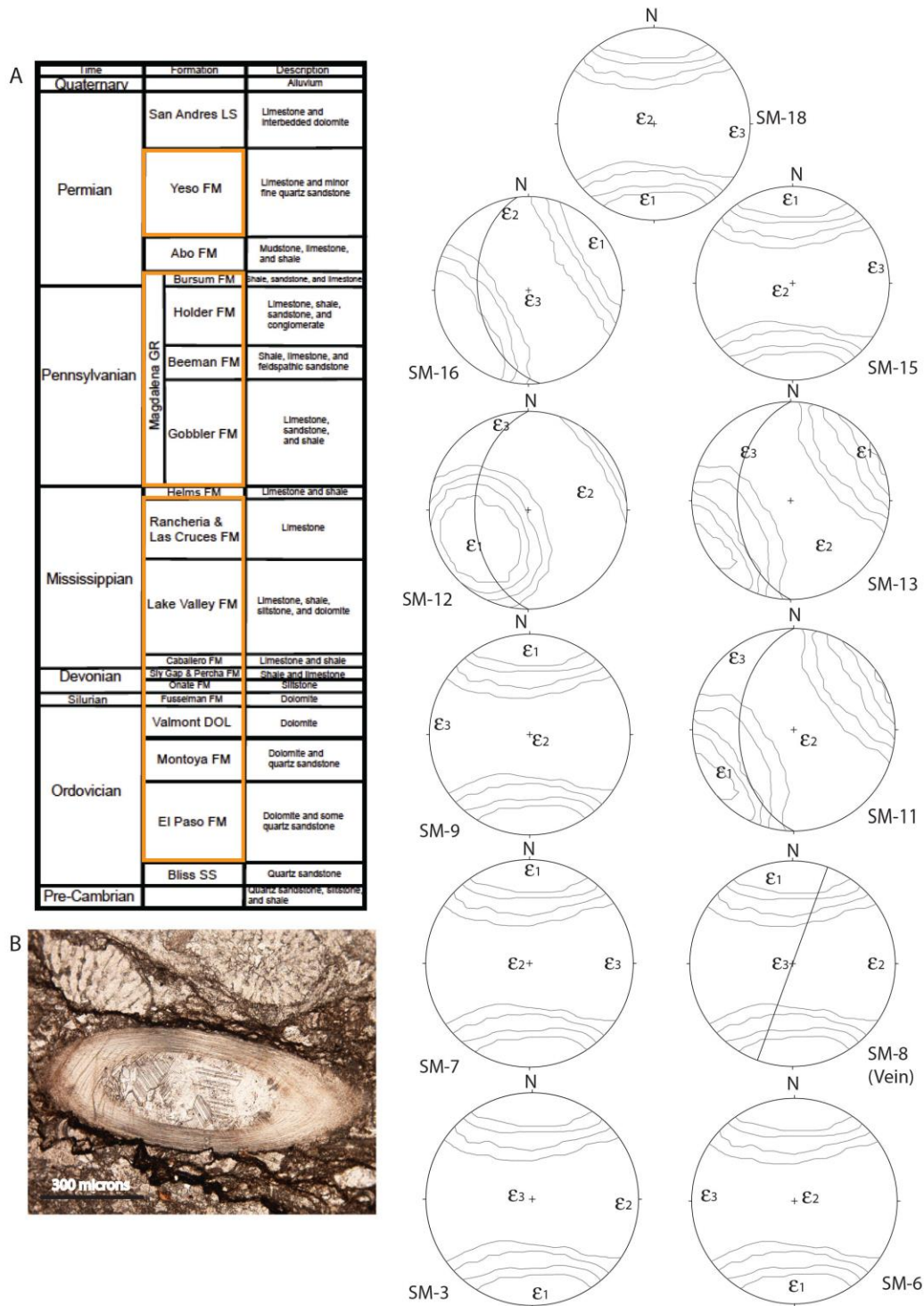


Figure 14: Geologic map of the western Sacramento Mountains, NM (modified from Scholle, 2003) with inset map of N. Mexico. Sampling localities are indicated by red stars (samples 3, 6-9 from Oliver Lee Park, others from the north). Yellow = Quaternary; Purple = Ordovician-Mississippian; Blue = Pennsylvanian and Permian; Tim = Tertiary intrusive rocks. See Figure 15 and Table 1.



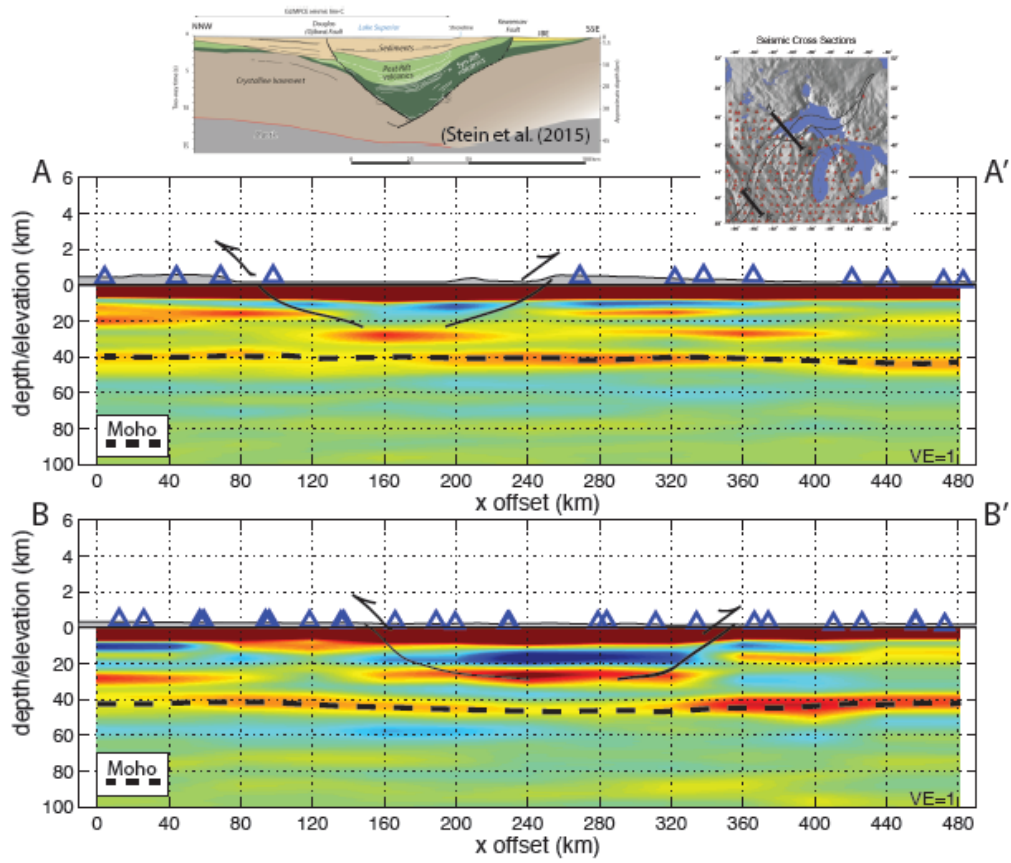


Fig. 16

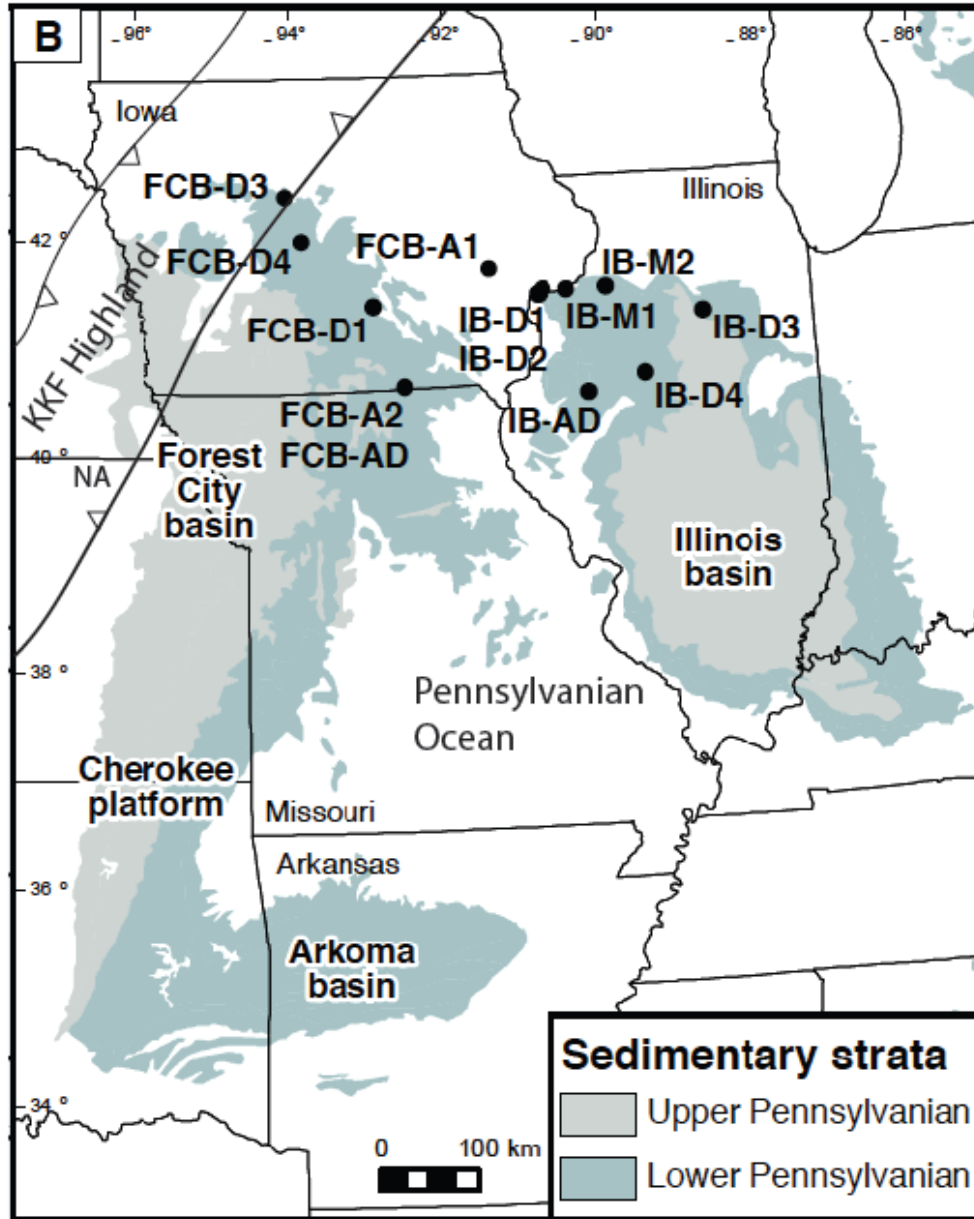


Figure 17: Mississippian-Permian features in the Midcontinent along the KKF including the structurally high Mississippian Nemaha Arch (NA), deposition of Pennsylvanian sediments east of the KKF which include detrital zircons (sample sites indicated) only from eastern sources (Kissock et al. 2016), and the lack of Permian sedimentation east of the KKF.

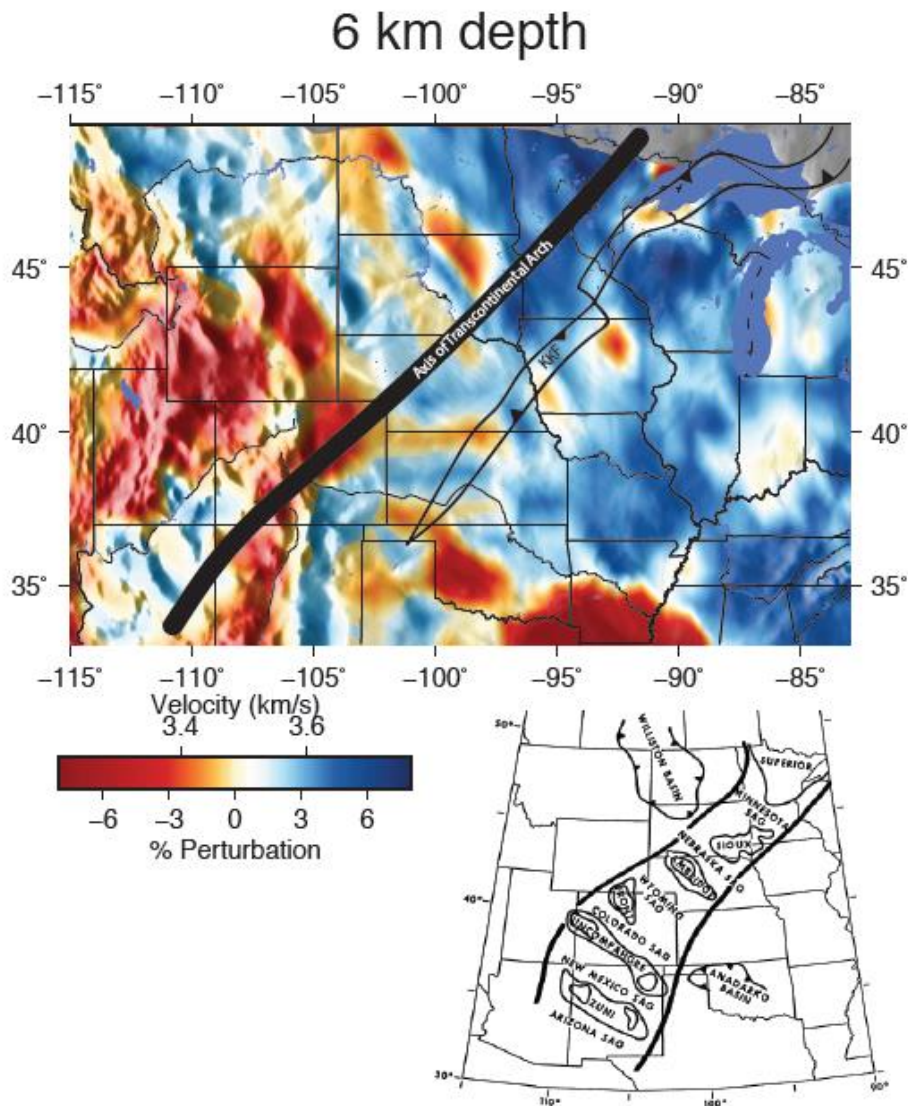


Figure 18: Shear wave velocities at 6 km calculated using ambient noise tomography and wave gradiometry (Porter et al., 2016; percent perturbation is calculated from the average for the region) with the supracrustal sediments removed to accentuate the relationship of the KKF and the Transcontinental Arch (Carlson, 1999).

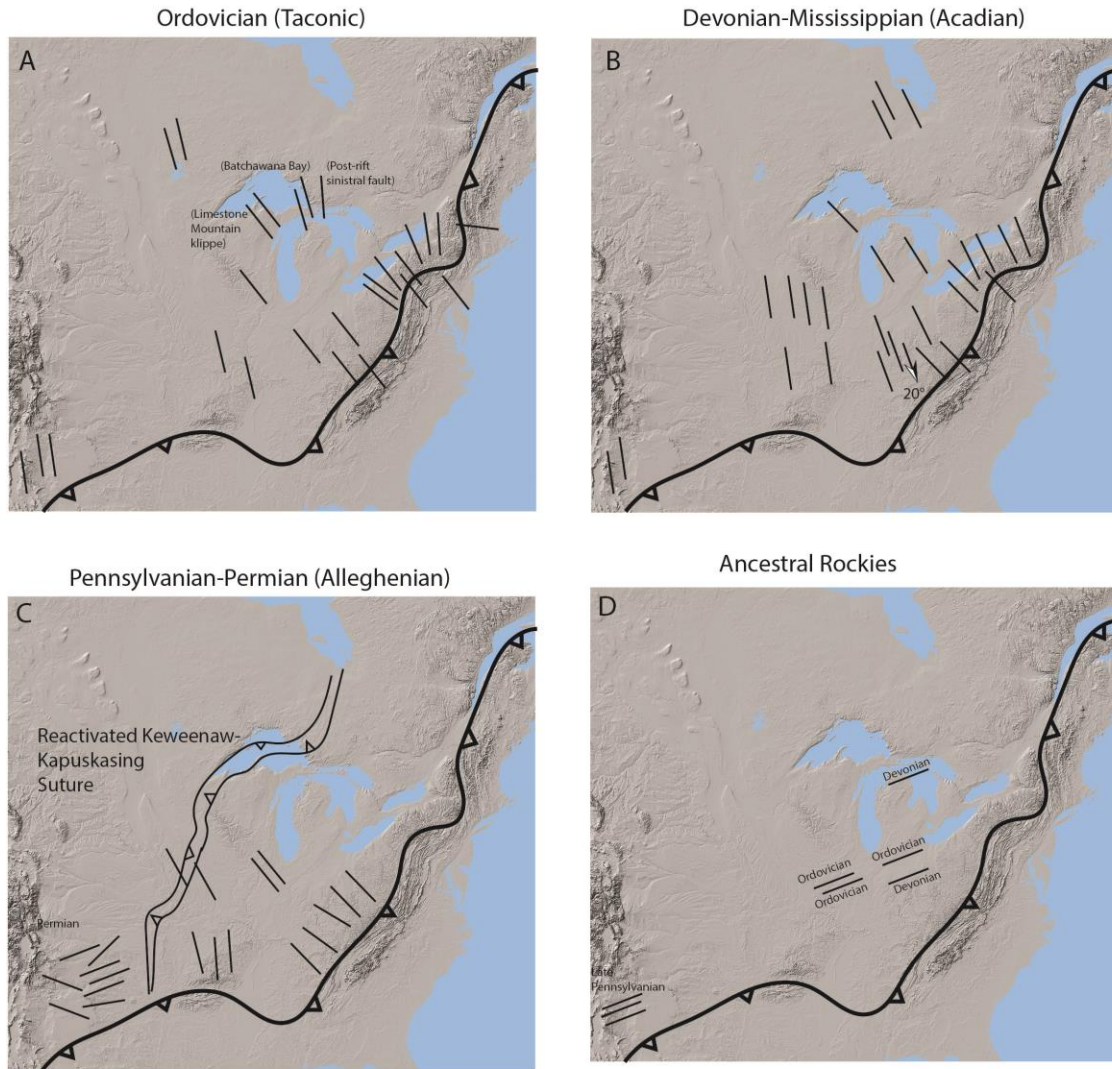


Figure 19: Layer-parallel shortening strain ( $e_1$  axes; Table 1, Appendices 1 & 2) recorded by twinned calcite presented by age of host limestone and correlative Appalachian-Ouachita-Marathon orogenic stages (A-C). Figure D includes shortening axes hosted by late Pennsylvanian limestones in the proximal Ancestral Rockies foreland and other AOM misfits that are better interpreted with this data grouping (eastern 3 samples from Craddock and van der Pluijm, 1989 and Craddock et al. 1993).

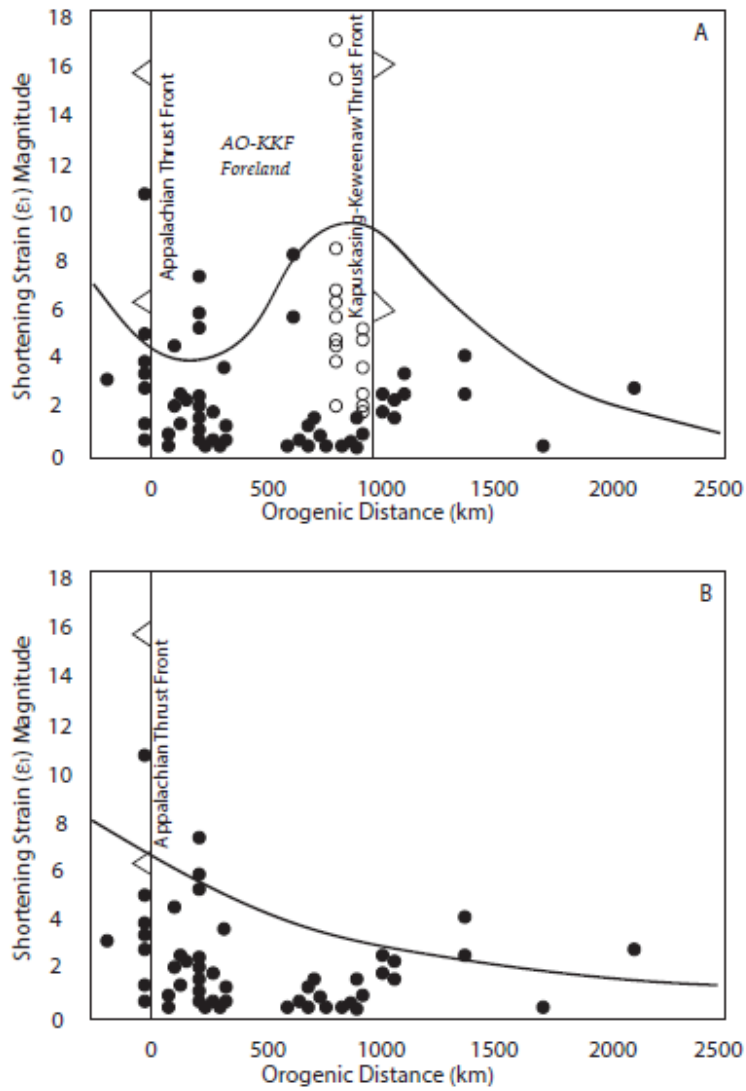


Figure 20: Layer-parallel shortening strain calcite twinning data for the Appalachian-Ouachita thrust belt and foreland (Appendices 1 and 2) with all the data (A) and then with the data proximal to the KKF removed (B). Closed circles are twinning strains for limestones, open circles are for veins (Table 1).

Y

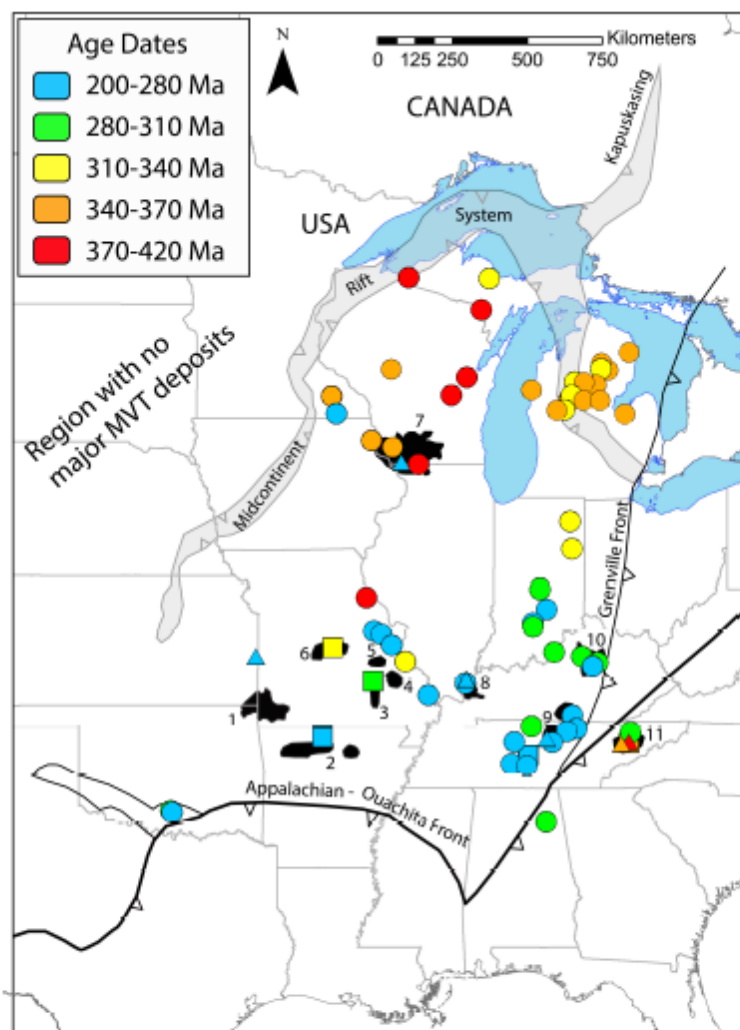


Figure 21: Map showing age dates for diagenetic minerals in the Midcontinent region of the United States. Major Mississippi Valley-type ore districts include: (1) Tri-State, (2) Northern Arkansas, (3) Viburnum Trend, (4) Old Lead Belt, (5) Southeast Missouri Barite, (6) Central Missouri Barite, (7) Upper Mississippi Valley, (8) Illinois-Kentucky Fluor spar, (9) Central Tennessee and Kentucky, (10) Central Kentucky, (11) Eastern Tennessee. Shapes indicate types of age dating techniques used: triangles indicate various age dates on ore-stage minerals such as sphalerite and calcite; circles indicate ages dates on on K-silicate minerals (feldspare and illite-smectite); and squares indicate paleomagnetic age dates. Age ranges for colors are shown in the inset legend. Data are from Duffin et al. (1989), Elliot and Aronson (1993), Girard and Barnes (1995), Hay et al. (1988), Leach et al. (2001, and references therein), Liu et al (2003), Marshal et al. (1986), Matthews (1988), Nakai et al. (1990), Robinson and LaBerge (2013) and Wheeler (1989).

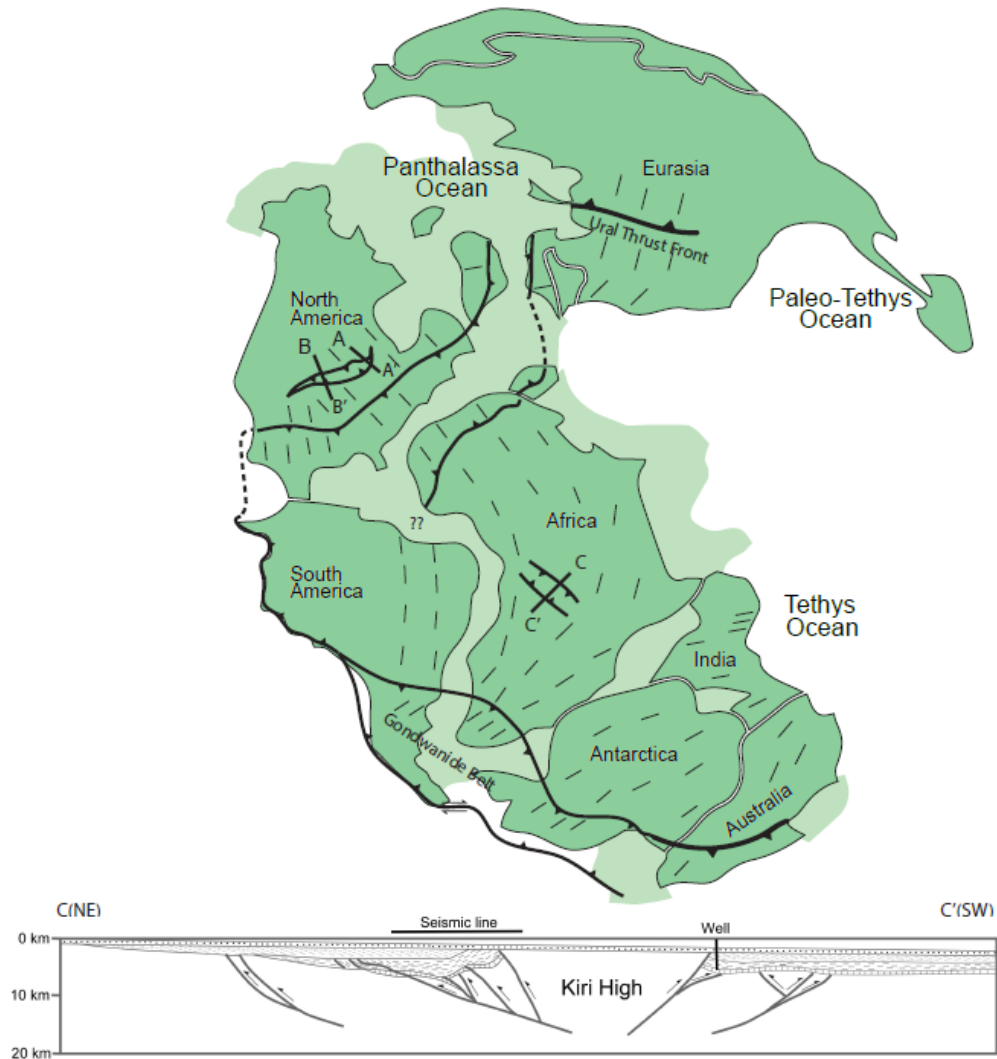


Figure 22: Pangea at ~240 Ma with closure of the Atlantic Ocean and corresponding orogenic belts (Alleghenian and Hercynian-Atlas) in the north, and the oblique Gondwanide orogen on the southern margin of Gondwana. Thick black lines are layer-parallel shortening axes, thin lines are the projection of that strain field across continents. Cross sections A-B, across the KKF, are from Figure 16 and the Kiri uplift profile is included here (Daley et al. 1991; C-C').

AC

Table 1: Calcite Twinning Strain Results

Kapuskasung Sinistral Shear Zone, Ontario													
Sample	Rock Unit	Fault		Grains (n=)	$\epsilon_1$	$\epsilon_2$	$\epsilon_3$	$\epsilon_1$ (%)	NEV (%)	$\Delta\sigma$ (bars)	Fabric Interp.	Orogenic Distance (km)	Comment
		Orientation											
1A	Striated Calcite	N0°E, 90°		36	1°, 2°	270°, 3°	116°, 87°	-6.9	1	-337	FPS	800	Top
2A	Striated Calcite	N0°E, 90°	No twins										
2B	Striated Calcite	N0°E, 90°		37	352°, 8°	82°, 1°	176°, 81°	15.5	1	-377	FPS	800	
3A	Striated Calcite	N0°E, 90°	No twins										
3B	Striated Calcite	N0°E, 90°		36	177°, 2°	267°, 2°	71°, 89°	17.1	11	-363	FPS	800	
4A	Striated Calcite	N0°E, 90°		22	302°, 22°	210°, 6°	106°, 66°	4.57	22	-351	FPS	800	
4B	Striated Calcite	N0°E, 90°	No twins										
5A	Striated Calcite	N0°E, 90°		10	159°, 8°	250°, 3°	1°, 81°	-6.5	0	-297	FPS	800	
5B	Striated Calcite	N0°E, 90°		36	173°, 4°	263°, 2°	5°, 85°	2.09	1	-386	FPS	800	
6A	Striated Calcite	N0°E, 90°		27	154°, 20°	60°, 11°	303°, 66°	-3.9	1	-354	FPS	800	
6B	Striated Calcite	N0°E, 90°		23	342°, 3°	211°, 84°	72°, 3°	-4.9	13	-357	FPS	800	Bottom
AL	Striated Calcite	N0°E, 90°		236	346°, 4°	256°, 2°	80°, 86°	-8.6	14	-368	FPS	800	
PEV	Striated Calcite	N0°E, 90°		199	353°, 4°	83°, 2°	165°, 85°	-	0	-343	FPS	800	

NE	Calcite	90°					6.09						
V	Striated Calcite	N0°E, 90°	37	248°, 30°	142°, 25°	19°, 48°	-5.2	100	-356	FPS	800		
							- 7.39						
		<b>Bedding</b>		<b>Batchawana Bay Shear Zone, Ontario</b>									
1	Synfaulting Calcite	310°, 60°S	36	303°, 2°	17°, 3°	159°, 86°	-1.8	8	-353	LPS	900	South	
2	Synfaulting Calcite	310°, 80°S	30	137°, 9°	258°, 5°	348°, 87°	5	1	-388	LPS	900		
3	Synfaulting Calcite	Horizo ntal	30	141°, 5°	225°, 3°	355°, 83°	2.05	6	-371	LPS	900		
4	Synfaulting Calcite	310°, 60°S	22	351°, 15°	280°, 6°	140°, 87°	5	1	-434	LNS	900	North	
5	Mamainse Point	345°, 90°	35	355°, 14°	88°, 8°	197°, 82°	-5.2	5	-372	VPS	900	Vein	
6	Mamainse Point	351°, 90°	37	3°, 5°	273°, 7°	98°, 83°	4.78	7	-368	VPS	900	Vein	
				<b>Silver Creek Cliff, Minnesota</b>									
1	Keweenaw Gabbro	301°, 28°SW	36	211°, 21°	109°, 3°	348°, 86°	-2.6	2	-323	LPS	Not Applicable	Fault gouge	
				<b>Limestone Mountain Klippe, Michigan</b>									
1	Devonian Limestone	N14°E, 37°N	42	326°, 25°	209°, 2°	107°, 81°	- 3.28	8	-366	LPS	1100	Limesto ne Mtn.	East Limb
2	Ordovician Limestone	N18°E, 27°S	37	116°, 17°	15°, 19°	262°, 83°	- 2.51	6	-343	LPS	1100	Limesto ne Mtn.	West Limb
3	Ordovician	N28°E,	34	133°, 4°	238°, 5°	347°,	-	11	-348	LPS	1100	Sherman	West

	Limestone	6°SE				86°	2.44					Hill	Limb	
<b>Iowa</b>														
1	Pennsylvania	Horizontal	19	323°, 6°	261°, 3°	112°, 88°	-	0.42	10	-295	LPS	600	Crescent	Dennis LS
2	Pennsylvania	Horizontal	31	172°, 5°	87°, 84°	268°, 4°	-	0.47	6	-323	LPS	620	Monarch	Dennis LS
3	Mississippi	Horizontal	24	343°, 3°	261°, 8°	117°, 83°	-	0.12	8	-342	LPS	700	Gilmore City	Eagle City LS
4	Mississippi	Horizontal	34	339°, 8°	72°, 81°	253°, 11°	-	-0.2	8	-324	LPS	670	Iowa Falls	Eagle City LS
5	Mississippi	Horizontal	15	171°, 5°	54°, 82°	251°, 2°	-	0.23	13	-352	LPS	650	LaGrand e	Eagle City LS
<b>LaSalle Anticline, Illinois</b>														
1	MacLeansburg Group		No twins										East Limb	Pennsylvanian
2	MacLeansburg Group	Horiz.	20	351°, 2°	271°, 3°	149°, 86°	-	-5.8	0	-278	LPS	600	Fold Hinge	Pennsylvanian
3	MacLeansburg Group	N-S, 12°E	36	355°, 5°	145°, 73°	265°, 3°	-	-8.3	0	-314	LPS	600	East Limb	Pennsylvanian
4	Platteville LS	N-S, 7°W	18	273°, 12°	6°, 12°	133°, 77°	1.72	5	11	-308	LPS	600	West Limb	Ordovician
5	Platteville LS	N-S, 30°W	18	268°, 15°	117°, 74°	352°, 7°	-	3.05	0	-256	LPS	600	West Limb	Ordovician
<b>Indiana</b>														
1	Valmeyeran Limestone	Horizontal	27	151°, 3°	254°, 4°	13°, 85°	-	2.24	11	-341	LPS	150	North	St. Louis Fm.
2	Valmeyeran Limestone	Horizontal	22	173°, 5°	258°, 4°	38°, 83°	-	1.37	9	-319	LPS	130		Salem Fm.
3	Valmeyeran Limestone	Horizontal	16	153°, 2°	47°, 13°	307°, -	-	-	12	-319	LPS	120		St.



		45°E				87°	3.00					vanian
							%					
							-					
15	Gobbler Fm.	Horizontal	36	4°, 03°	226°, 83°	87°, 6°	1.40		3	-372	LPS	Pennsylvanian
14	Gobbler Fm.	N-S, 45°W	Micrite				%					Pennsylvanian
13	Laborcita Fm. (Vein)	N-S, 45°W	38	63°, 02°	194°, 42°	333°, 48°	12.10	21.0		-382	LPS	Latest Penn.
12	Holder Fm.	N-S, 45°W	38	243°, 41°	68°, 12°	341°, 26°	1.80	5.0		-346	LPS	Pennsylvanian
11	Holder Fm.	N-S, 45°W	36	247°, 28°	336°, 18°	95°, 84°	1.30	13.0		-304	LPS	Pennsylvanian
10	Rancheria Fm.	N-S, 45°W	Micrite				%					Mississippian
9	Lake Valley Fm.	Horizontal	36	357°, 4°	275°, 12°	346°, 48°	2.10		13	-314	LPS	Mississippian
8	Caballero Fm. (L. Lake)	Horizontal	38	348°, 4°	78°, 2°	238°, 88°	2.00	8.0		-394	LPS	Mississippian
							%					Vein: 20°, 90°
7	Sly Gap Fm.	Horizontal	36	3°, 6°	227°, 86°	86°, 4°	1.30	8.0		-362	LPS	Devonian
6	Onate Fm.	Horizontal	38	181°, 5°	47°, 85°	268°, 05°	5.10	10.0		-350	LPS	Devonian
5	Fusselman Fm.	Horizontal	Micrite				%					Ordovician
4	Valmont Fm.	Horizontal	Micrite				%					Ordovician

3	Montoya Fm. Upper El	Horizontal	29	175°, 5°	77°, 4°	315°, 84°	- 1.10 %	15.0	-347	LPS	Ordovician
2	Paso Fm. Middle El	Horizontal	Micrite								Ordovician
1	Paso Fm.	Horizontal	Micrite								Ordovician

ACCEPTED MANUSCRIPT

**Table 2: O and C Isotopes from Synfaulting Calcite**

	<b>d13C</b> <b>(VPDB)</b>	<b>d18O</b> <b>(VPDB)</b>
KSZ-1	-8.63	-15.22
KSZ-2	-8.46	-17.09
KSZ-3	-8.75	-15.60
BB-1	-4.46	-8.28
BB-2	-5.73	-18.93
BB-3	-5.39	-13.31
BB-5	-5.08	-16.57
MP-1	-5.31	-15.32
MP-2	-5.37	-16.01

KSZ-Kapuskasing strike-slip samples

BB-Batchawana Bay samples

MP-Mamainse Point

Table 3

Sample / Wt. %	Major-Element Analyses of Microtektites by Electron Microprobe, Limestone Mountain															
	G1-1	G1-2	G1-3	G1-4	G1-5	G2-1	G2-2	G2-3	G2-4	G2-5	G3-1	G3-2	G3-3	G3-4	G3-5	G3-6
SiO <sub>2</sub>	71.38	71.67	71.23	71.82	71.98	71.47	71.68	70.72	71.37	71.09	72.76	72.69	71.89	72.94	72.47	72.63
TiO <sub>2</sub>	0.05	0.04	0.02	0.03	0.02	0.05	0.06	0.03	0.02	0.04	0.02	0.03	0.03	0.02	0.03	0
Al <sub>2</sub> O <sub>3</sub>	1.39	1.4	1.42	1.39	1.42	1.41	1.43	1.4	1.39	1.41	1.23	1.16	1.2	1.2	1.31	1.22
FeO	0.09	0.01	0.04	0.06	0.07	0.06	0.06	0.04	0.03	0.04	0.04	0.03	0.02	0.05	0.02	0.04
MgO	3.77	3.76	3.75	3.81	3.7	3.86	3.8	3.73	3.75	3.73	3.41	3.37	3.4	3.38	3.47	3.41
CaO	5.96	5.86	5.89	6.01	6.01	6	6.06	5.92	5.98	5.95	5.53	5.48	5.54	5.49	5.56	5.52
Na <sub>2</sub> O	15.78	16.09	15.7	15.79	16.12	16.18	16.02	15.58	15.95	16.04	15.37	15.08	14.98	15.28	14.85	15.54
K <sub>2</sub> O	0.38	0.35	0.36	0.35	0.37	0.39	0.37	0.36	0.39	0.4	0.3	0.31	0.31	0.3	0.3	0.29
MnO	0.01	0	0.01	0	0.05	0	0.01	0.03	0	0	0	0.02	0	0.02	0.01	0.01
Cl	0.03	0.02	0.02	0.02	0.03	0	0.02	0.03	0.01	0.02	0.03	0.03	0.01	0.03	0.03	0.04
SO <sub>3</sub>	0.29	0.28	0.32	0.3	0.28	0.33	0.25	0.34	0.31	0.33	0.24	0.26	0.21	0.25	0.23	0.24
Total	99.13	99.48	98.76	99.58	100.05	99.75	99.76	98.18	99.2	99.05	98.93	98.37	97.59	98.88	98.28	98.94

Sample / Wt. %	Major-Element Analyses of Microtektites by Electron Microprobe, Limestone Mountain															
	G4-1	G4-2	G4-3	G4-4	G4-5	G4-6	G4-7	G4-8	G5-1	G5-2	G5-3	G5-4	G5-5	G5-6	Av.	St. Dev.
SiO <sub>2</sub>	71.48	70.72	71.87	70.64	71.23	70.76	71.74	71.65	71.78	71.34	71.03	72.08	72.41	72.55	71.68	0.65
TiO <sub>2</sub>	0.03	0.03	0.03	0.05	0.03	0.03	0	0.02	0	0.01	0	0.03	0.01	0.01	0.03	0.02
Al <sub>2</sub> O <sub>3</sub>	1.44	1.41	1.42	1.41	1.4	1.41	1.43	1.43	1.3	1.31	1.3	1.33	1.34	1.33	1.35	0.08
FeO	0	0.06	0.03	0.03	0.06	0.04	0.06	0.07	0.07	0.01	0.04	0.05	0	0.05	0.04	0.02
MgO	3.78	3.73	3.74	3.68	3.67	3.66	3.71	3.75	3.42	3.42	3.37	3.41	3.43	3.44	3.61	0.17
CaO	6.01	5.92	5.99	6.01	5.97	5.93	6.02	5.92	5.61	5.55	5.55	5.56	5.57	5.52	5.8	0.22
Na <sub>2</sub> O	15.87	15.43	15.53	15.32	16.22	15.93	15.86	16.49	16.07	15.97	15.56	16.19	15.85	15.52	15.74	0.40
K <sub>2</sub> O	0.36	0.34	0.35	0.35	0.38	0.37	0.37	0.36	0.63	0.6	0.61	0.63	0.62	0.62	0.4	0.11

<b>MnO</b>	0	0.01	0	0.03	0.04	0.01	0	0.01	0	0.01	0.03	0.01	0	0.02	0.01	0.01
<b>Cl</b>	0.03	0.04	0.05	0.04	0.03	0.02	0.04	0.05	0.01	0.01	0.02	0.02	0.01	0.02	0.03	0.01
<b>SO3</b>	0.28	0.29	0.29	0.28	0.26	0.36	0.28	0.29	0.22	0.25	0.22	0.27	0.25	0.24	0.27	0.04
<b>Total</b>	99.2 8	97.9 8	99.3	97.8 4	99.29	98.5 2	99.5 1	100	99.1 1	98.4 8	97.7 3	99.5 8	99.4 9	99.3 2	98.9 6	

**Table 4: Conodont Populations, Limestone Mountain and Sherman Hill, Michigan**

	Plectodina aculeata	Fibrous conodonts	Icriodella superba	Periondon grandis	Scalopodus insculptus	Amorphognathus ordovicicus	Phragmodus undatus	Plectodina furcata	Belodina compressa	Drepanodus suberectus	Disctacodus sp.	Panderodus feulneri
<b>Limestone Mountain</b>												
8 (top)							4	8		1		25
7				2					1	1		16
6		2										
5	2	5							1			4
4			3	4		16	10	19	9	7	8	21
3				2	3	10	3	4	4	3	6	40
2					2	10	3	7	3	2	4	15
1 (bottom)								2	1	4	2	5
<b>Sherman Hill</b>												
2 (top)								3	5		14	22
1 (bottom)								8	3		8	17

**Table 5. U-Pb geochronologic analyses of Monzonite dike intruding deformed Permian strata east of Ruidoso, New Mexico**

Analysis	Isotope ratios										Apparent ages (Ma)							
	U (ppm)	206Pb 204Pb	U/Th	206Pb* 207Pb*	± (%)	207Pb* 235U*	± (%)	206Pb* 238U	± (%)	error corr.	206Pb* 238U*	± (Ma)	207Pb* 235U	± (Ma)	206Pb* 207Pb*	± (Ma)	Best age (Ma)	± (Ma)
Lincoln-10-19	122	6100	0.7	20.0857	5.7	0.0480	###	0.0070	8.7	0.84	44.9	3.9	47.6	4.8	185.0	132.4	44.9	3.9
Lincoln-10-13	421	3126	0.5	21.8442	1.0	0.0469	3.0	0.0074	2.9	0.94	47.7	1.4	46.5	1.4	-14.0	24.8	47.7	1.4
Lincoln-10-4	525	1745	0.5	18.6595	5.6	0.0551	6.2	0.0075	2.7	0.44	47.9	1.3	54.5	3.3	353.9	126.4	47.9	1.3
Lincoln-10-12	138	1035	1.4	22.4928	5.0	0.0458	6.0	0.0075	3.2	0.54	48.0	1.5	45.4	2.7	-85.2	123.6	48.0	1.5
Lincoln-10-20	80	1080	1.4	20.6970	4.7	0.0525	5.1	0.0079	2.1	0.40	50.6	1.0	51.9	2.6	114.8	110.7	50.6	1.0
Lincoln-10-3	655	5950	0.5	21.4595	1.7	0.0526	1.9	0.0082	0.9	0.47	52.5	0.5	52.0	1.0	28.7	40.5	52.5	0.5
Lincoln-10-21	209	2020	0.6	20.5605	3.1	0.0559	3.2	0.0083	0.9	0.28	53.5	0.5	55.2	1.7	130.4	73.3	53.5	0.5
Lincoln-10-9	194	88916	1.9	10.7451	0.8	3.4796	2.6	0.2712	2.4	0.94	1546.8	33.4	1522.6	20.3	1489.2	15.9	1489.2	15.9
Lincoln-10-11	199	38271	2.0	10.7438	0.8	3.3712	2.8	0.2627	2.7	0.96	1503.6	36.2	1497.7	22.0	1489.4	14.7	1489.4	14.7
Lincoln-10-10	158	49627	1.9	10.7292	1.0	3.5165	2.4	0.2736	2.1	0.90	1559.2	29.5	1530.9	18.7	1492.0	19.3	1492.0	19.3
Lincoln-10-15	122	82266	3.2	9.6569	1.0	4.4045	1.9	0.3085	1.6	0.85	1733.2	24.4	1713.2	15.6	1688.7	18.1	1688.7	18.1
Lincoln-10-17	100	27565	2.6	9.6560	0.7	4.3870	3.4	0.3072	3.3	0.98	1727.1	50.3	1709.9	28.1	1688.9	13.8	1688.9	13.8
Lincoln-10-14	182	55938	9.5	9.6414	0.7	4.3401	1.2	0.3035	1.0	0.83	1708.6	15.3	1701.0	10.1	1691.7	12.5	1691.7	12.5
Lincoln-10-16	116	46733	1.6	9.5820	0.5	4.2815	2.3	0.2975	2.2	0.97	1679.1	32.7	1689.8	18.8	1703.1	9.9	1703.1	9.9

1. Analyses with >10% uncertainty (1-sigma) in 206Pb/238U age are not included.
2. Analyses with >10% uncertainty (1-sigma) in 206Pb/207Pb age are not included, unless 206Pb/238U age is <500 Ma.
3. Best age is from 206Pb/238U age for analyses with 206Pb/238U age <1000 Ma or 206Pb/207Pb age for 206Pb/238U age > 1000 Ma.
4. Analyses with 206Pb/238U age > 500 Ma and with >20% discordance (<80% concordance) are not included.
5. Analyses with 206Pb/238U age > 500 Ma and with >5% reverse discordance (<105% concordance) are not included.
6. All uncertainties are reported at the 1-sigma level, and include only measurement errors.

7. Systematic errors are as follows (at 2-sigma level): [sample 1: 2.5% ( $^{206}\text{Pb}/^{238}\text{U}$ ) & 1.4% ( $^{206}\text{Pb}/^{207}\text{Pb}$ )]
8. Analyses conducted by LA-MC-ICPMS, as described by Gehrels et al. (2008).
9. U concentration and U/Th are calibrated relative to Sri Lanka zircon standard and are accurate to ~20%.
10. Common Pb correction is from measured  $^{204}\text{Pb}$  with common Pb composition interpreted from Stacey and Kramers (1975).
11. Common Pb composition assigned uncertainties of 1.5 for  $^{206}\text{Pb}/^{204}\text{Pb}$ , 0.3 for  $^{207}\text{Pb}/^{204}\text{Pb}$ , and 2.0 for  $^{208}\text{Pb}/^{204}\text{Pb}$ .
12. U/Pb and  $^{206}\text{Pb}/^{207}\text{Pb}$  fractionation is calibrated relative to fragments of a large Sri Lanka zircon of  $563.5 \pm 3.2$  Ma (2-sigma).
13. U decay constants and composition as follows:  $^{235}\text{U} = 9.8485 \times 10^{-10}$ ,  $^{238}\text{U} = 1.55125 \times 10^{-10}$ ,  $^{238}\text{U}/^{235}\text{U} = 137.88$ .
14. Weighted mean determined with Isoplot (Ludwig, 2008).